

UNCLASSIFIED

AD NUMBER

AD872980

NEW LIMITATION CHANGE

TO

Approved for public release, distribution  
unlimited

FROM

Distribution authorized to U.S. Gov't.  
agencies and their contractors;  
Administrative/Operational use; Aug 1970.  
Other requests shall be referred to Air  
Force Aero Propulsion Laboratory, [APFL],  
Wright-Patterson Air Force Base, Ohio  
45433.

AUTHORITY

AFAPL, ltr, 2 Sept 1971

THIS PAGE IS UNCLASSIFIED

AD872980

AFAPL-TR-65-45

Part IX

(T)  
JG

## ROTOR-BEARING DYNAMICS DESIGN TECHNOLOGY

### Part IX: Thrust Bearing Effects on Rotor Stability

AD No. —

DDS FILE COPY

AUG 14 1970

R. Cundiff  
J. Vahr

RT

Mechanical Technology Incorporated

## TECHNICAL REPORT AFAPL-TR-65-45, PART IX

August 1970

This document is subject to special export controls  
and each transmittal to foreign governments or  
foreign national may be made only with prior approval  
of the Air Force Aero Propulsion Laboratory (APFL),  
Wright-Patterson Air Force Base, Ohio 45433.

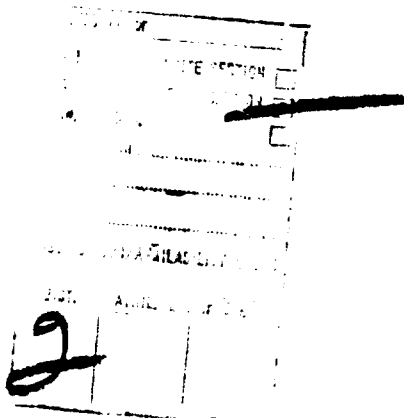
Air Force Aero Propulsion Laboratory  
Air Force Systems Command  
Wright-Patterson Air Force Base, Ohio

Best Available Copy

NOTICE

When Government drawings, specifications, or other data are used for any purpose other than in connection with a definitely related Government procurement operation, the United States Government thereby incurs no responsibility nor any obligation whatsoever; and the fact that the government may have formulated, furnished, or in any way supplied the said drawings, specifications, or other data, is not to be regarded by implication or otherwise as in any manner licensing the holder or any other person or corporation, or conveying any rights or permission to manufacture, use, or sell any patented invention that may in any way be related thereto.

This document is subject to special export controls and each transmittal to foreign governments or foreign nationals may be made only with prior approval of the Air Force Aero Propulsion Laboratory (APFL), Wright-Patterson Air Force Base, Ohio 45433.



Copies of this report should not be returned unless return is required by security considerations, contractual obligations, or notice on a specific document.

Declassify At:

**AFAPL-TR-65-45**

**Part IX**

**ROTOR-BEARING DYNAMICS DESIGN TECHNOLOGY**

**Part IX: Thrust Bearing Effects  
on Rotor Stability**

R. Cundiff  
J. Vehr

**Mechanical Technology Incorporated**

**TECHNICAL REPORT AFAPL-TR-65-45, PART IX**

**August 1970**

This document is subject to special export controls  
and each transmittal to foreign governments or  
foreign national may be made only with prior approval  
of the Air Force Aero Propulsion Laboratory (APFL),  
Wright-Patterson Air Force Base, Ohio 45433.

**Air Force Aero Propulsion Laboratory  
Air Force Systems Command  
Wright-Patterson Air Force Base, Ohio**

**Best Available Copy**

FOREWORD

This report was prepared by Mechanical Technology Incorporated, 968 Albany-Shaker Road, Latham, New York 12110 under USAF Contract No. AF33(615)-3238. The contract was initiated under Project No. 3048, Task No. 304806. The work was administered under the direction of the Air Force Aero Propulsion Laboratory, with Mr. M. Robin Chasman and Mr. Everett A. Lake (APFL) acting as project engineer.

This report covers work conducted from 1 October 1968 to 1 January 1970.

This report was submitted by the authors on June 5, 1970.

This report is Part IX of final documentation issued in multiple parts.

Publication of this report does not constitute Air Force approval of the report's findings or conclusions. It is published only for the exchange and stimulation of ideas.



HOWARD F. JONES, Chief  
Lubrication Branch  
Fuel, Lubrication & Hazards Division  
Air Force Aero Propulsion Laboratory

ABSTRACT

This volume presents a study conducted to determine the effects thrust bearings have on rotor-bearing stability. A computer program was written in order to study these effects and permits the inclusion of the thrust bearing characteristics into the rotor system. A manual is provided for the program, containing a listing of the program and detailed instructions for preparation of input data. A technique is also presented which permits the user a convenient method of evaluating the stability of a rotor system with and without the thrust bearing data. Extensive design data are presented for gas-lubricated, externally pressurized thrust bearings.

This abstract is subject to special export controls  
and each transmittal to foreign governments or foreign  
nationals may be made only with prior approval of the  
Air Force Aero Propulsion Laboratory (APFL), Wright-  
Patterson Air Force Base, Ohio 45433.

TABLE OF CONTENTS

	<u>Page</u>
I. INTRODUCTION -----	1
II. THE DETERMINATION OF THRESHOLD SPEED FOR WHIRL INSTABILITY OF A ROTOR -----	2
1. General Discussion -----	2
2. Analysis of Stability of Arbitrary, Non-Symmetrical Rotor... 10	
3. Determination of Rotor-Bearing Stability by Means of Critical Speed Maps-----	13
III. EFFECT OF THRUST BEARING STIFFNESS AND DAMPING ON ROTOR-BEARING STABILITY -----	18
1. Discussion-----	18
2. Sample Calculations-----	22
IV. ANGULAR STIFFNESS COEFFICIENTS FOR HYDROSTATIC THRUST BEARINGS ... 50	
APPENDIX I: Computer Program - PN400 - The Threshold of Instability of a Flexible Rotor in Fluid Film Bearings.. 61	
REFERENCES -----	86

## ILLUSTRATIONS

<u>Figure</u>	<u>Page</u>
1. Coordinate System for Forces and Displacement-----	4
2. Loci of Roots for Real and Imaginary Parts of Equation (10)-----	9
3. Sign Convention for Amplitude, Slope, Bending Moment and Shear Force Illustrated in x-z Plane-----	11
4. Coordinate Axis System-----	19
5. Conical Instability Rotor Model 1-----	23
6. Conical Instability Rotor Model 2-----	24
7. Critical Speed Map of Rotor 1-----	33
8. Loci for Roots of Real and Imaginary Parts of Stability Determinant-----	35
9. Loci for Roots of Real and Imaginary Parts of Stability Determinant-----	40
10. Critical Speed Map of Rotor 2-----	44
11. Loci of Roots for Real and Imaginary Parts of Stability Determinant-----	46
12. Sketch of Hydrostatic Thrust Bearing-----	51
13. Hydrostatic Thrust Bearing, $R_o/R_i = 1.25$ . Dimensionless Angular Stiffness vs. Restrictor Coefficient-----	54
14. Hydrostatic Thrust Bearing, $R_o/R_i = 1.5$ . Dimensionless Angular Stiffness vs. Restrictor Coefficient-----	55
15. Hydrostatic Thrust Bearing, $R_o/R_i = 2$ . Dimensionless Angular Stiffness vs. Restrictor Coefficient-----	56
16. Hydrostatic Thrust Bearing, $R_o/R_i = 3$ . Dimensionless Angular Stiffness vs. Restrictor Coefficient-----	57
17. Dynamic Angular Stiffness for the Hydrostatic Thrust Bearing $R_o/R_i = 1.5$ . Inherent Compensation-----	58
18. Dynamic Angular Stiffness for the Hydrostatic Thrust Bearing $R_o/R_i = 3$ . Inherent Compensation-----	59
19. Minimum Number of Feeder Holes-----	60

## SYMBOLS

$a$	Orifice radius, inch
$a_{mn}$	Dynamic influence coefficients
$A$	Defined by Eq. (20)
$B$	Single effective bearing damping, defined by Eq. (19), lbs.sec/in
$B_{major}$	Maximum value of $B$ , lbs.sec/in
$B_{minor}$	Minimum value of $B$ , lbs.sec/in
$B_{xx}, B_{xy}, B_{yx}, B_{yy}$	Dynamic bearing damping coefficients, lbs.sec/inch
$\bar{B}$	Dimensionalized bearing damping coefficient $= C_w B / P_a L D$
$C$	Radial clearance, inch
$D$	Bearing diameter, inch
$D_{xx}, D_{xy}, D_{yx}, D_{yy}$	Dynamic angular bearing damping coefficients, lbs.sec.inch/radians
$e$	Steady-state bearing eccentricity, inch
$F_x, F_y$	Bearing fluid film forces, lbs.
$G_{xx}, G_{xy}, G_{yx}, G_{yy}$	Dynamic angular bearing stiffness coefficients, lbs.inch/radian
$i$	$= \sqrt{-1}$
$Im\{\}$	Imaginary part of complex expression
$K$	Single effective spring stiffness, defined by Eq. (18), lb/in.
$K_{major}$	Maximum value of $K$ , lb/in.
$K_{minor}$	Minimum value of $K$ , lb/in.
$K_{xx}, K_{xy}, K_{yx}, K_{yy}$	Dynamic bearing stiffness coefficients, lbs/inch
$\bar{K}$	Dimensionalized stiffness coefficient $= C_K K / P_a L D$

L	Bearing length, inch
L	Half bearing span length, inch
= L <sub>1</sub> + L <sub>2</sub>	
L <sub>1</sub>	Distance from rotor C.G. to centerline of bearing number 1
L <sub>2</sub>	Distance from rotor C.G. to centerline of bearing number 2
M	Journal bearing mass (half rotor mass for rigid rotor), lbs.sec <sup>2</sup> /inch
M <sub>c</sub>	Critical mass per bearing, lbs.sec <sup>2</sup> /inch
M <sub>x</sub> , M <sub>y</sub>	x and y-component of rotor bending moment to the left of a rotor mass station, lbs.inch
M' <sub>x</sub> , M' <sub>y</sub>	x and y-component of rotor bending moment to the right of the rotor mass station, lbs.inch
n	Number of feeder holes
P <sub>a</sub>	Ambient pressure, psia
P <sub>s</sub>	Supply pressure, psia
R	Bearing radius, inch
Re()	Real part of complex expression
R <sub>o</sub>	Outer radius of thrust bearing, inch
R <sub>i</sub>	Inner radius of thrust bearing, inch
R	Gas constant, inch <sup>2</sup> /sec <sup>2</sup> °R
T	Temperature of gas lubricant, °R
t	Time, seconds
V <sub>x</sub> , V <sub>m</sub>	x and y-component of rotor shear force to the left of a rotor mass station, lbs.
V' <sub>x</sub> , V' <sub>y</sub>	x and y-component of rotor shear force to the right of a rotor mass station, lbs.
W	Static load on bearing, lbs.

$W_x, W_y$	External forces on rotor in x and y direction, lbs.
$Z_{xx}, Z_{xy}, Z_{yx}, Z_{yy}$	Complex notation of stiffness and damping axial coordinate, inch
$x, y$	Rotor amplitudes, inch
$x_c, x_s$	Cosine and sine component of rotor x-amplitude, inch
$y_c, y_s$	Cosine and sine component of rotor y-amplitude, inch
$z$	Axial coordinate, inch
$\gamma$	= $v/\omega$ , whirl frequency ratio
$\Delta$	Complex deterministic equation
$\Delta_c$	= $\text{Re}\{\Delta\}$ , real part of complex equation
$\Delta_s$	= $\text{Im}\{\Delta\}$ , imaginary part of complex equation
$\delta$	= $a^2/dC$ , inherent compensation factor
$e_B$	= $e/C$ , eccentricity ratio for bearing
$\theta$	Angular displacement of thrust bearing in x-z plane, radian
$\Lambda$	= $\frac{12\pi\mu N}{P_a} \left( \frac{R_o}{C} \right)^2$ , Compressibility number
$\Lambda_s$	= $\frac{6\mu n a^2 \sqrt{RT}}{P_s C^3 \sqrt{1 + \delta^2}}$ , restrictor coefficient
$\mu$	Lubricant viscosity, $\text{lbs}\cdot\text{sec/in}^2$
$\nu$	Whirl frequency, rad/sec
$\nu_c$	Critical whirl frequency at threshold of instability, rad/sec
$\sigma$	= $\frac{12\mu\nu}{P_a} \left( \frac{R_i R_o}{C^2} \right)$ , Squeeze number

$\Psi$	Angular displacement of thrust bearing in y-z plane, rad.
$\Phi$	Bearing attitude angle, deg.
$\dot{\Psi}$	Angular displacement of thrust bearing in y-z plane, rad.
$\omega$	Journal angular velocity, rad/sec
$\omega_T$	Journal angular velocity at threshold, rad/sec

Subscripts

B	Bearing
C,S	Cosine and sine component (real and imaginary part)
C	Critical value
e	Effective
j	Journal bearing
m	Number of total rotor stations
n	Rotor station number
T	Thrust bearing
x,y	x and y-direction

Superscripts

dot	Time derivative
bar	Dimensionless quantity

SECTION I  
INTRODUCTION

For rotors possessing a high degree of dissymmetry or for rather short rotors the instability whirl motion will have a substantial conical whirl component. Under such conditions the dynamic forces imposed on the rotor by the thrust bearing will have an important effect on the dynamical characteristics and the stability of the rotor-bearing system.

The purpose of the study described in this report was to develop the technology for determining effects of thrust bearing forces on the stability of rotors supported in fluid film bearings and to assess the significance of this effect on rotors of practical design. To this end, a computer program was developed to perform many of the complex calculations necessary for determination of the stability limits of complicated rotor-bearing systems which takes account of effects of thrust bearing stiffness and damping. This computer program is an extension and modification of a similar program developed in an earlier task performed under contract AF33(615) 3238 (Ref. 1). A complete description of the program including a computer listing is provided in the present report.

The present report provides angular stiffness data for hydrostatic thrust bearing geometries for use in the determination of rotor stability. Also a useful, simplified method for determining stability of rotors supported on bearings all of which are the same is described. Finally, several numerical examples of the calculation of thrust bearing effects on rotor stability are presented and the significance of these effects is discussed.

## SECTION II

### THE DETERMINATION OF THRESHOLD SPEED FOR WHIRL INSTABILITY OF A ROTOR

#### 1. General Discussion

As is well established, a fluid film bearing supporting a rotor may be likened to a spring-dashpot system in that the bearing reaction to small displacements may be expressed in terms of stiffness and damping coefficients. A mass supported by springs has a number of natural spring-mass frequencies depending on the complexity of the spring system and the possible modes of motion of the mass. If any mode of motion is excited at the natural frequency by an external harmonic force, then the response of the system will be at a maximum but, if the system possesses effective damping for this mode of excitation, then the response will be bounded and the system will not be unstable. If, on the other hand, the natural frequency of a mode of motion corresponds to a condition where the effective damping of the system is negative, then the motion of the system at that frequency will increase without bound without any external excitation, and the system is considered as being unstable, i.e. subject to self-excited vibration. If a natural frequency occurs at a condition of zero damping, then the system can be said to be at the threshold of instability, where infinitesimally small exciting forces applied over a period of time will result in ever increasing amplitudes of response.

The so-called critical speeds of a rotor-bearing system refer to resonant responses of the system to unbalance forces of the system which, by their nature, are applied at a frequency synchronous with the rotational speed of the shaft. Since fluid film bearings in general have positive damping to synchronous speed oscillations, critical speeds are not instabilities but simply represent a condition of large resonant response to inherent unbalance forces. Fluid film bearings, however, do have an effective damping to various modes of motion which does tend toward zero when the motion occurs at some fraction of the running speed, usually at half the running speed. Thus, as the running speed of a rotor increases beyond the first critical speed or natural frequency speed, the rotor will begin to approach the condition where the first resonant or natural frequency of the system will coincide with the fractional frequency at which effective damping goes to zero. When this coincidence occurs, the rotor is said to have reached the whirl threshold speed. A

further increase in rotor speed usually results in a very rapid growth of whirl amplitude and, in almost all cases, the whirl threshold speed represents the upper limit for safe operation of the rotor.

We might note at this time that because effective damping of fluid film bearings tends toward zero for half-frequency oscillations, the rule of thumb has arisen that the threshold of instability is reached at about twice the first critical speed of the rotor. The basis for this rule of thumb will be examined in more detail in subsection 3 where there is discussed a procedure for using critical speed maps for predicting threshold of whirl instability.

Having briefly discussed the qualitative nature of whirl instability and its distinction from critical speeds, we will now proceed to show the nature of the linearized analysis required to determine the whirl threshold speed. In the illustrative treatment below, we shall consider only the translatory mode of a symmetric rotor supported on two identical bearings. The more general case of the translatory, conical and bending modes of a non-symmetric rotor will be considered in subsection 2. For this general case, determination of whirl threshold speed requires use of the computer program developed in this study. For the simpler case presented below, whirl threshold speed can be determined analytically.

For the translatory mode of a rigid symmetric rotor the gravity and inertia (D'Alembert) forces are equally borne by the two bearings. The kinematic relationships between the rotor and stator bearing surfaces at one bearing are at every instant identical as those of the other. It is therefore only necessary to consider the motion of one journal which has a mass equal to one-half the rotor mass. Let the rotor mass be  $2M$  and the journal center amplitudes be  $x$  and  $y$ .

At any given rotor speed and with a known static load on the bearing, the journal center occupies a certain unique equilibrium position relative to the bearing center. When the journal whirls around its equilibrium position in a small orbit, hydrodynamic bearing forces are generated in the bearing fluid film. These dynamic forces can be expressed in a linearized form by expanding the film forces into a first order Taylor series. With the bearing fluid film dynamic forces represented by  $F_x$  and  $F_y$  and with the dynamic external forces on the rotor represented by  $w_x$  and  $w_y$  as shown in Fig. 1, the linearized equation of motion become:

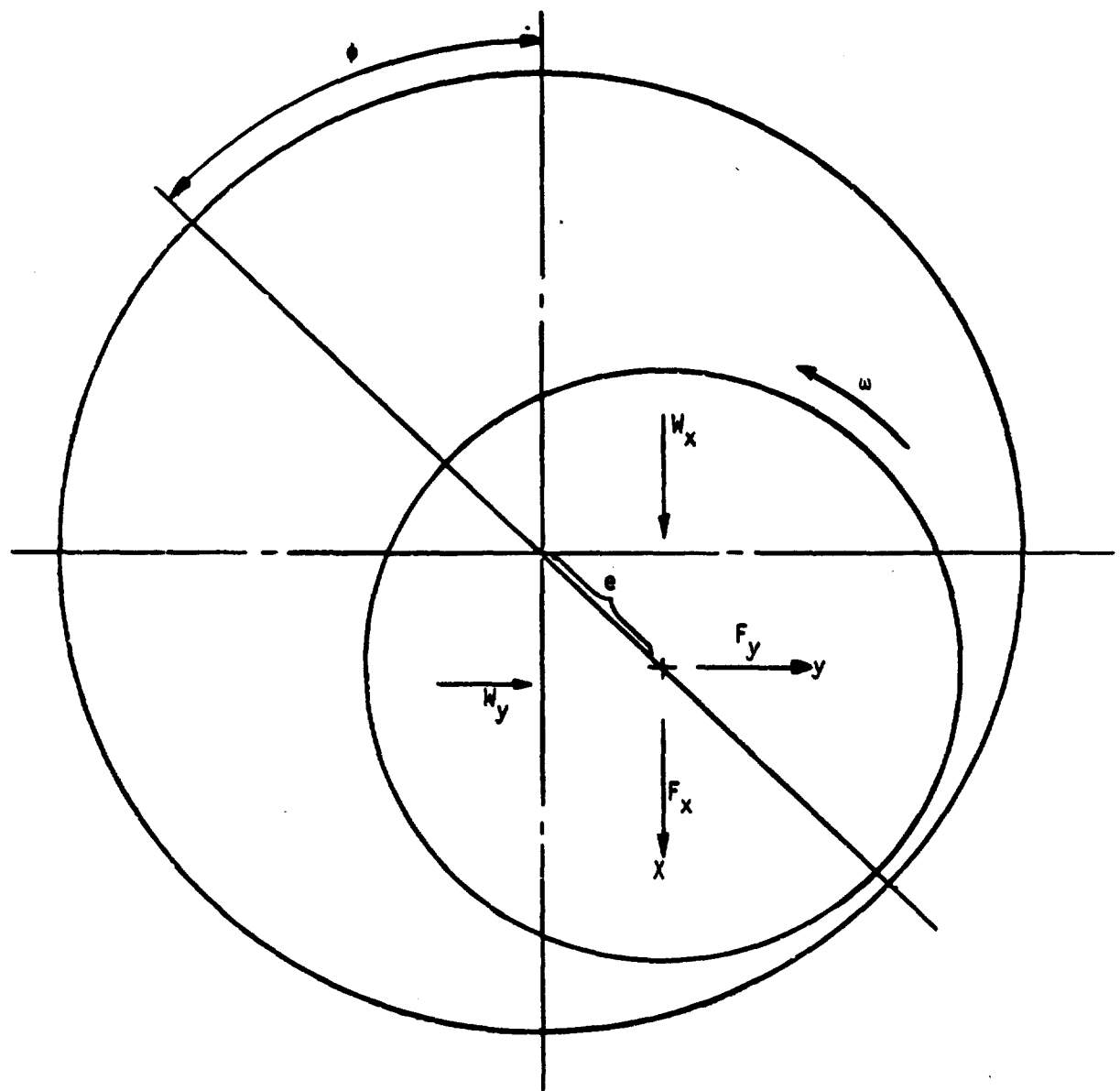


Fig. 1 Coordinate System for Forces and Displacements

$$M \frac{d^2x}{dt^2} = F_x + W_x = -K_{xx}x - B_{xx}\dot{x} - K_{xy}y - B_{xy}\dot{y} + W_x$$

(1)

$$M \frac{d^2y}{dt^2} = F_y + W_y = -K_{yy}y - B_{yy}\dot{y} - K_{yx}x - B_{yx}\dot{x} + W_y$$

where  $x$  and  $y$  are the whirl amplitudes measured from the static equilibrium position,  $t$  is time, and the four radial stiffness coefficients and the four radial damping coefficients are computed from the lubrication equation (Reynolds equation) as described in Ref. 2. For a given bearing geometry and known lubricant properties, the eight coefficients are functions of the bearing load and the rotor speed and, if the lubricant is compressible like a gas, they are also functions of the whirl frequency. At the threshold of instability,  $x$  and  $y$  are pure harmonic motions and can be conveniently expressed in terms of the whirl frequency  $\nu$ :

$$x = x_c \cos(\nu t) - x_s \sin(\nu t)$$

(2)

$$y = y_c \cos(\nu t) - y_s \sin(\nu t)$$

These equations can also be expressed in complex form:

$$x = \operatorname{Re} \{(x_c + ix_s) e^{i\nu t}\} = x_c \cos(\nu t) - x_s \sin(\nu t)$$

(3)

$$y = \operatorname{Re} \{(y_c + iy_s) e^{i\nu t}\} = y_c \cos(\nu t) - y_s \sin(\nu t)$$

where  $\operatorname{Re} \{ \}$  indicates that only the real part of the complex equation is applicable. For convenience the  $\operatorname{Re} \{ \}$  notation is dropped and Eq. (3) is expressed:

$$x = (x_c + ix_s) e^{i\nu t}$$

(4)

$$y = (y_c + iy_s) e^{i\nu t}$$

When these equations are used in the analysis their complete meaning is defined by Eq. (3). Time derivatives can also be carried out in the complex notation,

bearing in mind that only the real part is of significance; e.g.

$$\begin{aligned}\dot{x} &= \frac{\partial}{\partial t} \operatorname{Re} \left\{ (x_c + ix_s) e^{ivt} \right\} \\ &= \operatorname{Re} \left\{ (x_c + ix_s) \frac{\partial}{\partial t} (e^{ivt}) \right\} \\ &= \operatorname{Re} \left\{ iv (x_c + ix_s) e^{ivt} \right\} \\ &= -v x_c \sin vt - v x_s \cos vt\end{aligned}$$

By differentiating Eqs. (4) and substituting into Eqs. (1) the equations of motion can be written:

$$\begin{aligned}M \ddot{x} &= -z_{xx} x - z_{xy} y + w_x \\ M \ddot{y} &= -z_{yx} x - z_{yy} y + w_y\end{aligned}\tag{5}$$

where:

$$\begin{aligned}z_{xx} &= K_{xx} + iv B_{xx} \quad (\text{Similarly for } z_{xy}, z_{yx}, z_{yy}) \\ &= K_{xx} + i\gamma\omega B_{xx}\end{aligned}\tag{6}$$

$$\gamma = v/\omega\tag{7}$$

Here,  $\omega$  is the angular speed of rotation and  $\gamma$  is the ratio of the whirl frequency to the rotational frequency. In this form, the equations are equally valid for an incompressible and a compressible lubricant. In matrix form Eqs. (5) can be expressed:

$$\begin{Bmatrix} (z_{xx} - Mv^2) & z_{xy} \\ z_{yx} & (z_{yy} - Mv^2) \end{Bmatrix} \begin{Bmatrix} x \\ y \end{Bmatrix} = \begin{Bmatrix} w_x \\ w_y \end{Bmatrix} \quad (8)$$

For the rotor-bearing represented by Eq. (8) to be unstable, it is necessary and sufficient that Eq. (8) yield a non-zero solution for the amplitudes  $x$  and  $y$  when the external forces  $w_x$  and  $w_y$  are zero, i.e. for the system to be unstable a non-trivial solution to Eq. (9) below must be found.

$$\begin{Bmatrix} (z_{xx} - Mv^2) & z_{xy} \\ z_{yx} & (z_{yy} - Mv^2) \end{Bmatrix} \begin{Bmatrix} x \\ y \end{Bmatrix} = 0 \quad (9)$$

For a non-trivial solution to exist, the determinant of the matrix must vanish. Setting both the real and imaginary parts of the determinant to zero gives;

$$\Delta = \Delta_c + i\Delta_s = (z_{xx} - Mv^2)(z_{yy} - Mv^2) - z_{xy} z_{yx} = 0 \quad (10)$$

$$\begin{aligned} \Delta_c &= \operatorname{Re}\{\Delta\} = (K_{xx} - Mv^2)(K_{yy} - Mv^2) - K_{xy} K_{yx} \\ &\quad - \gamma^2 (\omega B_{xx} \omega B_{yy} - \omega B_{xy} \omega B_{yx}) = 0 \end{aligned} \quad (11)$$

$$\begin{aligned} \Delta_s &= I_m \{\Delta\} = \gamma \left[ (K_{xx} - Mv^2) \omega B_{yy} + (K_{yy} - Mv^2) \omega B_{xx} \right. \\ &\quad \left. - K_{xy} \omega B_{yx} - K_{yx} \omega B_{xy} \right] = 0 \end{aligned} \quad (12)$$

Thus, when both the real and imaginary parts of the determinant vanish simultaneously harmonic motion or whirl is present and this whirl is referred to as rotor instability. Every combination of  $\gamma$  and  $\omega$  satisfying either Eq. (11) or Eq. (12) can be represented by a point in a  $\gamma$ - $\omega$  plot. Typically the locii of these points appear as shown in Fig. 2.

Eqs. (11) and (12) contain two unknowns, the whirl frequency ratio,  $\gamma$ , and the angular speed of rotation,  $\omega$ . For incompressible fluids, the eight dynamic film coefficients are independent of  $\gamma$ , thus Eqs. (11) and (12) may be solved yielding two expressions for  $Mv^2$  and  $\gamma^2$ .

$$Mv^2 = \frac{K_{xx} \omega B_{yy} + K_{yy} \omega B_{xx} - K_{xy} \omega B_{yx} - K_{yx} \omega B_{xy}}{\omega B_{xx} + \omega B_{yy}} \quad (13)$$

$$\gamma^2 = \frac{(K_{xx} - Mv^2)(K_{yy} - Mv^2) - K_{xy} K_{yx}}{\omega B_{xx} \omega B_{yy} - \omega B_{xy} \omega B_{yx}} \quad (14)$$

At a given rotational speed and load and with the eight coefficients known,  $Mv^2$  may be calculated from Eq. (13) and when substituted into Eq. (14) gives the whirl frequency ratio squared value  $\gamma^2$ . Two methods of establishing an instability criteria may be obtained from these two values. First, the actual mass at the journal bearing may be substituted into the  $Mv^2$  term to solve for the  $v^2$  value which when substituted into the  $\gamma^2$  value yields the apparent threshold frequency. If this threshold frequency is identical to the rotor speed at which the coefficients were based then the threshold speed has been obtained. The second method substitutes the rotor speed,  $\omega$ , in the  $\gamma^2$  term to find the whirl frequency  $v$  which, when substituted into the  $Mv^2$  term, yields a critical mass  $M_c$  for onset of instability. If the actual journal bearing mass  $M$  is less than  $M_c$ , then the system is stable; if  $M$  is greater than  $M_c$ , the system is

unstable. The mathematical derivation of this stability criterion is given in Ref. 4.

From compressible fluids, the eight radial dynamic fluid film coefficients are functions of both  $\gamma$  and  $\omega$ , making a closed form solution to the simultaneous Eqs. (11) and (12) impossible and the solution is most conveniently obtained graphically. For any fixed value of  $\omega$ ,  $\Delta_c$  and  $\Delta_s$  can be plotted as functions of  $\gamma$  to find their zero points. With  $\gamma > 0$  it is seen that  $\Delta_s$  has one zero point and  $\Delta_c$  has up to two zero points (only true in this simple case). The calculation is repeated for several values of  $\omega$  and the results for the various zero points may be plotted as shown:

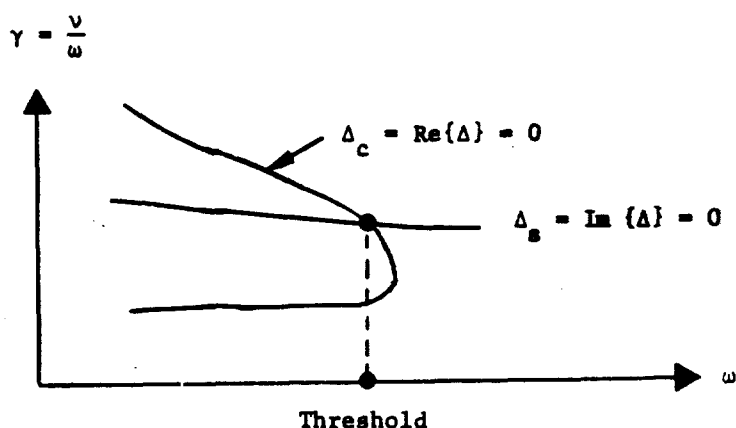


Fig. 2 Loci of Roots for Real and Imaginary Parts of Eq. (10)

The intersection of the two curves define the speed at which instability sets in or the point at which both the real and imaginary parts of the simplified determinant vanish simultaneously.

## 2. Analysis of Stability of Arbitrary, Non-Symmetrical Rotor

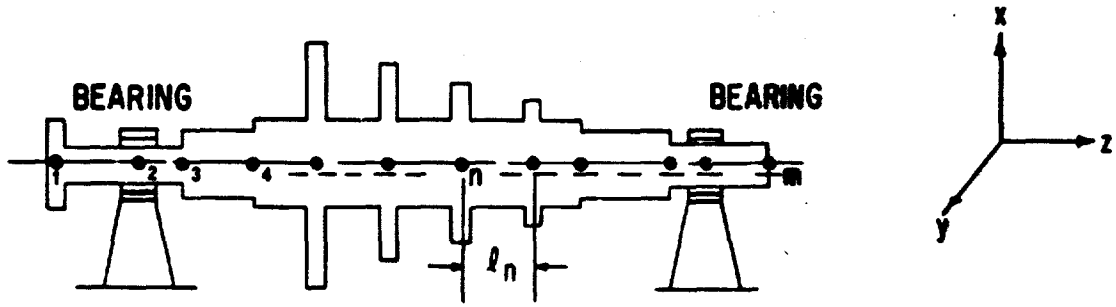
Consider the arbitrary rotor shown in Fig. 3. Assuming that the two ends of the rotor are free, the bending moments  $M'_{xm}$  and  $M'_{ym}$  and shear forces  $V'_{xm}$  and  $V'_{ym}$  at the rotor end will be linearly proportional to the displacements  $x_1$  and  $y_1$  and bending angles  $\theta_1$  and  $\varphi_1$  of the shaft at station 1 provided these displacements and bending angles are small enough such that linearized analysis applies. Mathematically we can write this linear relationship as

$$\begin{Bmatrix} V'_{xm} \\ V'_{ym} \\ M'_{xm} \\ M'_{ym} \end{Bmatrix} = \begin{Bmatrix} a_{11} & a_{12} & a_{13} & a_{14} \\ a_{21} & a_{22} & a_{23} & a_{24} \\ a_{31} & a_{32} & a_{33} & a_{34} \\ a_{41} & a_{42} & a_{43} & a_{44} \end{Bmatrix} \begin{Bmatrix} x_1 \\ y_1 \\ \theta_1 \\ \varphi_1 \end{Bmatrix} \quad (15)$$

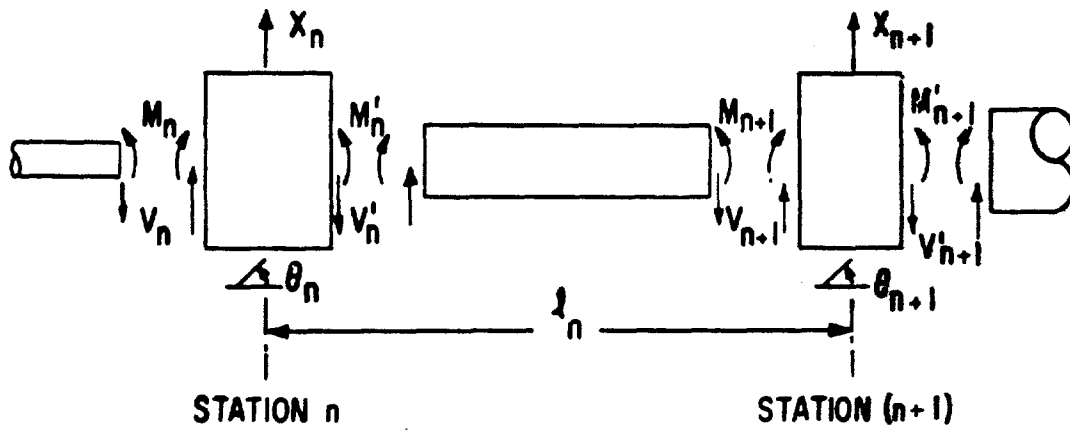
where the terms  $a_{11}$ ,  $a_{12}$ , etc., are the dynamic influence coefficients which relate the forces at station m to the motions at station 1. These coefficients are functions of the rotor inertia, rotor flexibility, and the dynamic stiffness and damping coefficients of the bearings supporting the rotor. Since  $a_{11}$ ,  $a_{12}$ , etc., are dynamic coefficients, they explicitly depend upon the rotor speed  $\omega$  and the frequency ratio  $\gamma = v/\omega$  where  $v$  is the frequency of the shaft motions being considered. For gas bearing, the stiffness and damping coefficients contained in  $a_{11}$ ,  $a_{12}$ , etc., are also functions of  $\omega$  and  $\gamma$ .

For symmetrical, rigid rotors for which only translatory motions  $x_1$  and  $y_1$  are considered, Eq. (15) above reduces to

$$\begin{Bmatrix} V'_{xm} \\ V'_{ym} \end{Bmatrix} = \begin{Bmatrix} a_{11} & a_{12} \\ a_{21} & a_{22} \end{Bmatrix} \begin{Bmatrix} x_1 \\ y_1 \end{Bmatrix} \quad (16)$$



Outline of Rotor with Location of Rotor Stations



Sign Convention for Amplitude, Slope, Bending Moment and Shear Force Illustrated in x-z Plane

Fig. 3

This is the situation considered in the previous section, and we see by comparison of Eq. (15) with Eq. (8) that the coefficients  $a_{11}$ ,  $a_{12}$ ,  $a_{21}$ , and  $a_{22}$  are given by the analytical expressions

$$\begin{aligned}a_{11} &= (z_{xx} - M\nu^2) \\a_{12} &= z_{xy} \\a_{21} &= z_{yx} \\a_{22} &= (z_{yy} - M\nu^2)\end{aligned}\tag{17}$$

For the more general case of an arbitrary flexible rotor supported on dissimilar bearings, the coefficients  $a_{11}$ ,  $a_{12}$ , etc., are very complex functions and usually cannot be expressed in analytical form but must be calculated by means of a computer program. Therefore, one of the principal tasks to be performed by a computer program written for analyzing the stability of arbitrary rotors is that of calculating all of the dynamic influence coefficients as a function of rotor geometry, rotor speed, frequency ratio  $\nu$  and the dynamic bearing coefficients supplied as input to the program. The procedure by which these influence coefficients are calculated is described in Ref. 3, Appendix VIII.

Once the dynamic influence coefficients are calculated for an appropriate range of  $\omega$  and  $\nu$ , the various thresholds of stability of the rotor-bearing system are determined by essentially the same procedure as for the simple, symmetrical rotor-bearing system discussed in the previous section. That is, thresholds of instability are found by determining the values of  $\omega$  and  $\nu$  at which both the real and the imaginary parts of the determinant of the matrix of dynamic influence coefficients simultaneously go to zero. Again, this is accomplished by plotting on a graph of  $\nu$  versus  $\omega$  separate curves for the conditions where the real and the imaginary parts of the determinant go to zero, and determining the thresholds of instability from the intersections of these curves.

In the case of an arbitrary rotor which is flexible and unsymmetric, determining

the real and imaginary parts of the determinant of the matrix of influence coefficients cannot, in general, be accomplished analytically but must be accomplished numerically by the computer program for analyzing stability. The procedure is essentially one of having the computer program calculate the values of the real and imaginary parts of the determinant over a specified range of whirl frequency ratios at a fixed rotor speed. The program then determines the zero points of the real and imaginary parts of the determinant by quadratic interpolation each time a change in the sign of these functions occurs. It should be clearly noted here that the computer program itself does not determine thresholds of stability; this remains to be accomplished by the designer by plotting the curves of the loci of the real and imaginary roots of the stability determinant.

The discussion presented above serves to describe in a qualitative way the nature of the process of determining the stability of an arbitrary rotor and how this process is implemented by means of a computer program. A detailed description of the computer program developed in the present project for the purpose of analyzing rotor-bearing stability is given in Appendix I.

### 3. Determination of Rotor-Bearing Stability by Means of Critical Speed Maps.

For a flexible rotor with two translatory and two angular degrees of freedom, i.e.,  $x_1$ ,  $y_1$ ,  $\theta_1$  and  $\omega_1$  the determinant of the matrix of influence coefficients is a higher order polynomial in  $\gamma$  and  $\omega$  than is the simple determinant from Eq. (9). Consequently, there are many real and imaginary roots of the determinant and a number of different thresholds of instability, i.e., a plot such as that shown in Fig. 2 will, for an arbitrary flexible rotor, contain many curves for  $\Delta_c = 0$  and  $\Delta_s = 0$  and many curve intersections. Each different intersection or threshold of stability will correspond to a different mode of instability motion, e.g., translatory whirl, conical whirl, etc. In general, only the mode occurring at the lowest value of  $\omega$  is of interest since this defines the practical operating limits of the system. However, the presence of a number of modes of instability makes the determination of the lowest mode a very complex and costly task, even with the aid of the computer program. Hence, it is desirable to find methods of approximately determining thresholds of instability so that the exact process of determinin

such thresholds by means of the stability program can be accomplished with a minimum of costly searching.

One convenient approach for approximately locating the instabilities of most rotors can be had by use of a critical speed map for the rotor in question. A critical speed map shows the various natural or resonant frequencies of a rotor as a function of a single value of spring stiffness  $K$  assigned to the bearings supporting the shaft. A typical critical speed map is shown in Fig. 10. For complex rotors, such maps are usually obtained by means of a computer program written specifically for this purpose.

As was discussed earlier in subsection 1., whirl instability can be viewed as a condition of undamped resonance. In particular Lund (Ref. 4) has shown that if this view point is taken, then at the threshold of stability the fluid film bearing can be represented by a single effective spring stiffness coefficient  $K$  and damping coefficient  $B$  given by

$$K = \frac{1}{2}(K_{xx} + K_{yy}) - \frac{\frac{1}{4}(K_{xx} - K_{yy})(\gamma_{\omega}B_{xx} - \gamma_{\omega}B_{yy}) + \frac{1}{2}(K_{xy}\gamma_{\omega}B_{yx} + K_{yx}\gamma_{\omega}B_{xy})}{A} \quad (18)$$

$$B = \frac{1}{2}(\gamma_{\omega}B_{xx} + \gamma_{\omega}B_{yy}) - A \quad (19)$$

where  $A$  is expressed by the following quartic equation:

$$\begin{aligned} A^4 + & \left[ \frac{1}{4}(K_{xx} - K_{yy})^2 + K_{xy}K_{yx} - \frac{1}{4}(\gamma_{\omega}B_{xx} - \gamma_{\omega}B_{yy})^2 - \gamma_{\omega}B_{xy}\gamma_{\omega}B_{yx} \right] A^2 \\ - & \left[ \frac{1}{4}(K_{xx} - K_{yy})(\gamma_{\omega}B_{xx} - \gamma_{\omega}B_{yy}) + \frac{1}{2}(K_{xy}\gamma_{\omega}B_{yx} + K_{yx}\gamma_{\omega}B_{xy}) \right]^2 = 0 \end{aligned} \quad (20)$$

Since  $B$  is real, Eq. (20) has only two solutions for  $A$  which are of equal magnitude but of opposite sign. In order for the effective bearing damping to become zero (corresponding to the undamped resonance criteria) at some value of  $\gamma$ , then  $A$  must be positive from Eq. (20) since  $(\gamma\omega B_{xx} + \gamma\omega B_{yy})$  is always positive. Therefore, only the real, positive value of  $A$  is used to define the stiffness coefficient in Eq. (18).

Another method of obtaining the effective stiffness and damping bearing coefficients at the threshold of stability is by replacing  $Mv^2$  by  $Z$  in Eq. (9) and then solving for  $Z$ . From Eq. (9):

$$\begin{Bmatrix} (Z_{xx} - Z) & Z_{xy} \\ Z_{yx} & (Z_{yy} - Z) \end{Bmatrix} \begin{Bmatrix} x \\ y \end{Bmatrix} = 0 \quad (21)$$

Since two solutions of  $Z$  are obtained, the following notation is used:

$$z_1, z_2 = \begin{Bmatrix} z_{\text{major}} \\ z_{\text{minor}} \end{Bmatrix} = \frac{1}{2} \left[ (Z_{xx} + Z_{yy}) \pm \sqrt{(Z_{xx} - Z_{yy})^2 + 4Z_{xy}Z_{yx}} \right] \quad (22)$$

where:

$$Z_{xx} = K_{xx} + i\gamma\omega B_{xx} \quad (\text{Similarly for } Z_{xy}, Z_{yx}, Z_{yy})$$

$$z_{\text{major}} = K_{\text{major}} + i\gamma\omega B_{\text{major}} \quad (\text{Similarly for } z_{\text{minor}})$$

The condition for the lowest threshold speed is that  $\gamma\omega B_{\text{minor}} = 0$ . Thus the  $K_{\text{minor}}$  and  $B_{\text{minor}}$  are equivalent to the two expressions shown in Eqs. (18) and (19).

In arriving at a  $K_{\text{minor}}$  and a  $B_{\text{minor}}$  value, the negative sign in front of the radical in Eq. (22) is generally used. An evaluation of the value of the radical is somewhat difficult since the coefficients of the bearing change constantly with increasing eccentricity. Various bearing types and coefficients have been evaluated and this sign convention has proven correct. This sign convention is also consistent with the analysis by Lund (Ref. 4).

The importance of  $K_{\text{minor}}$  lies in the convenience with which it can be used in conjunction with a rotor critical speed map to determine the onset of instability. By cross-plotting the minor stiffness of the bearing as a function of rotor speed, several critical speed curves may be crossed before the rotor design speed is reached. The threshold speed is obtained when the first critical speed corresponding to  $K_{\text{minor}}$ , divided by the critical whirl frequency ratio  $\gamma$ , gives the rotor speed at which the  $K_{\text{minor}}$  and  $\gamma$  were evaluated. The critical whirl frequency ratio is defined as the value of  $v/\omega$  at which  $B$  evaluated from Equation (19) goes to zero. In most instances, the critical frequency ratio is nearly 1/2, and since  $K_{\text{minor}}$  tends not to change very rapidly with rotor speed, this gives rise to the rule of thumb that the whirl threshold speed is approximately twice the first critical speed of the rotor bearing system. The critical whirl frequency ratio can be determined from Eq. (14).

The specific steps involved in determining threshold speed from a critical speed map are as follows:

- (1) Obtain a critical speed map of the rotor as a function of support stiffness.
- (2) Calculate the eight radial bearing coefficients over some specified speed range which one estimates will contain the whirl threshold speed.
- (3) Compute the  $K_{\text{minor}}$  and  $\gamma$  values from Eqs. (18) or (22) and (14), for various shaft speeds.

- (4) For each of the  $K_{\text{minor}}$  values, enter the critical speed map at each value and obtain the first natural frequency or critical speed.
- (5) For each shaft speed selected divide the critical speed by the computed whirl frequency ratio. When the resulting speed, which we shall refer to as apparent threshold speed, equals the shaft speed at which the  $K_{\text{minor}}$  value was evaluated, then the actual threshold speed has been determined.

For incompressible lubricated bearings the stiffness and damping coefficients are independent of the whirl frequency ratio, whereas the compressible lubricated bearing coefficients must be obtained at the critical whirl frequency ratio. In general these gas bearing coefficients may be obtained at  $v/\omega = 0.50$  with sufficient accuracy since the critical whirl frequency ratio is usually close to this value.

It should be noted that use of a critical speed map together with values of  $K_{\text{minor}}$  to determine the stability threshold is valid for rotors of arbitrary shape and flexibility but does rely upon the bearings supporting the rotor being quite similar, since the critical speed map is plotted in terms of only one value of bearing stiffness. However, if the bearings supporting the rotor are not too dissimilar, the present approach will serve to indicate at least approximately the critical speed and critical speed ratio by using values of  $K_{\text{minor}}$  for any one of the bearings. A more exact value for critical speed can then be determined by using the computer program developed for calculating rotor bearing stability.

An example calculation of how to determine whirl threshold speed from a critical speed map is given in the next section.

### SECTION III

#### EFFECT OF THRUST BEARING STIFFNESS AND DAMPING ON ROTOR-BEARING STABILITY

##### 1. Discussion

Since a thrust bearing exhibits no radial stiffness or radial damping properties, the threshold speed of a rotor which whirls in the lateral or radial mode will not be affected. However, if the rotor motion is angular or conical, considerable restraint can be imposed on the rotor by the angular thrust bearing properties. Thus, if the lowest critical speed of the rotor is conical, the threshold speed of the rotor could be significantly influenced by the addition of the thrust bearing coefficients. The computer program described in Appendix I of this report allows for the inclusion of these thrust bearing coefficients. In this present section we will consider some simplified relations which enable us to estimate the effects of thrust bearing stiffness on the conical stability of a symmetric rotor.

First let us define the axes about which the rotor undergoes angular displacement while whirling in a conical mode. Consider Fig. 4. The two coordinates which serve to define the angular displacement of each thrust bearing are the  $\theta$  coordinate, which measures rotation about the  $y$  axis and the  $\varphi$  coordinate which measures rotation about the  $x$  axis. Both of these coordinates are shown about point 0 at the center of the rotor bearing system. These angular rotations are defined by  $\tan \theta = dx/dz^*$  and  $\tan \varphi = dy/dz^*$ . The equations defining the angular dynamic coefficients are:

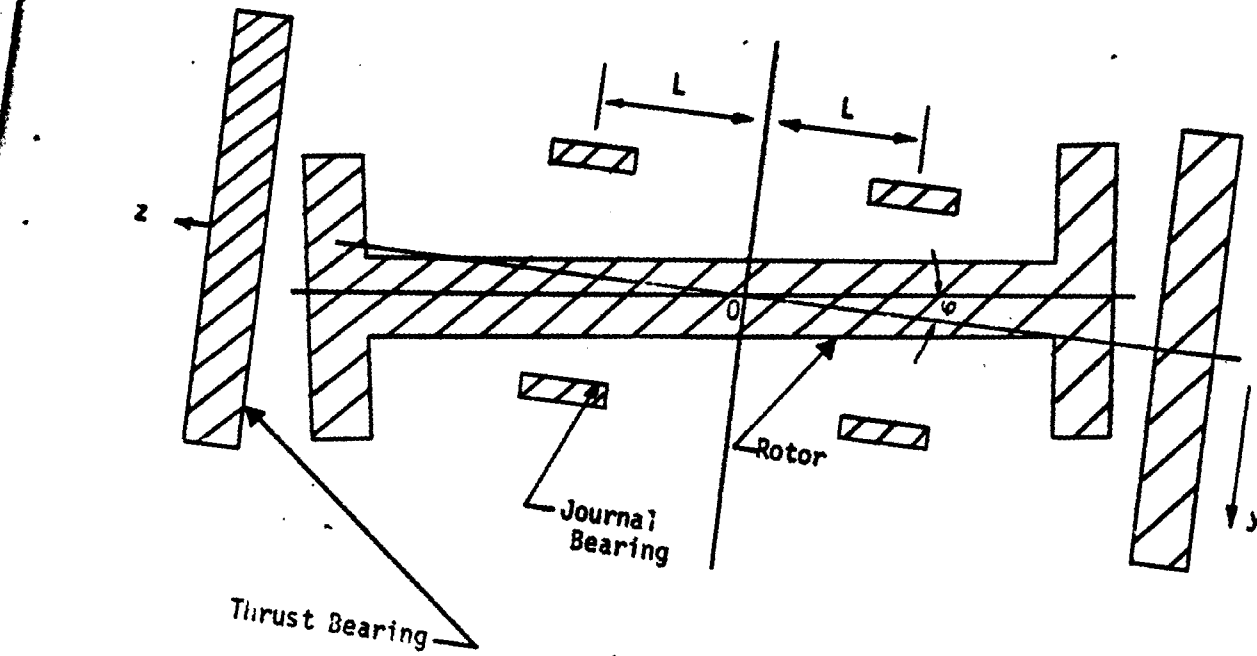
$$M_x = -G_{xx} \theta - D_{xx} \frac{d\theta}{dt} - G_{xy} \varphi - D_{xy} \frac{d\varphi}{dt} \quad (23)$$

$$M_y = -G_{xy} \theta - D_{yx} \frac{d\theta}{dt} - G_{yy} \varphi - D_{yy} \frac{d\varphi}{dt} \quad (24)$$

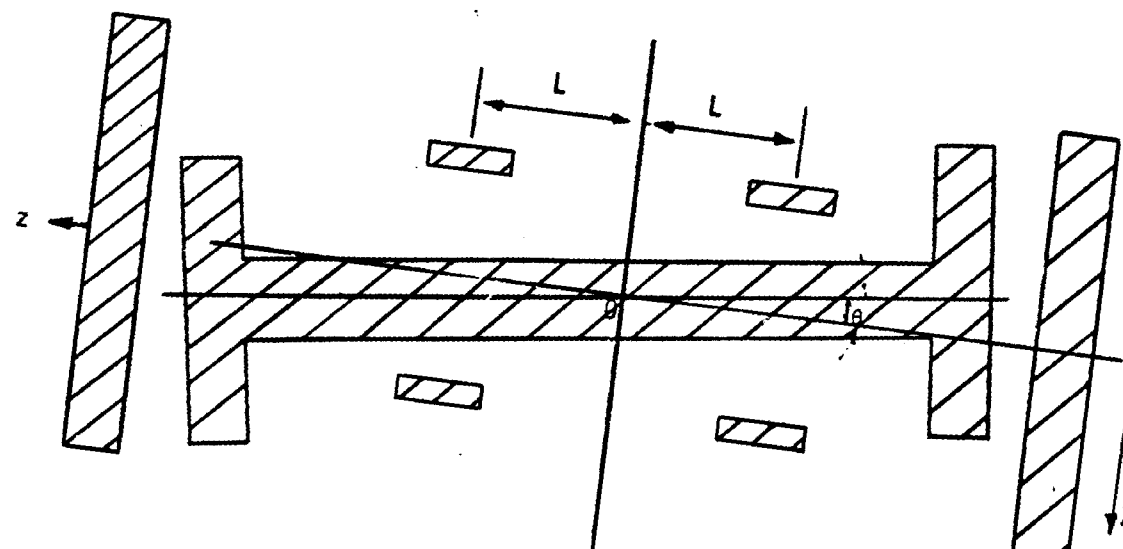
where  $M_x$  and  $M_y$  are the dynamic moments acting on the rotor resulting from the angular displacements and velocities  $\theta, \varphi, d\theta/dt$  and  $d\varphi/dt$ .  $M_x$  is in the  $x-z$  plane while  $M_y$  is in the  $y-z$  plane.

-----

\*For a flexible rotor, local values of  $dx/dz$  and  $dy/dz$  serve to define the angular rotations  $\theta$  and  $\varphi$  at local points along the rotor.



TOP VIEW



SIDE VIEW

Fig. 4 Coordinate Axis System

The computer program written to analyze rotor-bearing stability accepts the eight angular stiffness and damping coefficients  $G_{xx}$ ,  $\omega D_{xx}$ ,  $G_{xy}$ , etc., directly as bearing input data along with the translatory coefficients  $K_{xx}$ ,  $\omega B_{xx}$ ,  $K_{xy}$ , etc. However, in order to gain an estimate of the effect of thrust bearing angular stiffness on rotor-bearing stability, it is convenient to try to use the critical speed map approach for determining whirl-instability that was described earlier in the report. To use this approach, it is necessary to relate the thrust bearing angular coefficients to effective translatory stiffness and damping coefficients of the journal bearings supporting the rotor. For a symmetrical rotor-bearing system this can be accomplished by the following geometrical considerations. Referring to Fig. 4 we see that the restoring moment  $(M_x)_j$  in the x-z plane exerted by each journal bearing in response to a static angular displacement  $\theta$  about an axis through the point 0 parallel to the  $\theta$  axis is

$$(M_x)_j = -K_{xx} L^2 \theta \quad (25)$$

Similarly, the restoring moment  $(M_y)_j$ , due to each journal bearing is

$$(M_y)_j = -K_{yx} L^2 \theta \quad (26)$$

On the other hand, the restoring moments  $(M_x)_T$  and  $(M_y)_T$  exerted by each thrust bearing due to the angular displacement  $\theta$  are given by Eqs. (23) and (24), i.e.,

$$(M_x)_T = -G_{xx} \theta \quad (27)$$

$$(M_y)_T = -G_{yx} \theta \quad (28)$$

Therefore, we see that for angular displacement in this symmetrical system, the restoring moments of thrust bearings can be represented simply by adding the "effective" stiffness coefficients  $G_{xx}/L^2$  and  $G_{yx}/L^2$  respectively to the existing coefficients  $K_{xx}$  and  $K_{yx}$  of the journal bearings. This applies as well to all of the stiffness and damping coefficients. This, for angular displacements about axes through the point 0, the restoring moments can be determined by assuming that each journal bearing has effective stiffness and damping coefficients  $(K_{xx})_e$ ,

$(B_{xx})_e$ ,  $(K_{xy})_e$ , etc., given by

$$(K_{xx})_e = K_{xx} + G_{xx}/L^2$$

$$(K_{xy})_e = K_{xy} + G_{xy}/L^2$$

$$(K_{yx})_e = K_{yx} + G_{yx}/L^2$$

$$(K_{yy})_e = K_{yy} + G_{yy}/L^2$$

$$(B_{xx})_e = B_{xx} + D_{xx}/L^2$$

$$(B_{xy})_e = B_{xy} + D_{xy}/L^2$$

$$(B_{yx})_e = B_{yx} + D_{yx}/L^2$$

$$(B_{yy})_e = B_{yy} + D_{yy}/L^2$$

(29)

The approach of taking account of thrust bearing effects on conical motions of symmetrical systems by means of adding effective stiffness and damping to existing journal bearings permits one to use the critical speed map method for estimating whirl instability as described in the previous section. This would be accomplished by using the total effective values of stiffness for conical motion of the rotor, as defined in Eqs. (29) to evaluate  $K_{\text{minor}}$  and overall damping  $B$  as defined by Eqs. (18), (19) and (20). Note that this procedure is valid for conical whirl instability only. Thrust bearings would have no effect on the translatory whirl mode and their angular coefficients should not be included in the evaluation of  $K_{\text{minor}}$  and  $B$  if this mode of instability is being determined.

Some sample calculations were performed by the critical speed map method to examine the effect of independently adding principal angular stiffness,  $G_{xx}$  and  $G_{yy}$  and principal angular damping  $D_{xx}$  and  $D_{yy}$  on the conical stability of a symmetrical rotor. The conclusions reached were that:

- (1) Addition of principal angular stiffnesses  $G_{xx}$  and  $G_{yy}$  does not change the critical value of frequency ratio  $\gamma_c$  for instability but can increase the threshold speed  $\omega_c$  for instability by increasing the natural frequency of the conical mode.
- (2) Addition of principal angular damping,  $D_{xx}$  and  $D_{yy}$ , does not change the natural frequency of the rotor-bearing system, but does decrease the critical frequency ratio for instability (i.e., the frequency ratio at which damping B goes to zero) thereby increasing the threshold speed  $\omega_c$  at which instability occurs.

In the sub-section below are discussed various specific design examples for which the effect of thrust bearings on rotor-bearing stability are investigated.

## 2. Sample Calculations

The basic tool used in computing the threshold speed is computer program PN400. With this program it was possible to obtain the threshold speeds exactly with and without the thrust bearing effects. However, since much time searching for threshold speeds is generally required when using this program alone, the shorter critical speed map technique for locating threshold speeds, outlined in this report, was first used to obtain an approximate value of threshold speed with an exact solution being then obtained using the computer program.

Two rotors will be analyzed to determine their threshold speeds with and without the addition of a thrust bearing system. These two rotor models are shown in Figures 5 and 6.

The first rotor, Figure 5, weighs approximately 7.2 lbs. and is supported by two gas-lubricated hydrodynamic journal bearings. The load is identical on each bearing. Air at 100°F and ambient pressure (14.7 psia) is supplied to each bearing. Thrust bearing surfaces are available at either end of the rotor.

The second rotor, Figure 6, weighs approximately 18.75 lbs. and is supported by

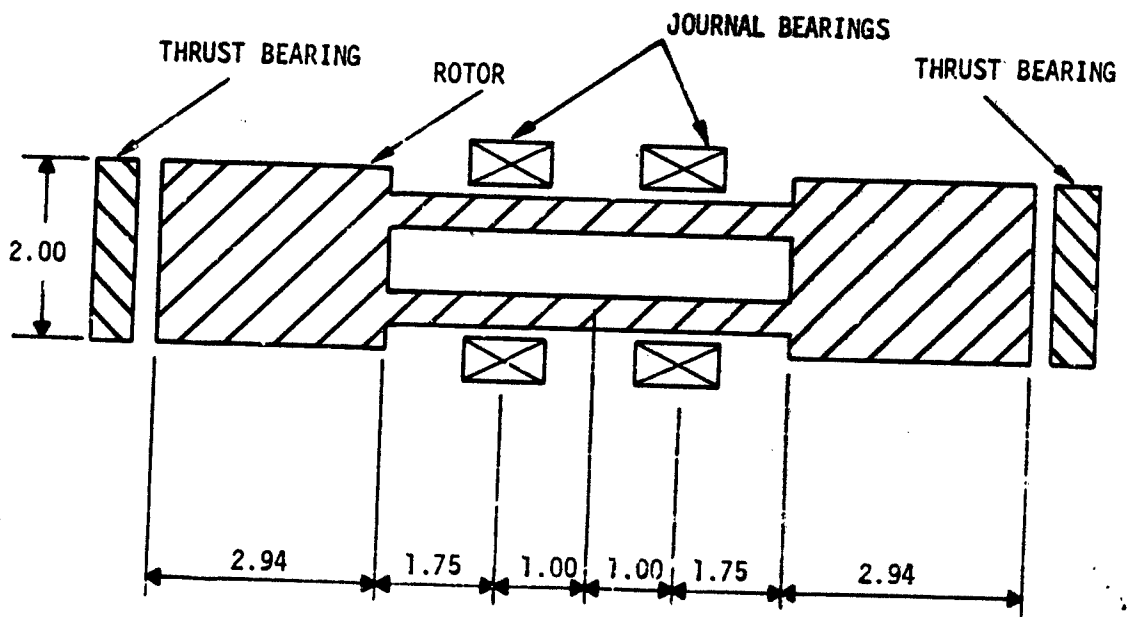
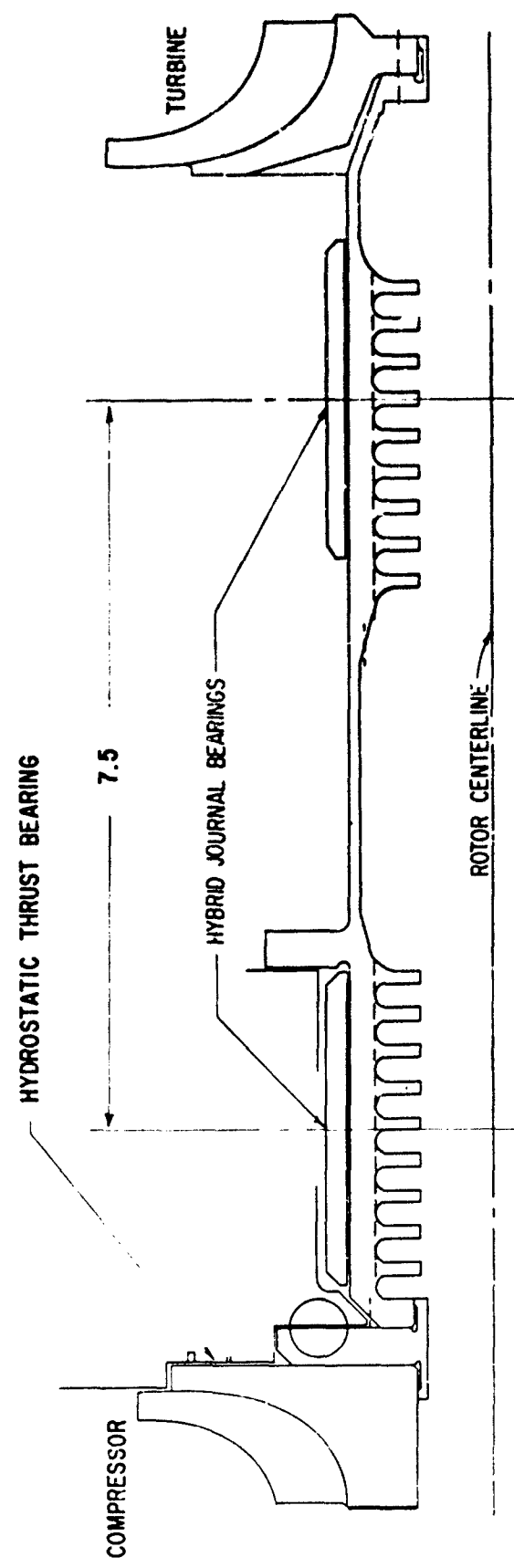


Fig. 5 Conical Instability Rotor Model 1



WTI-9052

Fig. 6 Conical Instability Rotor Model 2

two gas-lubricated hybrid journal bearings. The loads are different for each bearing. A thrust bearing is shown at the left hand end of the rotor. This particular model was designed as a high pressure (HP) spool for an actual high temperature turbo-compressor but the design was rejected based on its threshold speed. No consideration was given to the thrust bearing effects on the rotors' stability behavior. In this example the thrust bearing effects will be computed.

Tables I and III list the nondimensional dynamic coefficients for the hydrodynamic and hybrid gas-lubricated journal bearing designs respectively. Table I lists the eight stiffness and damping coefficients as a function of eccentricity (or load), bearing number  $\Lambda$  and whirl frequency ratio  $v/\omega$  for a length-to-diameter ratio of 1.00. For a constant load on a bearing ( $W$  constant) and varying speed the coefficients must be obtained by double interpolation on  $\Lambda$  and load in Table I since  $\Lambda$  changes with speed. Although data are shown for  $v/\omega = 0.3, 0.5$  and 1.00, only the  $v/\omega = 0.5$  data was used in the first example.

The data for rotor No. 1 are given below

Rotor Model #1

Journal Bearing Design (Hydrodynamic)

D = 1.50 in.  
L = 1.50 in.  
C/R = .001 in/in.  
 $P_a$  = 14.7 psia  
W = 3.62 lbs. (each bearing)  
 $\mu$  =  $2.7 \times 10^{-9}$  lb.sec/in<sup>2</sup> (air at 100°F)

Thrust Bearing Design (Hydrostatic)

$R_o$  = 1.00 in.  
 $R_i$  = 0.333 in.  
 $P_a$  = 14.7 psia  
 $P_s$  = 73.5  
C = .0011 in.

Inherent compensation

$\Lambda_s$  = 1.0

**TABLE I**  
**PLAIN CYLINDRICAL BEARING**  
**COMPRESSIBLE DATA**

L/D = 1

$\nu/\omega$	$\Lambda$	$\epsilon_B \cos \phi_B$	$\epsilon_B$	$\phi_B$	$\bar{w}$	$\bar{K}_{xx}$	$\bar{K}_{xy}$	$\bar{K}_{yx}$	$\bar{K}_{yy}$	$\bar{B}_{xx}$	$\bar{B}_{xy}$	$\bar{B}_{yx}$	$\bar{B}_{yy}$
0.3	0.50	.075	.375	78.5	.052	1.54	3.49 -	3.10	1.78	4.98 -	1.30	3.30	8.50
	.10	.43	76.5	.063	1.55	3.30 -	2.50	1.90	4.30 -	1.10	3.30	7.60	
	.15	.51	73.0	.090	1.53	3.20 -	1.03	2.10	3.50 -	1.00	3.28	6.26	
	.20	.57	69.4	.110	1.69	3.22 -	1.16	2.32	3.16 -	.86	3.38	5.47	
1.00	.075	.27	73.8	.067	2.27	3.85 -	3.90	2.56	5.87 -	3.37	5.30	8.70	
	.10	.32	71.7	.083	2.10	3.40 -	3.00	2.50	4.80 -	2.83	4.70	7.00	
	.15	.40	68.0	.12	1.94	2.96 -	1.90	2.42	3.72 -	2.24	3.98	5.11	
	.20	.46	64.3	.15	2.00	2.78 -	1.27	2.48	3.17 -	1.90	3.64	4.02	
1.60		.006	.007	123.	43.0	-140.	140.	-207.	-117.	267.	7.17		
	.011	.014	61.6	21.4	-70.	70.6	-104.	-	56.6	132.	3.40		
	.028	.035	25.0	8.54	-27.5	28.4	-41.4	-	23.5	51.6	1.15		
	.055	.072	12.8	4.26	-13.4	14.3	-20.6	-	11.8	24.7	.41		
1.80		.006	.007	127.	40.8	-144.	145.	-222.	-110.	268.	5.44		
	.011	.014	63.7	20.4	-71.8	72.7	-111.	-	55.0	133.	2.56		
	.027	.036	25.8	8.14	-28.2	29.2	-44.0	-	22.0	51.8	.839		
	.055	.072	13.2	4.05	-13.7	14.7	-22.0	-	11.1	24.8	.280		
2.00		.075	.18	65.4	.080	3.70	4.20 -	5.00	4.00	5.30 -	7.20	9.00	8.30
	.10	.22	63.6	.10	3.20	3.50 -	3.60	3.40	4.20 -	5.70	7.00	6.10	
	.15	.30	60.0	.15	2.63	2.76 -	2.20	2.88	3.11 -	4.10	5.00	3.82	
	.20	.36	56.5	.19	2.46	2.41 -	1.43	2.67	2.51 -	3.27	4.00	2.65	

TABLE I (Continued)  
PLAIN CYLINDRICAL BEARING  
COMPRESSIBLE DATA  
L/D = 1

$v/w$	$\Lambda$	$\epsilon_B \cos \phi_B$	$\epsilon_B$	$\phi_B$	$\bar{w}$	$\bar{K}_{xx}$	$\bar{K}_{xy}$	$\bar{K}_{yy}$	$\bar{B}_{xx}$	$\bar{B}_{xy}$	$\bar{B}_{yx}$	$\bar{B}_{yy}$	
0.3	.00	.005	.009	.55.0	.007	67.2	57.1	- 98.0	77.5	7.50	-155.	218.	
	.01	.017	.54.8	.014	.34.0	28.7	- 48.6	39.0	3.88	- 78.0	109.	46.0	
	.025	.043	.54.1	.034	14.3	11.7	- 19.1	16.0	1.71	- 31.7	42.8	17.9	
	.05	.083	.52.9	.067	7.70	5.10	- 9.30	8.40	1.00	- 1.61	20.8	8.44	
	.075	.12	.52.3	.088	5.60	4.00	- 6.00	5.80	7.00	- 11.0	13.2	5.70	
	.10	.16	.51.0	.12	4.50	3.20	- 4.30	4.50	6.10	- 8.40	9.60	4.00	
	.15	.22	.48.0	.18	3.47	2.39	- 2.57	3.46	6.36	- 5.70	6.13	2.22	
	.20	.284	.45.2	.236	3.03	1.95	- 1.69	2.96	0.55	- 4.40	4.30	1.40	
6.00	.005	.007	.45.7	.007	84.5	55.2	-109.	98.4	-56.7	-163.	251.	57.4	
	.01	.014	.45.5	.014	42.7	27.7	- 54.2	49.4	-28.3	- 82.0	124.	28.3	
	.025	.035	.44.9	.034	17.6	11.2	- 21.3	20.0	-11.2	- 33.0	48.7	10.8	
	.05	.069	.43.8	.068	9.33	5.70	- 10.3	10.3	- 5.50	- 16.8	23.4	4.97	
	.075	.10	.43.7	.09	6.60	3.70	- 6.70	6.90	- 3.70	- 11.7	14.6	3.70	
	.10	.14	.42.5	.12	5.30	2.90	- 4.80	5.30	- 2.70	- 8.90	10.5	2.50	
	.15	.196	.40.0	.190	3.90	2.11	- 2.90	3.84	- 1.57	- 5.90	6.57	1.30	
	.20	.253	.37.7	.256	3.30	1.67	- 1.94	3.10	- 1.12	- 4.50	4.48	0.79	
	.50	.50	.005	.058	85.0	.008	4.80	16.4	- 22.6	5.57	33.1	- 8.45	11.4
	.010	.10	.84.5	.014	3.06	9.34	- 12.4	3.45	18.3	- 4.64	6.65	26.2	
	.025	.20	.82.9	.028	2.03	5.13	- 6.06	2.35	9.32	- 2.38	3.91	13.8	
	.050	.30	.80.6	.046	1.71	3.77	- 3.66	2.17	6.06	- 1.61	3.14	9.56	

**TABLE I (Continued)**  
**PLAIN CYLINDRICAL BEARING**  
**COMPRESSIBLE DATA**

<u>L/D = 1</u>													
v/w	A	$\epsilon_B \cos \phi_B$	$\epsilon_B$	$\phi_B$	$\bar{w}$	$\bar{k}_{xx}$	$\bar{k}_{xy}$	$\bar{k}_{yy}$	$\bar{B}_{xx}$	$\bar{B}_{xy}$	$\bar{B}_{yy}$		
.50	.50	.075	.375	.78.5	.052	1.77	3.41	-2.77	2.30	4.89	-1.28	3.10	8.30
	.10	.43	.76.5	.063	1.75	3.20	-2.20	2.40	4.20	-1.10	3.00	7.30	
	.15	.51	.73.0	.090	1.71	3.12	-1.25	2.55	3.45	-0.97	3.00	6.00	
	.20	.57	.69.4	.110	1.87	3.16	-0.69	2.75	3.10	-0.82	3.07	5.22	
.67	.005	.04	.83.0	.007	8.16	21.8	-30.4	9.86	44.2	-15.2	20.0	62.9	
	.01	.078	.82.6	.014	4.74	11.8	-15.9	5.57	23.4	-8.05	10.9	33.4	
	.025	.16	.81.2	.03	2.75	5.87	-7.19	3.21	11.0	-3.82	5.57	15.9	
	.05	.26	.78.9	.05	2.12	3.99	-4.08	2.63	6.75	-2.43	3.98	10.1	
	.075	.33	.76.8	.067	1.94	3.40	-2.89	2.55	5.24	-1.15	3.52	8.03	
1.00	.005	.027	.79.3	.007	16.2	29.7	-42.5	20.4	60.4	-31.5	40.8	87.7	
	.01	.052	.79.0	.014	8.76	15.4	-21.5	10.8	31.0	-16.2	21.0	45.0	
	.025	.12	.77.8	.03	4.36	7.00	-9.00	5.20	13.5	-7.10	9.43	19.4	
	.050	.20	.75.8	.056	2.96	4.39	-4.70	3.59	7.68	-4.13	5.74	11.0	
	.075	.27	.73.8	.067	2.66	3.48	-3.20	3.23	5.70	-3.10	4.70	8.4	
	.10	.32	.71.7	.083	2.47	3.10	-2.40	3.00	4.70	-2.6	4.00	6.8	
	.15	.40	.68.0	.12	2.20	2.70	-1.32	2.83	3.62	-2.06	3.38	4.89	
	.20	.46	.64.3	.15	2.22	2.56	-0.72	3.80	3.07	-1.74	3.03	3.87	
1.60	.006				.007	48.8	9.34	-26.7	146.	35.0	-96.0	286.	62.4
	.011				.014	24.9	4.64	-13.3	73.0	17.3	-47.8	142.	34.6
	.028				.035	10.5	1.82	-5.24	29.3	6.73	-19.0	56.0	13.8

**TABLE I (Continued)**  
**PLAIN CYLINDRICAL BEARING**  
**COMPRESSIBLE DATA**  
**L/D = 1**

$\nu/\omega$	$\Lambda$	$\epsilon_B \cos \phi_B$	$\epsilon_B$	$\phi_B$	$\bar{w}$	$\bar{k}_{xx}$	$\bar{k}_{xy}$	$\bar{k}_{yx}$	$\bar{k}_{yy}$	$\bar{B}_{xx}$	$\bar{B}_{xy}$	$\bar{B}_{yx}$	$\bar{B}_{yy}$
.50	1.60		.055		.072	5.76	0.89	- 2.50	14.8	3.20	- 9.40	27.2	6.80
2.00	.005	.014	69.4	.007	38.6	35.8	- 5.70	52.0	74.4	- 76.5	103.	119.	
.01	.028	69.2	.013	20.0	18.2	- 28.4	26.4	37.5	- 38.7	51.8	59.5		
.025	.068	68.3	.033	8.75	7.69	- 11.2	11.1	15.4	- 16.0	21.0	24.0		
.05	.13	66.7	.063	5.10	4.24	- 5.49	6.20	8.00	- 8.47	10.7	12.2		
.075	.18	65.4	.08	4.00	3.10	- 3.60	4.70	5.50	- 5.90	7.30	8.40		
.10	.22	63.6	.10	3.50	2.60	- 2.50	3.90	4.30	- 4.70	5.70	6.46		
.15	.30	60.0	.15	2.84	2.10	- 1.37	3.16	3.17	- 3.37	3.95	4.10		
.20	.36	56.5	.19	2.66	1.88	- .76	2.82	2.54	- 2.70	3.08	3.00		
4.00	.005	.009	55.0	.007	56.7	26.7	- 54.0	69.0	59.4	- 113.	175.	116.	
.01	.017	54.9	.013	29.0	13.5	- 27.0	44.7	30.0	- 56.6	87.4	57.8		
.025	.043	54.1	.034	12.2	5.52	- 10.6.	18.2	11.8	- 23.0	34.0	23.0		
.05	.083	52.9	.067	6.72	2.90	- 5.14	9.40	5.90	- 11.7	16.9	11.4		
.075	.12	52.3	.088	5.00	1.90	- 3.40	6.50	3.70	- 7.90	10.7	8.00		
.10	.16	51.0	.12	4.10	1.50	- 2.40	5.00	2.80	- 6.00	7.90	5.90		
.15	.22	48.0	.18	3.22	1.25	- 1.35	3.67	2.06	- 4.14	5.02	3.62		
.20	.284	45.2	.236	2.87	1.10	- .83	3.00	1.55	- 3.17	3.56	2.59		
6.00	.005	.007	45.7	.007	59.4	19.5	- 47.0	108.	47.6	- 118.	212.	104.	
.01	.014	45.5	.014	30.0	9.80	- 23.5	54.0	23.7	- 59.0	105.	52.0		
.025	.035	44.9	.034	12.7	3.96	- 9.30	21.8	9.33	- 23.7	41.5	20.7		

**TABLE I. (Continued)**  
**PLAIN CYLINDRICAL BEARING**  
**COMPRESSIBLE DATA**

L/D = 1

$\nu/\omega$	$\Lambda$	$\epsilon_B \cos \phi_B$	$\epsilon_B$	$\phi_B$	$\bar{w}$	$\bar{K}_{xx}$	$\bar{K}_{xy}$	$\bar{K}_{yx}$	$\bar{K}_{yy}$	$\bar{B}_{xx}$	$\bar{B}_{xy}$	$\bar{B}_{yx}$	$\bar{B}_{yy}$
.50	6.00	.05	.069	43.8	.068	6.90	2.00	-4.50	11.0	4.60	-12.0	20.0	10.2
	.075	.10	43.7	.09	5.10	1.20	-3.20	7.50	2.50	-8.00	12.8	7.50	
	.10	.14	42.5	.12	4.20	.93	-2.30	5.80	1.90	-6.00	9.30	5.50	
	.15	.20	40.0	.19	3.20	.82	-1.24	4.07	1.50	-4.10	5.84	3.33	
	.20	.25	37.7	.26	2.80	.69	-.80	3.24	1.07	-3.07	4.10	2.40	
1.00	0.50	.15	.51	73.0	.090	2.47	2.83	-.03	4.26	3.19	-.84	2.10	5.10
	.20	.57	69.4	.11	2.60	2.91	.59	4.28	2.82	-.70	2.04	4.34	
	.90	.005	.03	80.4	.007	27.2	17.7	-26.6	40.2	51.1	-19.8	26.1	71.0
	.01	.058	80.0	.014	14.5	9.34	-13.4	21.0	26.4	-10.3	13.4	36.6	
	.025	.13	78.8	.031	7.01	4.42	-5.37	9.90	11.6	-4.63	5.96	16.1	
	.05	.22	76.7	.054	4.58	2.86	-2.49	6.45	6.68	-2.76	3.53	9.22	
	.075	.28	74.6	.075	3.80	2.38	-1.39	5.39	5.00	-2.10	2.72	6.84	
1.00	.15	.40	68.0	.12	3.25	1.87	.069	4.37	3.13	-1.43	1.80	4.05	
	.20	.46	64.3	.15	3.15	1.86	.54	4.00	2.61	-1.19	1.52	3.23	
2.00	.15	.30	60.0	.15	4.00	.69	.15	4.88	2.77	-1.53	1.68	3.44	
	.20	.36	56.5	.13	3.59	.75	.39	4.10	2.16	-1.20	1.25	2.63	
4.00	.15	.22	48.0	.18	4.69	-.05	.48	5.72	2.48	-1.00	1.50	2.64	
	.20	.284	45.2	.236	3.94	.089	.489	4.54	1.82	-.77	1.08	1.97	
6.00	.15	.196	40.0	.19	5.2	-.17	.63	6.10	2.30	-.70	1.24	2.10	
	.20	.250	37.7	.256	4.24	-.03	.55	4.70	1.65	-.52	.88	1.55	

**TABLE II**  
**HYBRID BEARING DATA**  
 $L/D = 1.08, \nu/\omega = 0.50$

$P_s/P_a$	$\Lambda_s$	$\Lambda$	$\epsilon$	$\bar{W}$	$\bar{K}_{xx}$	$\bar{K}_{xy}$	$\bar{K}_{yy}$	$\bar{\omega}_B_{xx}$	$\bar{\omega}_B_{xy}$	$\bar{\omega}_B_{yx}$	$\bar{\omega}_B_{yy}$
4.0	1.00	0.50	.01	.018	1.81	.0756	-.0756	1.81	.152	-.014	.014
			.02	.036	1.181	.0756	-.0757	1.81	.152	-.014	.014
			.04	.0725	1.82	.0757	-.0757	1.815	.152	-.014	.014
			.06	.109	1.83	.0757	-.0758	1.818	.152	-.014	.014
			.08	.145	1.84	.0758	-.076	1.822	.152	-.014	.014
1.00	1.00	.01	.018	1.83	.148	-.147	1.83	.296	-.054	.054	.294
		.02	.0365	1.84	.148	-.148	1.83	.296	-.054	.054	.296
		.04	.073	1.84	.148	-.148	1.84	.296	-.054	.054	.296
		.06	.110	1.848	.148	-.148	1.838	.296	-.054	.054	.296
		.08	.147	1.860	.148	-.148	1.84	.296	-.054	.054	.296
1.00	3.0	.01	.0197	2.00	.35	-.35	2.00	.70	-.386	.386	.70
		.02	.0394	2.00	.35	-.35	2.00	.70	-.386	.386	.70
		.04	.0789	2.00	.35	-.35	2.00	.70	-.386	.386	.70
		.06	.1185	2.02	.351	-.352	2.00	.704	-.388	.386	.70
		.08	.158	2.03	.351	-.353	2.00	.704	-.388	.386	.702
1.00	5.00	.01	.022	2.186	.414	-.414	2.18	.828	-.758	.758	.828
		.02	.0438	2.187	.414	-.414	2.186	.828	-.758	.758	.828
		.04	.0876	2.193	.414	-.414	2.188	.828	-.758	.758	.828
		.06	.132	2.20	.414	-.415	2.19	.830	-.760	.758	.828
		.08	.176	2.22	.414	-.416	2.196	.832	-.762	.758	.828

**Dimensionless Operating Parameters for Journal Bearings:**

$$\Lambda = \frac{12\pi N}{P_a} \left(\frac{R_o}{C}\right)^2$$

$$= \frac{12\pi(2.7 \times 10^{-9})(N)}{14.7 (.001)^2}$$

$$= 6.95 \times 10^{-3} (N) \text{ where } N = \text{speed, rps}$$

$$= 1.16 \times 10^{-4} (N') \text{ where } N' = \text{speed, rpm}$$

$$\bar{W} = \frac{W}{P_a L D}$$

$$= \frac{3.62}{(14.7)(1.5)(1.5)}$$

$$= 0.11$$

Values of journal bearing stiffness and damping coefficients were obtained from Table I for various pertinent values of  $\Lambda$  at  $v/w = 0.5$  for  $\bar{W} = 0.11$ . Corresponding to these values of journal bearing coefficients, values of  $K_{\text{minor}}$  were calculated for the journal bearings from Eq. (22) neglecting thrust bearing effects.

The critical speed map for rotor #1 is given in Figure 7. This figure shows the first two critical speed curves as a function of support stiffness. Also shown is a curve of the minor stiffness for the bearings calculated in the manner described above.

Whirl threshold speed is obtained from Figure 7 in the following way. First, if we draw an appropriate vertical line on Fig. 7 it will intersect both the first critical speed curve and the curve of  $K_{\text{minor}}$  vs. speed. Let us denote the values of speed at these intersections as  $v_c$  and  $\omega_T$  respectively. Now, corresponding to

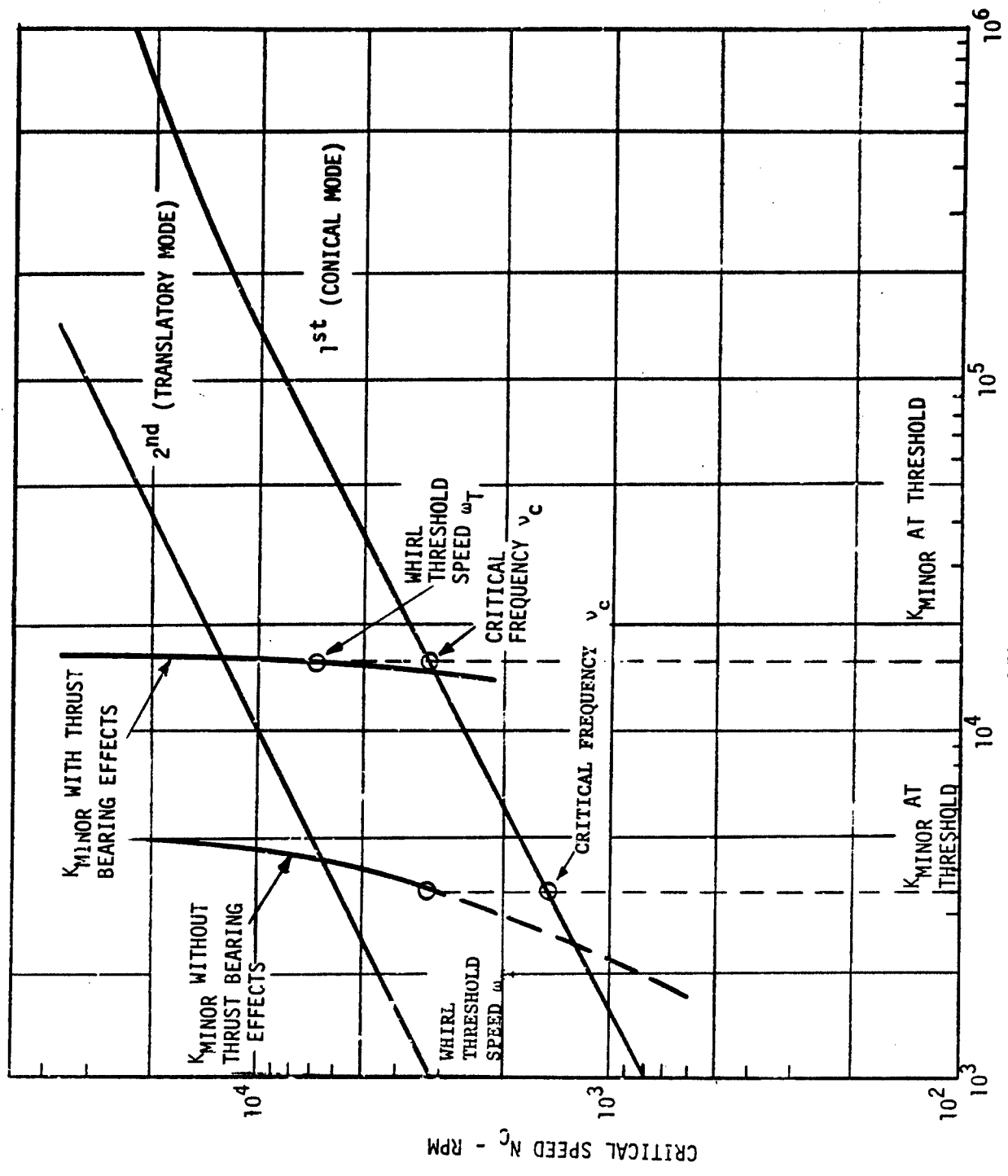


Fig. 7 Critical Speed Map of Rotor 1

these values of  $v_c$ , the natural frequency of oscillation and  $\omega_T$ , the rotor speed at which  $K_{\text{minor}}$  is calculated, there will be some value of whirl frequency ratio  $\gamma = v/\omega$  calculable from Eq. (14). If this calculated value of  $\gamma$  is exactly equal to  $v_c/\omega_T$ , then we have determined the whirl threshold condition and  $\omega_T$  will be our whirl threshold speed while  $v_c/\omega_T$  will be our whirl frequency ratio. If, say,  $v_c/\omega_T$  should prove to be less than our calculated value of  $\gamma$ , then we must try drawing another vertical line slightly further to the right and redetermine  $v_c/\omega_T$ . If  $v_c/\omega_T$  is less than the value of  $\gamma$  calculated from Eq. (14) then our new vertical line should be drawn slightly further to the left. Usually  $\gamma \approx 0.5$  so we would first try drawing a vertical line such that  $v_c/\omega_T = 0.5$ .

In the example shown, neglecting thrust bearing effects, the whirl threshold speed is found to be  $\omega_T = 3300$  rpm while the critical whirl frequency ratio is  $\gamma = v_c/\omega_T = 0.457$ .

It should be noted that in using this critical speed map approach, the curve of  $K_{\text{minor}}$  was calculated for the condition  $v/\omega = 0.5$  rather than for the condition  $v/\omega = 0.457$ . For greater accuracy, one could recalculate  $K_{\text{minor}}$  at the predicted critical whirl ratio of 0.457 and redetermine the whirl threshold. Usually, however, this would result in only a very small change in the value of threshold speed and is not necessary.

Next let us consider how we would determine the threshold speed of rotor No. 1 in a more precise manner using the computer program PN400. In using the program, we can take advantage of the fact that we have already determined the threshold speed in an approximate manner by the critical speed map approach as described above. Therefore, with the computer program, we look for the roots of the real and imaginary parts of Eq. (10) in the vicinity of  $\omega = 3300$  rpm and  $\gamma = 0.457$ .

The results obtained from the computer program are shown in Fig. 8. The straighter line represents the locus of roots of the imaginary part of Eq. (10), i.e., represents roots of Eq. (12), while the more curved line represents the locus of roots of the real part of Eq. (10), i.e., represents roots of Eq. (11). The intersection of these curves represents the condition at the threshold of whirl instability. As can be

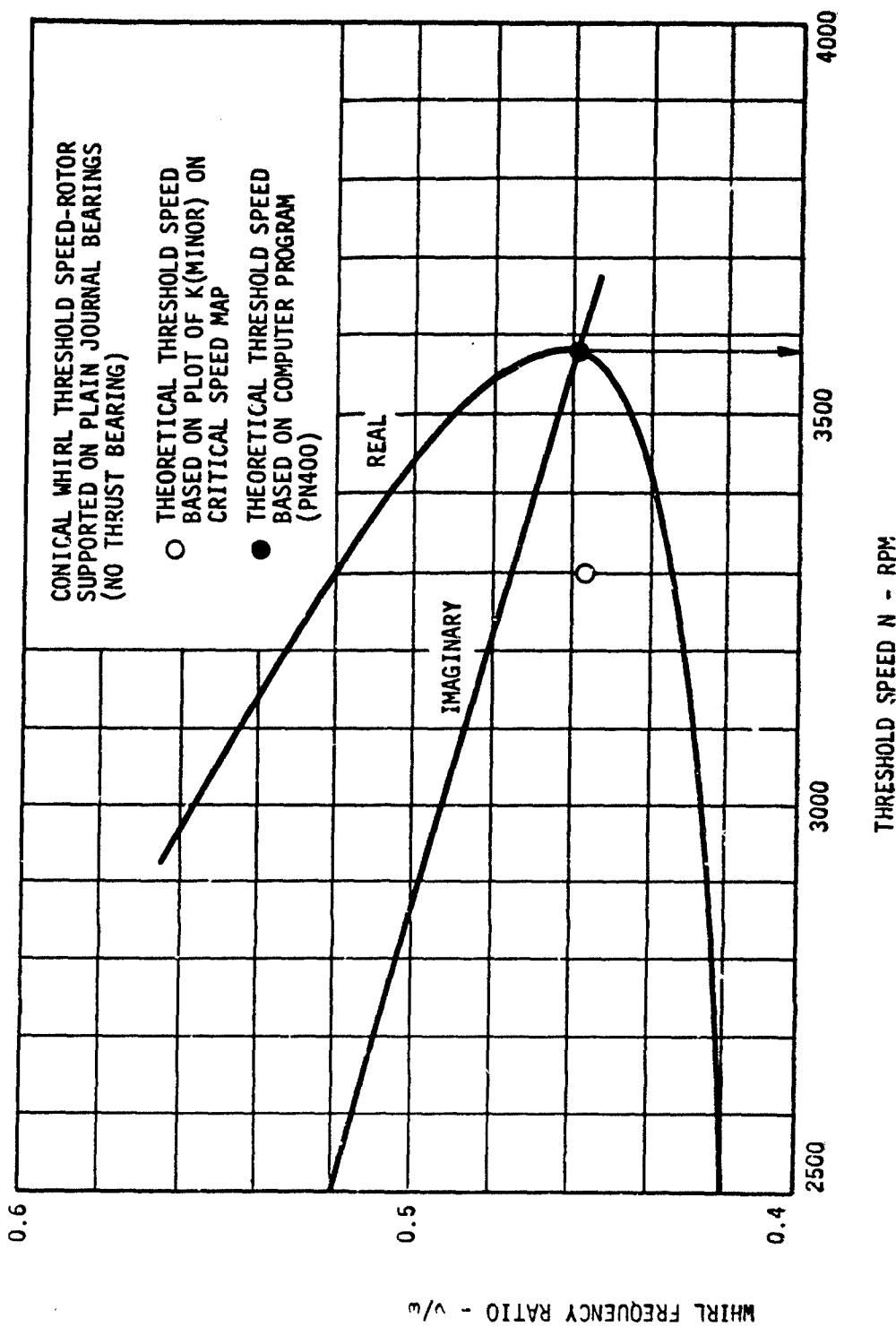


Fig. 8 Loci for Roots of Real and Imaginary Parts of Stability Determinant

seen, this occurs at a running speed of approximately 3570 rpm and at a frequency ratio of  $\gamma = 0.460$ .

For comparison, the whirl threshold solution obtained by the approximate critical speed map approach is also shown in Fig. 8. Agreement with the more precise computer solution is quite reasonable.

We can now proceed to investigate what change in the calculated value of whirl threshold speed for our example rotor No. 1 will result if we consider the thrust bearing angular stiffness and damping in our calculations. The thrust bearing for this rotor are hydrostatic with dimensions listed on page 25. In the case of hydrostatic thrust bearings, stiffness is the only bearing characteristic one usually needs consider in determining the influence of the thrust bearing on critical mode of whirl instability. This is so for the following reasons:

- (1) Damping, being the result of hydrodynamic forces rather than hydrostatic forces, is a very much weaker force in externally pressurized bearings than is the stiffness.
- (2) The "effective" angular damping in hydrostatic thrust bearings tends to zero at  $\gamma \approx 0.5$  much the same as does the effective radial damping in plain cylindrical journal bearings. Hence, for whirl frequency ratios near 0.5, hydrostatic thrust bearing damping will be quite ineffective in increasing the threshold speed for conical whirl instability.

To determine the effects of the hydrostatic thrust bearing stiffness on our calculated value of whirl threshold speed, we will first do a rough calculation using the critical speed map approach and then do a refined calculation using computer program PN400. Data for the angular stiffness of hydrostatic thrust bearings given in Figs. 13 through 16 in the next section as a function of the dimensionless parameter  $A_s$ . As discussed in the next section, this data is for static or steady state displacement of the bearing. However, in most cases this is applicable to dynamic displacement of the bearing if the frequency  $\nu$  of dynamic oscillation is low enough. To determine if steady state data is applicable, we

calculate the dimensionless squeeze number  $\sigma$

$$\sigma = \frac{12\mu v}{P_s} \frac{R_o R_i}{c^2}$$

$$= \frac{12(2.7 \times 10^{-9}) \nu (.333)}{14.7(.0011)^2}$$

$$= .605 \times 10^{-3} \nu$$

At

$$N_t = 3570 \text{ rpm}$$

$$\omega = 373 \text{ rad/sec}$$

$$\nu = (\nu/\omega)\omega$$

$$= 187 \text{ rad/sec}$$

Therefore

$$\sigma = .114$$

From Fig. 18, we see that squeeze number of  $\sigma = 0.114$  is sufficiently low such that steady state values for bearing stiffness apply (see discussion of Figs. 17 and 18 in the next section).

To determine the angular stiffness  $G$  from Fig. 16, we must determine the dimensionless feeding parameter  $\Lambda_s$ . Our approach is to set  $\Lambda_s$  at the value yielding maximum stiffness i.e.,  $\Lambda_s \approx 1.0$ . (This optimum value for  $\Lambda_s$  can be achieved for our bearing by the proper choice of  $na^2$  in  $\Lambda_s$ .) The maximum value of dimensionless angular stiffness  $\bar{G}$  is

$$\frac{1 + \delta^2}{1 + 2/3 \delta^2} \bar{G} \approx .12$$

Now, our bearing is inherently compensated, so  $\delta = a^2/cd$  is sufficiently large ( $d = 2a$  and  $c \ll a$ ) that the factor

$$\frac{(1 + \delta^2)}{(1 + 2/3 \delta^2)}$$

(See References 7 and 8)

as  $\delta \rightarrow \infty$  becomes approximately

$$\frac{\frac{1}{\delta^2} + 1}{\frac{\frac{1}{\delta^2} + \frac{2}{3}}{\delta^2}} = \frac{3}{2}$$

Solving for  $G$  from the expression given on Fig. 16 we have

$$G = \frac{\left[ \frac{(1 + \delta^2)}{1 + 2/3 \delta^2} \bar{G} \right] \pi (R_o^2 - R_i^2) R_o^2 (P_s - P_a)}{\frac{(1 + \delta^2)}{1 + 2/3 \delta^2} c}$$

$$= \frac{12 \pi [(1)^2 - (33)^2] (1)^2 (73.5 - 14.7)}{(3/2)(00110)}$$

$$= 1.15 \times 10^4 \text{ in-lb/radian}$$

As described earlier, this angular stiffness may be converted to an effective increase in journal bearing stiffness  $\Delta K_e$  which can be added to the existing journal bearing stiffness for purposes of determining whirl threshold speed

$$\Delta K_e = \frac{G}{L^2}$$

$$= \frac{1.15 \times 10^4}{(1)^2}$$

$$= 1.15 \times 10^4 \text{ lb/in.}$$

For a hydrostatic thrust bearing, the cross-coupling terms are zero and the stiffness in the two principal planes are identical. Since  $K_{\text{minor}}$  is increased directly by increases in  $K_{xx}$  and  $K_{yy}$ , the equivalent increase in stiffness  $\Delta K_e$  may be added directly to the  $K_{\text{minor}}$  obtained previously and the resultant curve for  $K_{\text{minor}}$  is plotted in Fig. 7. Using our graphical approach for determining whirl threshold speed, i.e.,  $v_c/\omega_T$  must equal  $\gamma$  calculated from Eq. (14), we find that the threshold speed with thrust bearings turns out to be at approximately 6900 rpm. Bearing stiffness and damping coefficients were therefore obtained for the hydrodynamic journal bearing at this value with  $\bar{W} = 0.11$  using the  $v/w = 0.50$  data. The journal bearing coefficients were then submitted along with the actual angular thrust bearing coefficients into the computer program. The results are shown plotted in Fig. 9 which yields a threshold speed of 7170 rpm at  $v/w = 0.477$ .

Rotor model No. 1 is an idealized model which serves as an example calculation of how thrust bearing stiffness may significantly improve the stability of the rotor to fractional frequency conical whirl instability, and how this improvement may be calculated. In rotor model No. 2 we have an example of an actual prospective design for a high temperature turbocompressor which was rejected on the basis of its poor stability characteristics. A simplified drawing of the rotor is shown in Fig. 6 and a brief description of the rotor was given earlier in this section. Due to the overhung nature of the design, the lowest mode of fractional frequency whirl instability was conical in nature. However, since the analytical tools were not available at the time this design was proposed, no account was taken of the effect of the thrust bearing in possibly enhancing the rotor stability. We shall examine the stabilizing influence of this thrust bearing in what follows below.

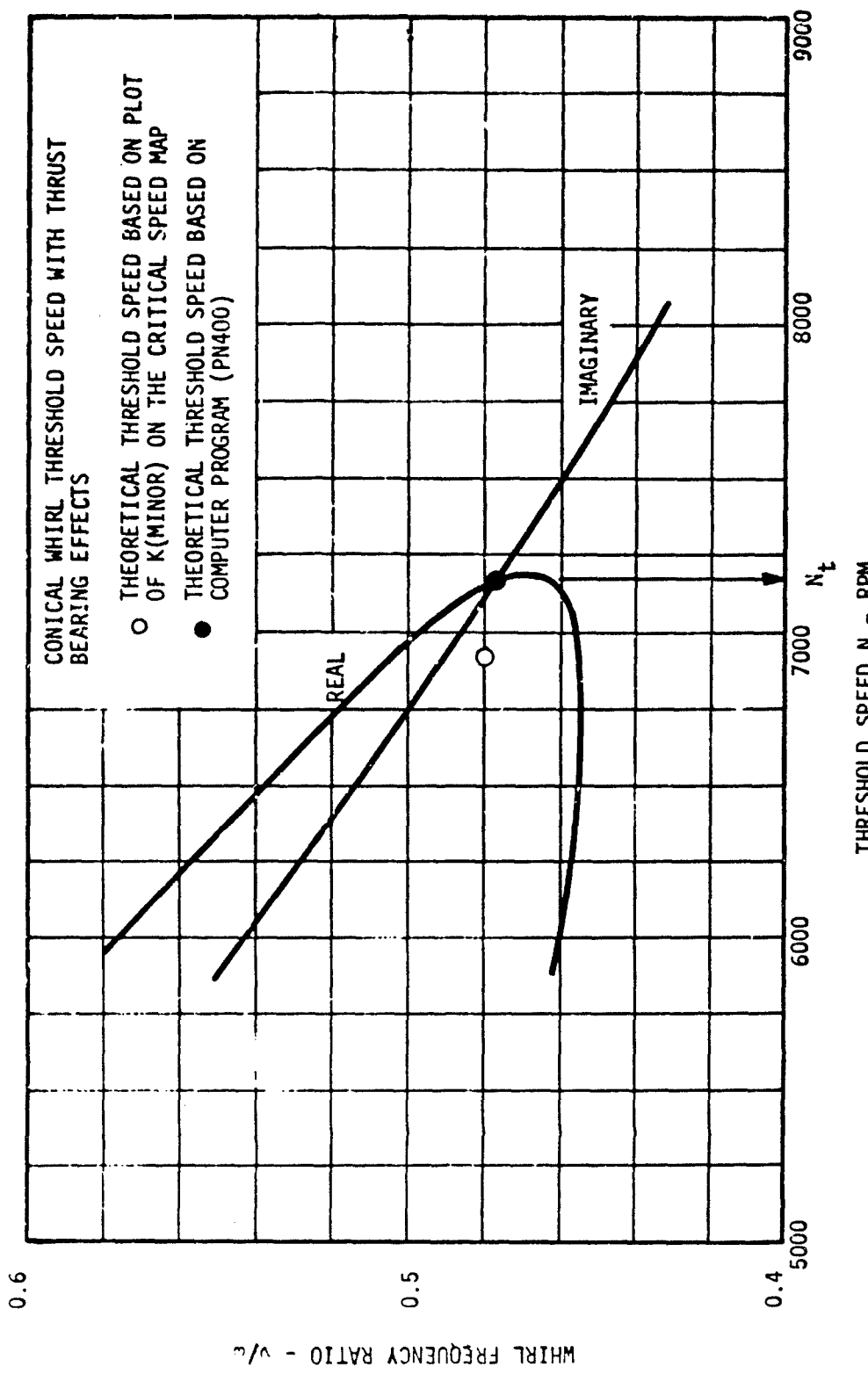


Fig. 9 Loci of Roots for Real and Imaginary Parts of Stability Determinant

The data for rotor No. 2 are as follows:

Rotor Model #2

Journal Bearing Design (Hybrid)

$D = 3.00$ in.	$R = 2.472 \times 10^5$ in. <sup>2</sup> /sec <sup>2</sup> $\omega_R$
$L = 3.25$ in.	$n = 32$ holes
$C = .0026$ in.	$a = .012$ in. (orifice radius)
$P_a = 18$ psia	Orifice compensation
$P_s = 72$ psia	Single Plane admission
$W = 6.95$ lb. (No. 1 bearing), 11.80 lb. (No. 2 bearing)	
$\mu = 3.40 \times 10^{-9}$ lb. sec./in. <sup>2</sup>	
$T = 760^\circ R$	

Thrust Bearing Design (Hydrostatic)

$R_o = 2.53$ in.	$M = 3.35 \times 10^{-9}$ lb.sec./in. <sup>2</sup>
$R_i = 1.55$ in.	$C = .0015$ in.
$P_a = 18$ psia	$n = 40$ holes
$P_s = 30.6$ psia	$a = .030$ in. = $d/2$ (inherently compensated)
$T_s = 1150^\circ R$	$\delta = a^2/cd = 10$

Table II gives the hybrid gas-lubricated journal bearing data for an  $L/D = 1.08$  with  $v/\omega = 0.50$  at  $P_s/P_a = 4.0$ . The hydrostatic effect parameter  $\Lambda_s$  for the journal bearing design with orifice compensation ( $\delta = 0$ ) and single plane admission is given by:

$$\begin{aligned} \Lambda_s &= \frac{6\mu n a^2}{P_s C^3} \frac{\sqrt{RT}}{\sqrt{1 + \delta^2}} \\ &= \frac{(6)(3.4 \times 10^{-9})(32)(.012)^2}{(72)(.0026)^3} \frac{\sqrt{2.472 \times 10^5 \times 760}}{} \\ &= 1.025 \end{aligned}$$

The data in Table II are applicable for  $\Lambda_s = 1.0$  with the only variables being the hydrodynamic effects  $\Lambda$  and load capacity  $W$ . Again double interpolation is required to obtain the necessary stiffness and damping coefficients at a constant  $\bar{W}$  value. The  $\bar{W}$  values for rotor No. 2 are

Journal Bearing Data

$$\bar{W}_1 = \frac{W_1}{P_a LD}$$

$$= \frac{6.95}{18(3.25)(3)}$$

$$= .0396 \text{ (bearing 1)}$$

$$\bar{W}_2 = \frac{W_2}{P_a LD}$$

$$= \frac{11.8}{18(3.25)(3)}$$

$$= .0672 \text{ (bearing 2)}$$

The relationship between bearing number  $\Lambda$  and rotational speed  $N$  is:

$$\begin{aligned} \Lambda &= \frac{12\pi N}{P_a} \left( \frac{R}{C} \right)^2 \\ &= \frac{12\pi (3.4 \times 10^{-9}) N}{18} \left( \frac{1.500}{.0026} \right)^2 \end{aligned}$$

$$= 2.38 \times 10^{-3} N \text{ (where } N = \text{ rps)}$$

$$= 3.96 \times 10^{-5} N' \text{ (where } N' = \text{ rpm)}$$

The bearing data shown in Table III are obtained from Table II, by interpolation, for  $\bar{W}_1 = .0396$  and  $\bar{W}_2 = .0672$ . The values of  $K_{\text{minor}}$  given in Table III are calculated from Eq. (18) or Eq. (22). The values of  $\gamma = v/\omega$ , the frequency ratio at which effective damping goes to zero, are calculated from Eq. (14).

The critical speed curves for rotor No. 2 are plotted in Figure 10. Also plotted is the curve of  $K_{\text{minor}}$  vs. speed. In this case  $K_{\text{minor}}$  varies hardly at all with speed, which makes calculation of the whirl threshold speed  $\omega_T$ , very easy. Noting that for instability  $v_c/\omega_T$  must equal  $\gamma$  (which in this case is very nearly exactly 0.5) and noting that  $v_c$  can now be given by the intersection of the curve of  $K_{\text{minor}}$  with the lowest critical speed curve, we have

$$v_c = 14,750 \text{ rpm (from Figure 10)}$$

$$\omega_T = v_c/0.5 = 29,500 \text{ rpm}$$

To obtain a more exact calculation for  $\omega_T$ , we use computer program PN400 with bearing input data obtained from Table III. The results obtained are shown in Fig. 11. The approximate solution obtained above from the critical speed map approach is shown as a circle in Figure 11. The solution curves for the real and imaginary parts of the stability determinant being equal to zero (the solution curves for Eq. (11) and (12)) are very nearly parallel for this example, making exact determination of the whirl threshold speed quite difficult. As can be seen, the whirl threshold speed lies somewhere in the range of 29,000 to 29,375 rpm and the whirl frequency ratio is between 0.499 and 0.504.

Next we compute the effect of the thrust bearing on this whirl threshold speed. Using the thrust bearing design data, the squeeze number  $\sigma$  evaluated at the previous calculated value of  $v_c$ , the oscillation frequency at whirl threshold is

$$\begin{aligned} \sigma &= \frac{12\mu v}{P_a} \left( \frac{R_i R_o}{c^2} \right) \\ &= \frac{12(3.35 \times 10^{-9})(1540)(2.53)(1.55)}{18 (.0015)^2} \\ &= 6.0 \end{aligned}$$

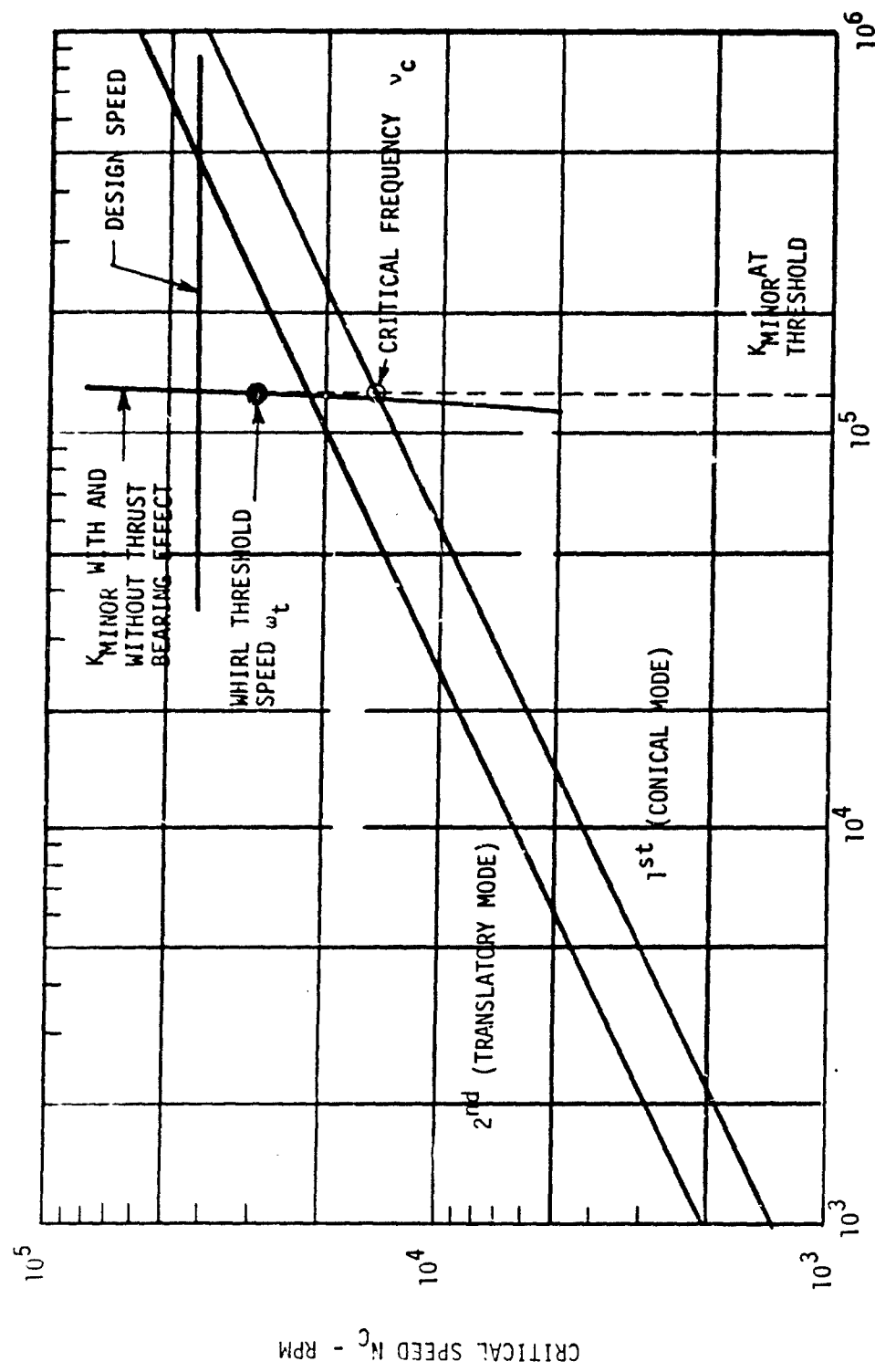


Fig. 10 Critical Speed Map of Rotor 2

TABLE III  
HYBRID GAS BEARING DATA  
 $L/D = 1.08$   $P_s/P_a = 4.0$

$\bar{W}$	$\Lambda$	$N$	$\gamma/\omega$	$\bar{K}_{\text{minor}}$	$K_{\text{minor}}$ (1b/in)	$K_{xx}$ (1b/in)	$K_{xy}$ (1b/in)	$K_{yy}$ (1b/in)	$\omega B_{xx}$ (1b/in)	$\omega B_{xy}$ (1b/in)	$\omega B_{yy}$ (1b/in)
.0396	.50	12400	.500	1.804	$1.22 \times 10^5$	$1.22 \times 10^5$	$5.06 \times 10^3$	$5.06 \times 10^3$	$1.22 \times 10^4$	$1.02 \times 10^4$	$8.70 \times 10^2$
1.00	24800	.499	1.808	$1.22 \times 10^5$	$1.24 \times 10^5$	$9.92 \times 10^3$	$9.99 \times 10^3$	$1.24 \times 10^4$	$2.00 \times 10^4$	$3.57 \times 10^3$	$2.00 \times 10^4$
1.75	43400	.499	1.806	$1.22 \times 10^5$	$1.28 \times 10^5$	$1.62 \times 10^4$	$1.62 \times 10^4$	$1.27 \times 10^4$	$3.23 \times 10^4$	$1.03 \times 10^4$	$3.24 \times 10^4$
3.00	74500	.492	1.812	$1.22 \times 10^5$	$1.35 \times 10^5$	$2.35 \times 10^4$	$2.35 \times 10^4$	$1.35 \times 10^4$	$4.72 \times 10^4$	$2.60 \times 10^4$	$2.61 \times 10^4$
5.00	124000	.500	1.809	$1.22 \times 10^5$	$1.48 \times 10^5$	$2.78 \times 10^4$	$2.79 \times 10^4$	$1.48 \times 10^4$	$5.76 \times 10^4$	$5.12 \times 10^4$	$5.11 \times 10^4$
.0672	.50	12400	.500	1.811	$1.22 \times 10^5$	$1.23 \times 10^5$	$5.06 \times 10^3$	$5.06 \times 10^3$	$1.23 \times 10^4$	$1.02 \times 10^4$	$8.70 \times 10^2$
1.00	24800	.499	1.812	$1.22 \times 10^5$	$1.24 \times 10^5$	$9.92 \times 10^3$	$9.99 \times 10^3$	$1.24 \times 10^4$	$1.99 \times 10^4$	$3.57 \times 10^3$	$3.57 \times 10^3$
1.75	43400	.499	1.804	$1.22 \times 10^5$	$1.27 \times 10^5$	$1.61 \times 10^4$	$1.61 \times 10^4$	$1.27 \times 10^4$	$3.24 \times 10^4$	$1.03 \times 10^4$	$1.04 \times 10^4$
3.00	74500	.512	1.809	$1.23 \times 10^5$	$1.35 \times 10^5$	$2.36 \times 10^4$	$2.31 \times 10^4$	$1.35 \times 10^4$	$4.71 \times 10^4$	$2.60 \times 10^4$	$2.60 \times 10^4$
5.00	124000	.499	1.809	$1.22 \times 10^5$	$1.48 \times 10^5$	$2.79 \times 10^4$	$2.79 \times 10^4$	$1.48 \times 10^4$	$5.31 \times 10^4$	$5.11 \times 10^4$	$5.11 \times 10^4$

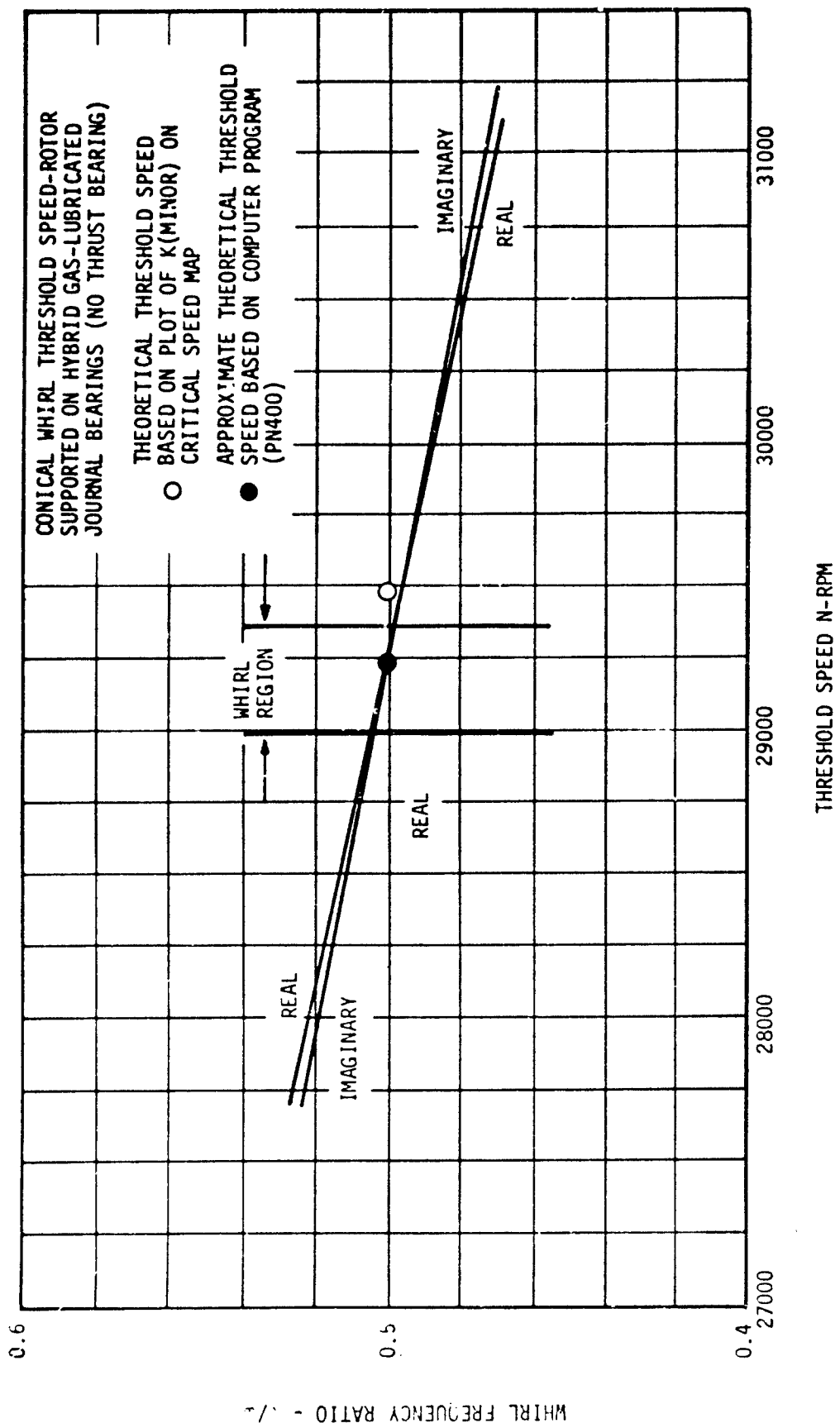


Fig. 11 Loci of Roots for Real and Imaginary Parts of Stability Determinant

The restrictor coefficient  $\Lambda_s$  equals:

$$\begin{aligned}\Lambda_s &= \frac{6 \mu n a^2 \sqrt{\rho T}}{P_s C^3 \sqrt{1 + \delta^2}} \\ &= \frac{(6)(3.35 \times 10^{-9})(40)(.03)^2 \sqrt{2.472 \times 10^5 \times 1150}}{(30.6)(.0015)^3 \sqrt{1 + 10^2}} \\ &= 11.80\end{aligned}$$

This value of  $\Lambda_s$  is significantly higher than the optimum value for maximum bearing stiffness (see Figure 15). This is because the operating condition being analyzed is the one at which stability of the rotor is poorest and is not the operating condition for which the bearing was designed. The curve of dynamic stiffness shown in Fig. 17 pertain to a value of  $\Lambda_s = 2.5$  which is optimum for a thrust bearing of radius ratio of  $R_o/R_i = 1.5$ . From this curve we see that such a bearing, operating at a squeeze number of  $\sigma = 6.0$  would be well within the range where steady state stiffness data apply; i.e., is operating at an oscillation frequency which is well below the frequency at which squeeze film effects become important. Physically, there is no reason to expect that this situation would be altered significantly when the bearing is operated at higher  $\Lambda_s$  (i.e., lower supply pressure). Therefore, we would readily expect that our example bearing at  $\Lambda_s = 11.8$  and  $\sigma = 6.0$ , would be in the "steady state" region where Fig. 15 could be used to calculate bearing stiffness. From Fig. 14, at  $P_s/P_a = 1.70$ , we determine that

$$\frac{1 + \delta^2 \bar{G}}{1 + 2/3 \delta^2} = 0.07$$

$$\bar{G} = (.07) \frac{1 + 2/3 \delta^2}{1 + \delta^2} = (.07) \frac{1 + 2/3 (10)^2}{1 + (10)^2}$$

$$= .0469$$

$$G = \frac{\pi(R_o^2 - R_i^2) R_o^2 (P_s - P_a) \bar{G}}{c}$$

$$= \frac{\pi [(2.53)^2 - (1.55)^2] (2.53)^2 (30.6 - 18)(.0469)}{.0015}$$

$$= 3.02 \times 10^4 \text{ in.lb/rad.}$$

Since we have only one thrust bearing, we must appropriately divide its effect among the two journal bearings to use the effective stiffness - critical speed map approach for approximately calculating the effect of the thrust bearing on whirl threshold speed. The distance of journal bearings 1 and 2 from the c.g. of the rotor are  $L_1 = 4.72"$  and  $L_2 = 2.78"$  respectively. By analogy with Eq. (29), which gives the relationships for adding an effective stiffness of one thrust bearing to one journal bearing, we can infer that a correct approach for adding an effective stiffness of one thrust bearing of angular stiffness  $G$  to two journal bearings of spans  $L_1$  and  $L_2$  would be by the relationship

$$K_e = \frac{G}{L_1^2 + L_2^2}$$

Therefore, the effective radial stiffness to be added to each journal bearing would be

$$K_e = \frac{G}{L_1^2 + L_2^2}$$

$$= \frac{3.02 \times 10^4}{30}$$

$$= 1010 \text{ lb/in}$$

This value is seen to be negligible compared with the values of stiffness associated with the journal bearings themselves. Hence, in this case, the thrust bearing would have negligible effect on conical motions of the shaft.

The above conclusion reached for rotor No. 2 probably pertains to most rotor designs. In general, such rotors will be designed so that the span between journal bearings is efficiently great that these bearings will exert a much greater restraining force on conical motions of the shaft than will the thrust bearings. However, this need not always be true. It is easy to conceive of systems where the thrust loads dominate and where journal bearings are needed only to locate the shaft. In such systems a designer could take advantage of the now available technology for including thrust bearing effects in whirl threshold speed calculations, and design the rotor such that the thrust bearing could assume the responsibility of restraining conical motions of the rotor.

SECTION IV  
ANGULAR STIFFNESS COEFFICIENTS FOR HYDROSTATIC THRUST BEARINGS

The hydrostatic bearing data presented in this section are based on an analysis by Lund described in Reference [5]. Basically, the analysis involves the assumption that discrete feeding holes arranged in an annular thrust bearing (see Fig. 12) can be represented approximately by a continuous "line source" of feeding as if the bearing were fed by a continuous circular slot rather than by discrete holes. This approximation tends to be absolutely correct in the limit as the number of feeding holes approaches an infinite number, but tends to somewhat overestimate bearing load and stiffness for bearings having a finite number of holes. A line source correction factor to account for this overestimation has been worked out by comparing a detailed discrete feeding analysis with the simpler line source analysis. The correction factor to be applied depends on the product  $n\zeta$  and  $d/\xi D$  where  $n$  is the number of feeding holes,  $\zeta = 1/2 \log_e (R_o/R_i)$ ,  $d$  is the diameter of the feeding holes,  $D = 2 \sqrt{R_o R_i}$ ,  $R_o$  and  $R_i$  are the outer and inner radii of the thrust bearings having a practical number of holes, the correction factor to be applied is  $2/3$ , i.e., the line source analysis overestimates the stiffness by 50%. This correction factor has been built into the design curves presented in this section. Figure 19 shows a curve of  $n\zeta$  vs.  $d/\xi D$  giving the recommended size and number of feedings for which this correction applies. If more feeding holes are used, stiffness will be higher than that predicted by the design charts in this section and conversely.

The stiffness of compressible hydrostatic bearings is dependent upon the frequency of excitation  $\nu$  of the bearing if this frequency is high enough. This is because, at large values of  $\nu$ , the gas in the bearing film tends to be dropped and compressed rather than squeezed out of the film, and this contributes to a higher level of bearing stiffness. This effect is illustrated in Figures 17 and 18 where dimensionless stiffness  $\bar{G} = CG/[c(R_o^2 - R_i^2) R_o^2 (P_s - P_a)]$  is plotted vs. the dimensionless excitation frequency  $\sigma$  (known as squeeze number)

$$\sigma = \frac{12 \cdot \nu}{P_s} \left( \frac{R_i R_o}{C^2} \right)$$

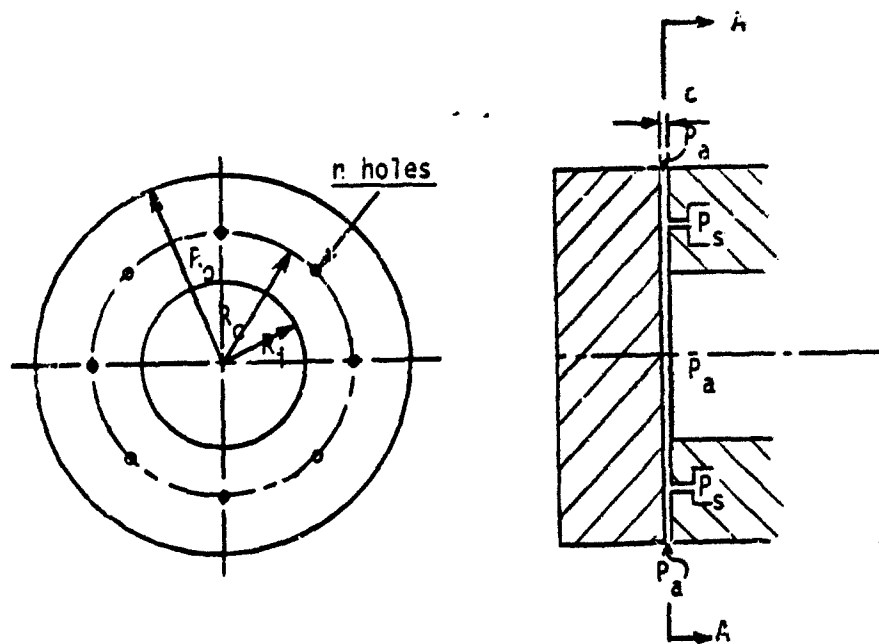


Fig. 12 Sketch of Hydrostatic Thrust Bearing

as can be seen, for small  $\sigma$ , the stiffness remains constant at its steady state value independent of excitation frequency. However, once  $v$  becomes large enough, the bearing stiffness begins to increase with  $v$  due to the above mentioned squeeze film effect.

In general, for rotors supported on hydrostatic bearings, the running speed will be in the range such that an excitation frequency  $v \approx \omega/2$  will lead to squeeze numbers sufficiently low such that steady state bearing stiffness data will apply. This is generally so because if shaft speeds are high enough such that compressibility becomes significant in the squeeze film effect, then the shaft speed will tend to be high enough such that hydrodynamic bearings could be used for load support. Figures 17 and 18 will be used, therefore, primarily to define the limits below which steady state bearing data apply rather than being used as a source of dynamic stiffness data.

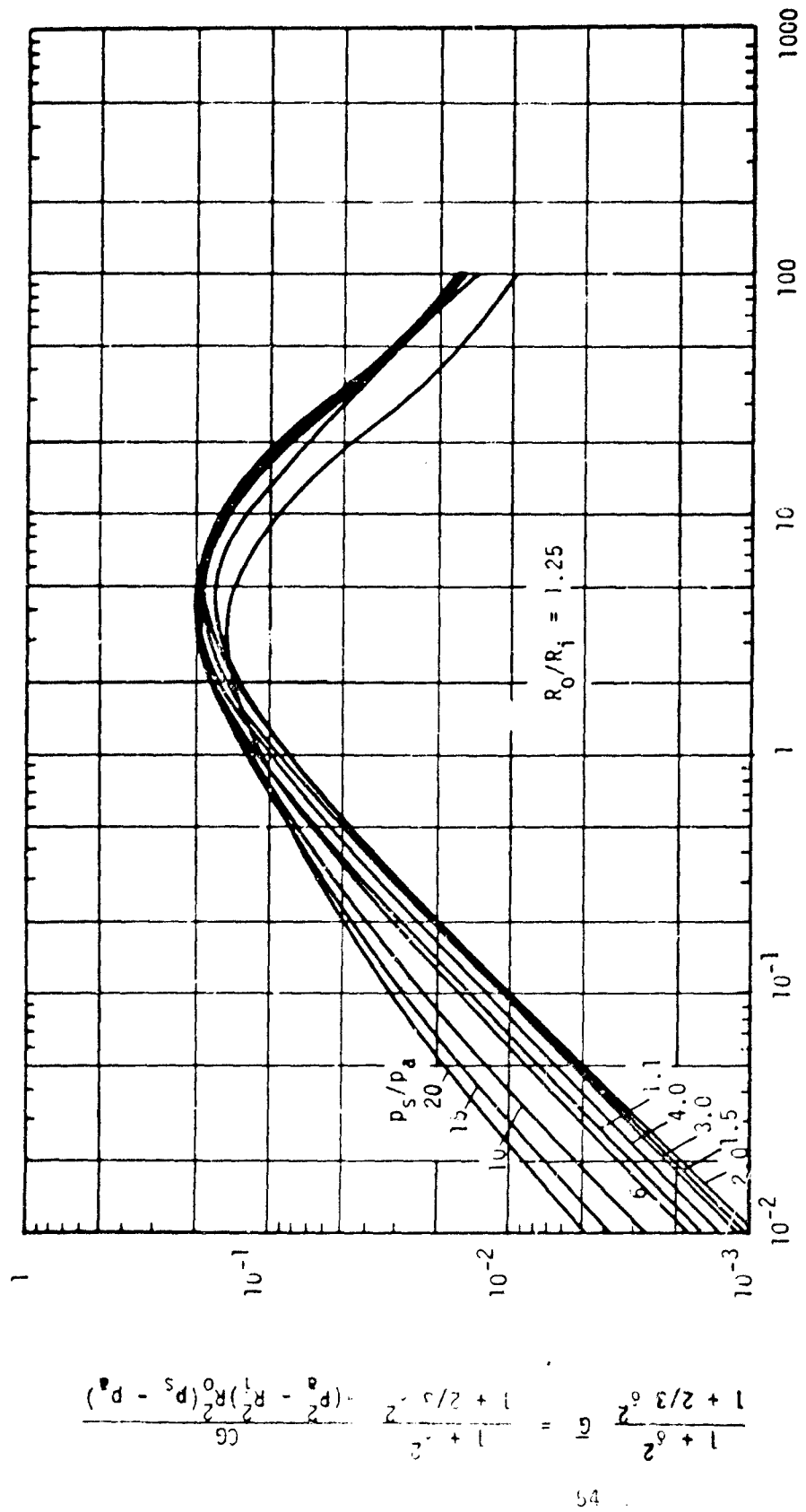
In Figures 13 through 16 are presented dimensionless angular stiffness  $\bar{G}$  vs. the feeding parameter  $\Lambda_s$

$$\Lambda_s = \frac{6\pi a^2 \sqrt{\frac{RT}{P_s C^3}}}{\sqrt{1 + \delta^2}} \quad (31)$$

for radius ratios of  $R_o/R_i = 1.25, 1.5, 2.0$ , and  $3.0$ . The dimensionless stiffness  $\bar{G}$  is pre-multiplied by the factor  $1 + \delta^2/(1 + 2/3 \delta^2)$  where  $\delta = a^2 cd$ , known as the inherent compensation factor, gives the ratio of orifice area  $\pi a^2$  to inherent restriction area  $\pi cd$  (see Figure 12). Curves are provided for different values of pressure ratio  $P_s/P_a$ . Usually, the hydrostatic thrust bearings are designed for a value of  $\Lambda_s$  which provides near maximum stiffness; i.e.,  $\Lambda_s$  is in the range 1.0 to 4.0, depending on radius ratio. Hence, the dynamic curves in Figs. 17 and 18 are presented for near optimum values of  $\Lambda_s$ .

Only stiffness data is provided for the hydrostatic bearings. This is for the following reasons:

- (1) Damping in hydrostatic bearings results, essentially, from hydrodynamic forces which are usually much weaker than the hydrostatic forces producing bearing stiffness.
- (2) More importantly, in hydrostatic thrust bearings, "effective" bearing damping tends to zero for wobbling or nutating modes of motion which occur at half the rotational speed of the thrust runner. In examining the stability of rotors, it is invariably the influence of precisely this kind of thrust bearing motion on rotor dynamics that we are attempting to calculate. Hence in such calculations, it is quite reasonable to presume that the effects of thrust bearing damping will be zero or near zero and only consider the effects of thrust bearing stiffness.



$$\Lambda_s = \frac{6 \mu n a^2 \sqrt{RT}}{p_s C^3 \sqrt{1 + \delta^2}}$$

Fig. 13 Hydrostatic Thrust Bearing,  $R_o/R_i = 1.25$   
Dimensionless Angular Stiffness vs. Restrictor Coefficient

NTI-9044

$$C_4 = \frac{(p_s - p_2)(R_o^2 - R_i^2)}{1 + 2/3 \delta^2} \cdot \frac{1 + 2/3 \delta^2}{1 + \delta^2} \cdot \frac{1 + 2/3 \delta^2}{1 + 2\delta^2}$$

54

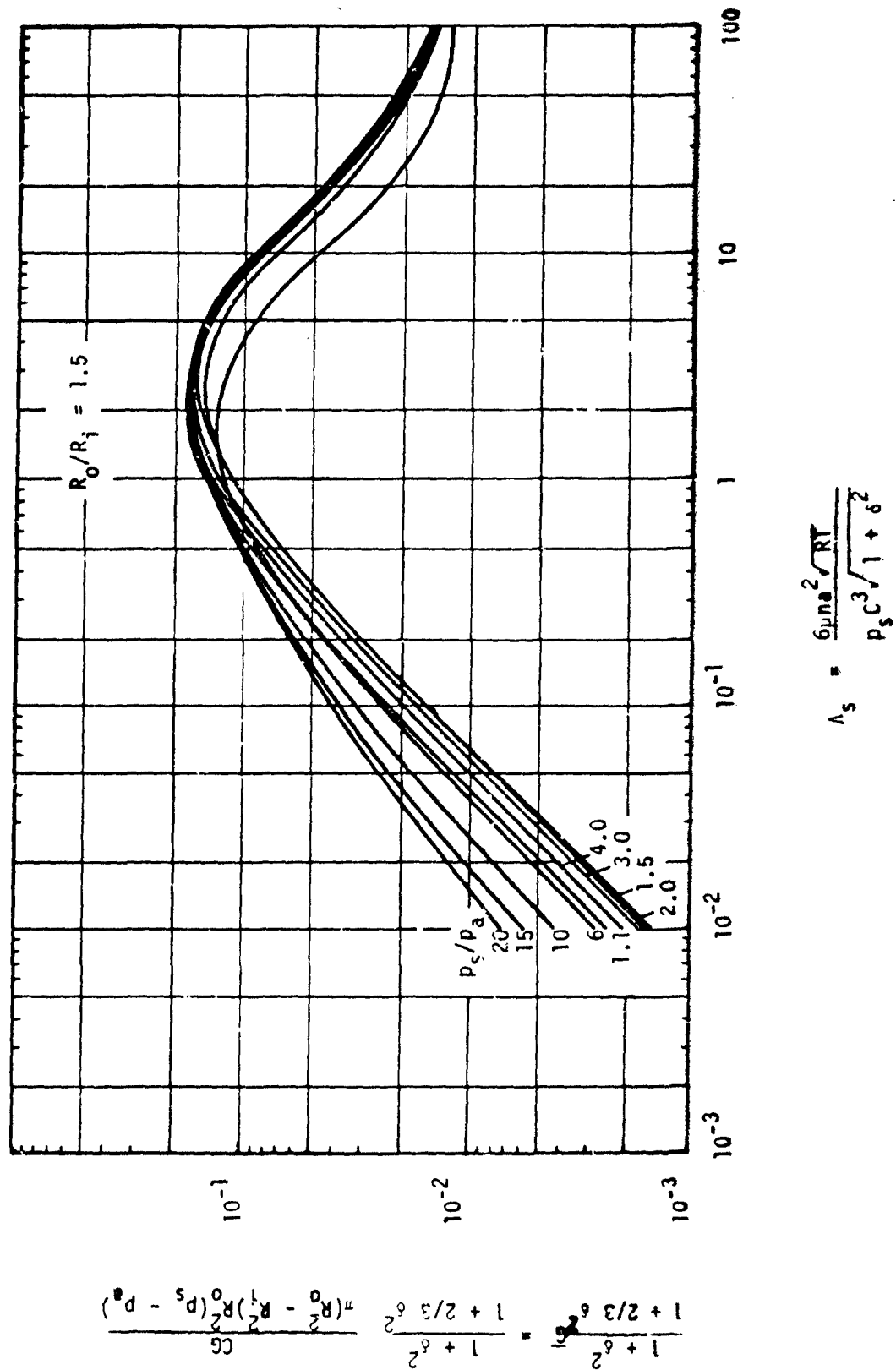
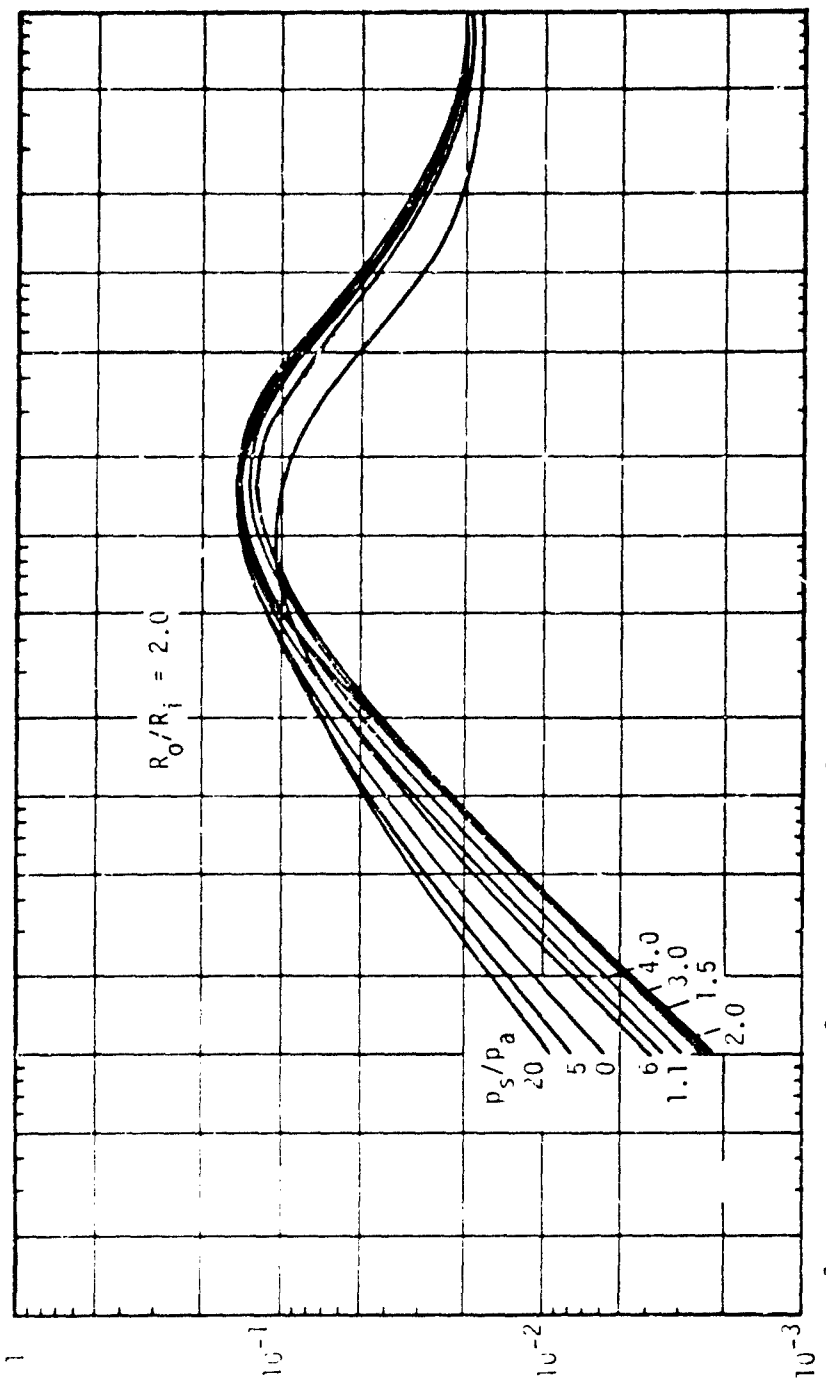


Fig. 14 Hydrostatic Thrust Bearing,  $R_o/R_i = 1.5$   
Dimensionless Angular Stiffness vs. Restrictor Coefficient

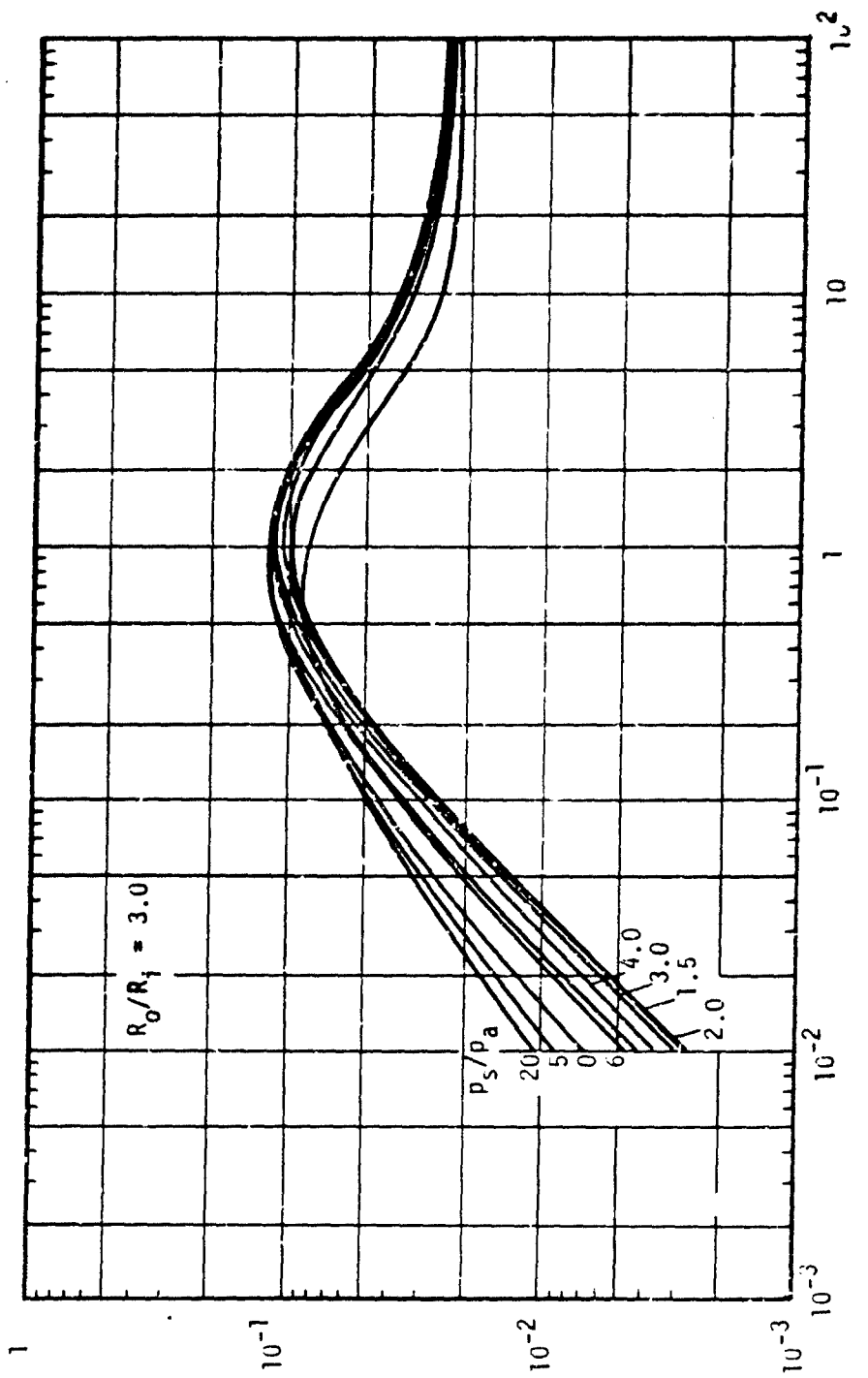
KRI-9050



$$\lambda_S = \frac{\epsilon_{uniax}^2 \sqrt{RT}}{p_s c^3 / 1 + \delta^2}$$

Fig. 15 Hydrostatic Thrust Bearing,  $R_0/R_i = 2$   
Dimensionless Angular Stiffness vs. Restrictor Coefficient

MTL-9051



$$\frac{\lambda_s}{Cg} = \frac{1 + 2/3 \delta^2}{1 + \delta^2} \frac{(R_0^2 - R_j^2) R_j^2 (P_s - P_a)}{\delta^2}$$

Fig. 16 Hydrostatic Thrust Bearing.  $R_0/R_j = 3$   
Dimensionless Angular Stiffness vs. Restrictor Coefficient

MRI-9053

$$\lambda_s = \frac{C_{\text{fun}}^2 \sqrt{RT}}{P_s C^3 / 1 + \delta^2}$$

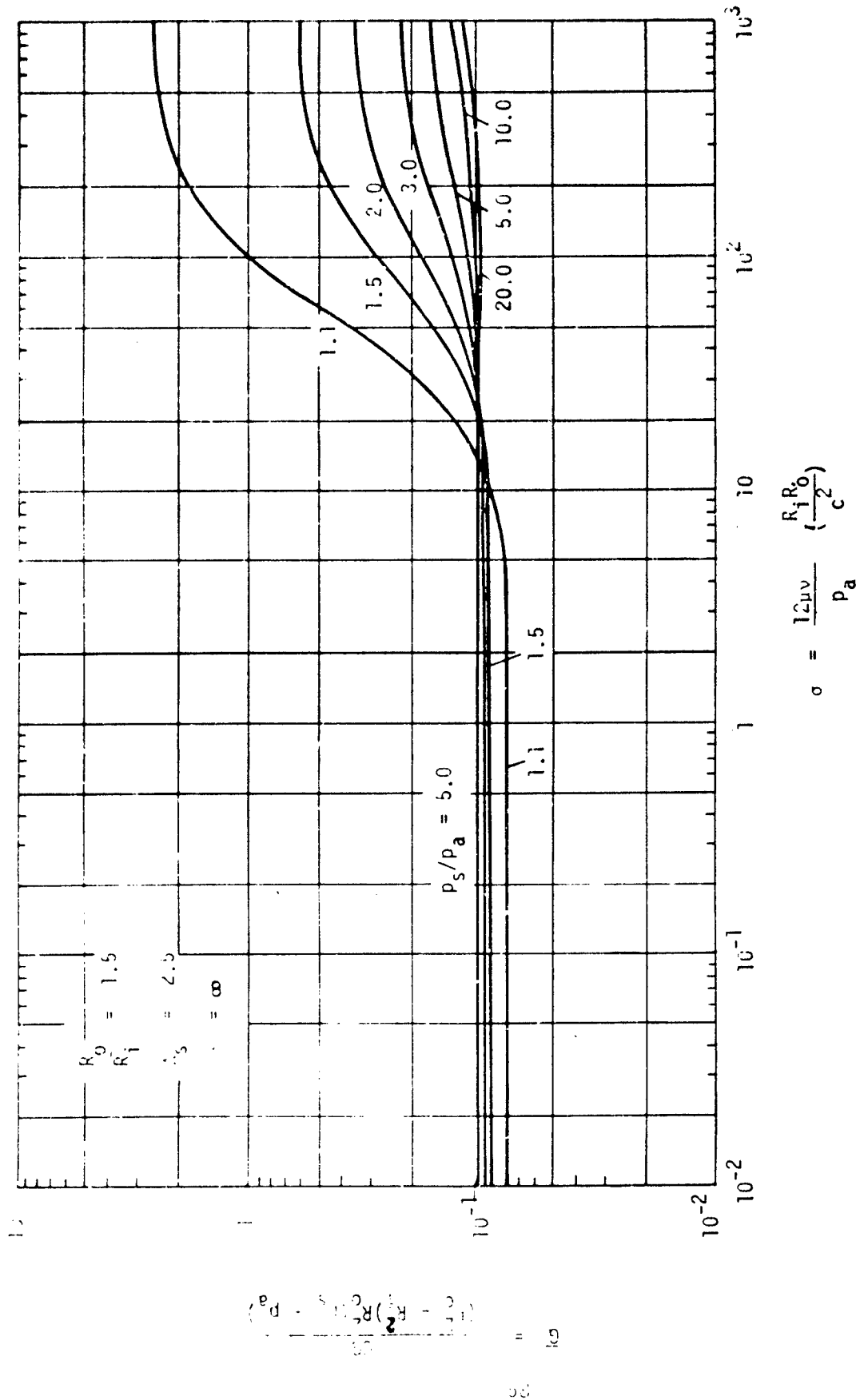


Fig. 17 Dynamic Angular Stiffness for the Hydrostatic Thrust Bearing  
 $R_o/R_i = 1.5$ . Inherent Compensation

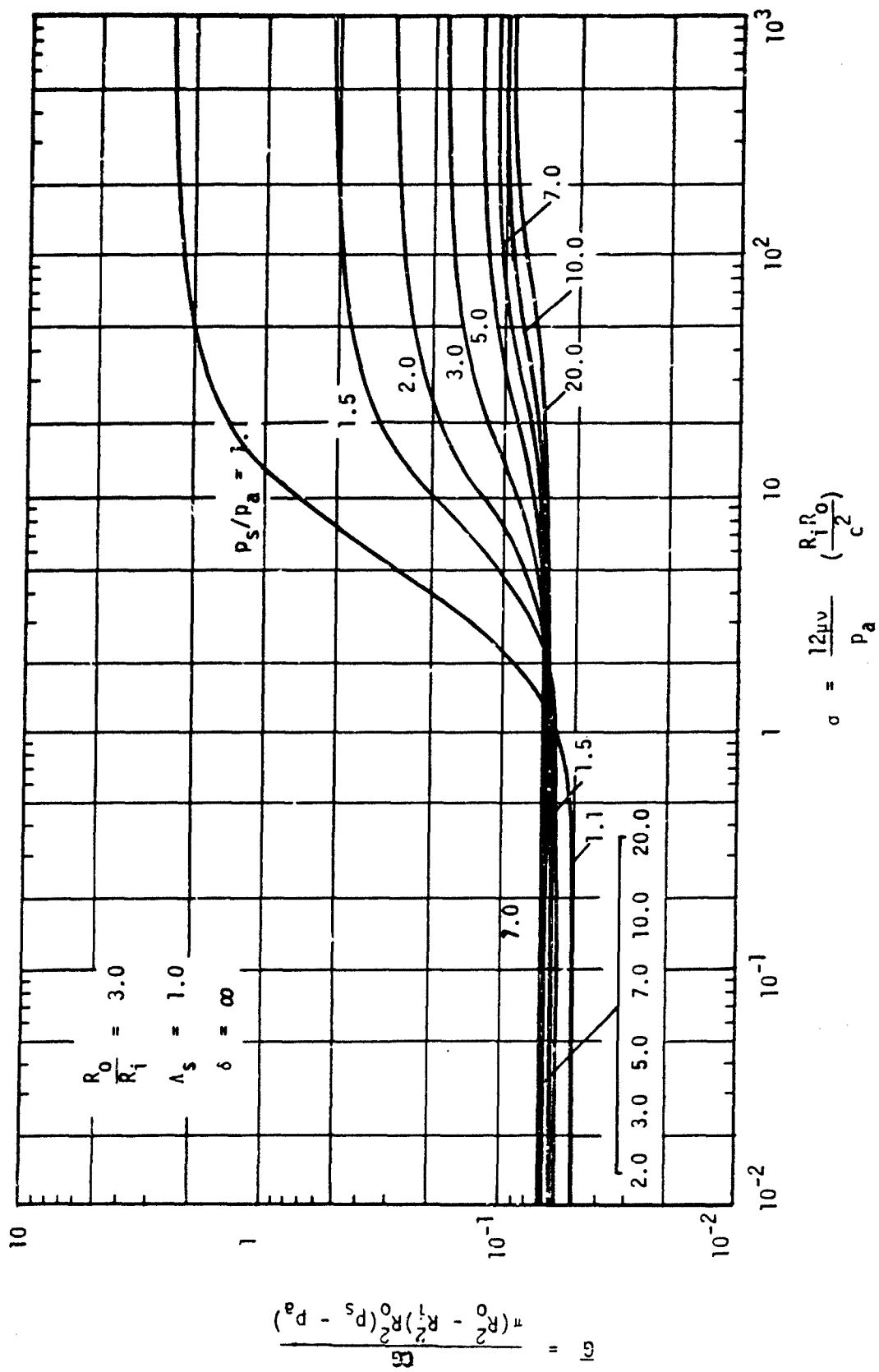


Fig. 18 Dynamic Angular Stiffness for the Hydrostatic Thrust Bearing  
 $R_0/R_i = 3.$  Inherent Compensation  
 MTI-9049

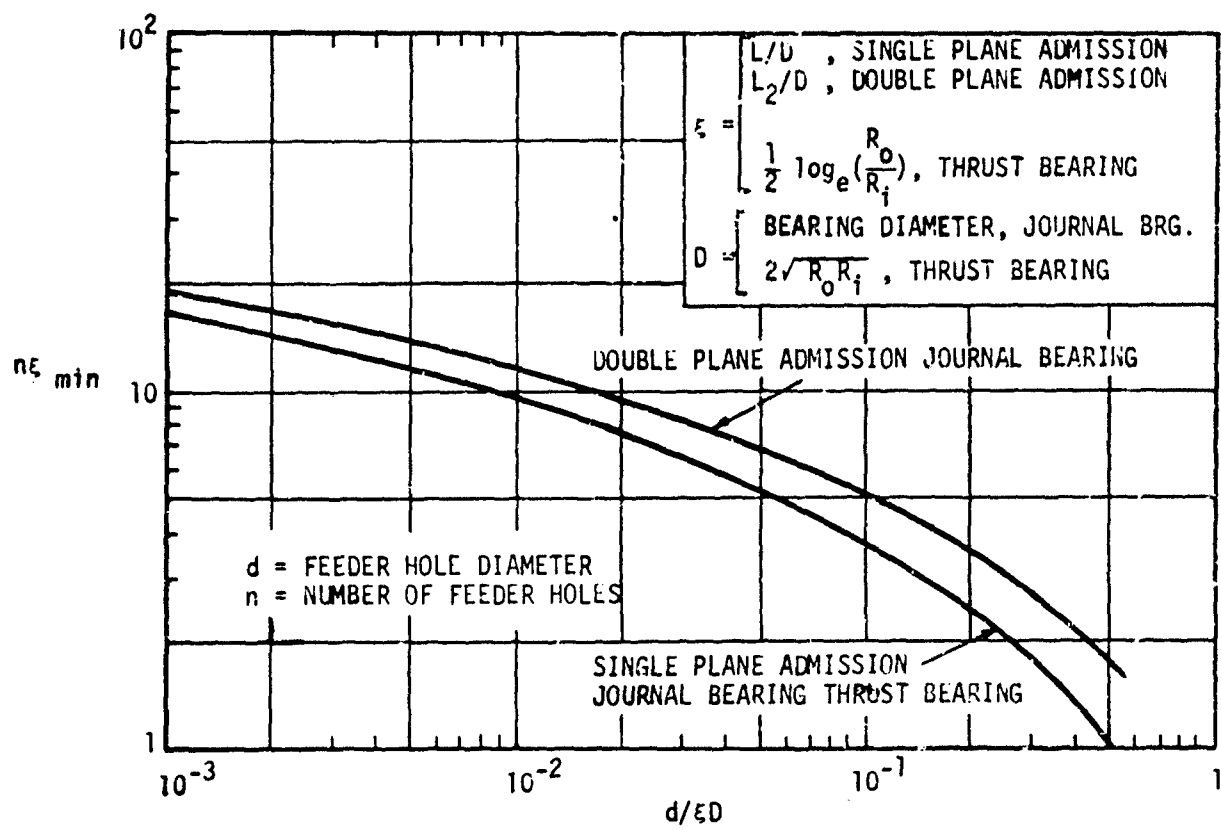


Fig. 19 Minimum Number of Feeder Holes

APPENDIX I  
COMPUTER PROGRAM  
THE THRESHOLD OF INSTABILITY OF A FLEXIBLE ROTOR IN FLUID FILM BEARINGS

This section describes the rotor stability computer program PN400: "The Threshold of Instability of a Flexible Rotor in Fluid Film Bearings". This program is quite similar to the computer program PN0017 given in Reference 1.

The new program described in this volume is a modification and extension of the previous version. The amount of plotting has been significantly reduced in that a quadratic interpolation<sup>1</sup> routine now automatically performs much of the plotting previously required to find the zero point solutions for both the real and imaginary parts of the complex determinant. This program also now accepts the angular thrust bearing properties and is also set up to handle both liquid-lubricated and gas-lubricated bearings. In addition a more refined rotor model is employed which describes the rotor in terms of stiffness and mass diameters, lengths, concentrated values of mass, and mass moments of inertia. The new rotor model is discussed in Reference 3.

Analysis

The rotor analysis is described in detail in Reference 3, Appendix VIII. Consider the rotor shown in Fig. 3 and assuming the two ends of the rotor to be free, the bending moment and the shear force at one rotor end are directly proportional to the unknown amplitude and slope at the opposite rotor end. The proportionality coefficients are the dynamic influence coefficients which are computed by the program, and the final equation is given in the following matrix form (see Eq. (H.61) in Appendix VIII of Reference 3 neglecting magnetic influence coefficient matrix).

---

<sup>1</sup> Second-order polynomial interpolation. See Reference 6.

$$\begin{Bmatrix} V'_{xm} \\ V'_{ym} \\ M'_{xm} \\ M'_{ym} \end{Bmatrix} = \begin{Bmatrix} a_{11} & a_{12} & a_{13} & a_{14} \\ a_{21} & a_{22} & a_{23} & a_{24} \\ a_{31} & a_{32} & a_{33} & a_{34} \\ a_{41} & a_{42} & a_{43} & a_{44} \end{Bmatrix} \begin{Bmatrix} x_1 \\ y_1 \\ \theta_1 \\ \varphi_1 \end{Bmatrix} \quad (32)$$

Here,  $V'_{xm}$  and  $V'_{ym}$  are the shear force components at one rotor end (station m),  $M'_{xm}$  and  $M'_{ym}$  are the bending moment components at the same location, and  $x_1$ ,  $y_1$ ,  $\theta_1$  and  $\varphi_1$  are the unknown amplitudes and slopes at station 1. The a's are the dynamic influence coefficients which depend on the whirl frequency ratio and the rotor speed. They include the effect of rotor inertia, rotor flexibility and the dynamic bearing coefficients. Since the ends of the rotor are free,  $V'_{xm} = V'_{ym} = M'_{xm} = M'_{ym} = 0$ . Thus,  $x_1$ ,  $y_1$ ,  $\theta_1$  and  $\varphi_1$  are only different from zero when the determinant of the matrix of influence coefficients is zero which, then, determines the threshold of instability:

$$\Delta = \Delta_c + i\Delta_s = \begin{vmatrix} a_{11} & a_{12} & a_{13} & a_{14} \\ a_{21} & a_{22} & a_{23} & a_{24} \\ a_{31} & a_{32} & a_{33} & a_{34} \\ a_{41} & a_{42} & a_{43} & a_{44} \end{vmatrix} = 0 \quad (33)$$

For each given angular speed,  $\omega$ , of the rotor, the program calculates  $\Delta_c$  and  $\Delta_s$  for specified values of the whirl frequency ratio  $\gamma = v/\omega$  and determines the zero points of  $\Delta_c$  and  $\Delta_s$  within the given range. The results can be plotted directly to find the threshold of instability.

## COMPUTER INPUT

### Card 1 (72H)

Any descriptive text may be given to identify the calculation.

### Card 2 (1415)

This is the "control card" whose values control the rest of the input. The control card has 10 items:

1. NS, the number of rotor stations, see "Rotor Data" ( $1 \leq NS \leq 100$ )
2. NB, the number of bearings ( $1 \leq NB \leq 10$ )
3. NPST. The program provides for including the response characteristics of the bearing pedestals. When it is desired to include this effect, set NPST = 1 and give the required input data as explained later. When NPST = 0, the pedestals are assumed to be rigid and no pedestal data are required in the input.
4. NANG. The dynamic forces of the fluid film in the journal bearings resist both radial motion and angular motion. In most cases, only the radial forces are significant in which case NANG is set equal to zero. However, long journal bearings and especially thrust bearings may exert considerable constraint on the angular motion of the rotor. When it is desired to include this effect, set NANG = 1 and give the required input data as explained later.
5. NFR is the number of whirl frequency ratios specified in the input list below, see explanation later ( $3 \leq NFR \leq 50$ ).
6. INC. If the bearing lubricant is compressible (gas bearings), set INC = 1 in which case the dynamic bearing coefficients must be specified for each whirl frequency ratio in the input. If INC = 0, the lubricant is incompressible and the dynamic bearing coefficients are independent of whirl frequency.

7. NIT. As discussed previously, the program searches for the zero points of the instability determinant. To do this, the instability determinant is computed as a function of the whirl frequency ratio. The input gives NFR values of the whirl frequency ratio in sequence, and the determinant is calculated for each of these values. In addition, each interval is subdivided into NIT increments and the determinant is also computed at these intermediate frequency ratio values. Whenever the program detects a change in sign of the determinant between two consecutive calculations, it uses quadratic interpolation to find the accurate zero point.

By subdividing the intervals in the given frequency ratio list, the list can be shortened without loss of accuracy. Furthermore, when the bearing lubricant is a gas it is necessary to provide the dynamic coefficients for each specified frequency ratio. Thus, to minimize the input data it is desirable to keep this number low. Then the program automatically calculates the coefficients for the intermediate points by quadratic interpolation.

NIT should be equal to or greater than 1. When NIT = 1, no subdivision takes place.

8. METR. This item should always be zero. It is included for diagnostic purposes which, however, is of no value to the general user of the program.

9. NCAL, specifies the number of rotor speed ranges. For each speed range it is necessary to give input data for the dynamic bearing coefficients. There is no limit for NCAL.

10. INP. If INP = 0, the present set of input data is followed by a new set, starting from Card 1. If INP = 1, this is the last set of input.

Card 3 (1F6E12.5)

1. YM is Youngs modulus E for the shaft material in lbs/inch<sup>2</sup>. If E actually changes along the rotor it should be noted that the program only uses E in the product EI where I is the cross-sectional moment of inertia of the shaft. Since

$I = \frac{\pi}{64} \left[ (d_o)^4_{\text{stiff}} - d_i^4 \right]$  where  $(d_o)_{\text{stiff}}$  is the outer shaft diameter and  $d_i$  is the inner diameter, any variation in  $E$  can be accounted for by changing  $(d_o)_{\text{stiff}}$  (see "Rotor Data").

2. DENST gives the weight density of the shaft material in lbs/inch<sup>3</sup>. The program converts it into the mass density  $\rho = \text{DENST}/386.069$ . If the density actually changes along the rotor it should be noted that the weight of the shaft per unit length is  $\rho \frac{\pi}{4} \left[ (d_o)^2_{\text{mass}} - d_i^2 \right]$  where  $(d_o)_{\text{mass}}$  is the outer shaft diameter (see "Rotor Data"). Thus,  $(d_o)_{\text{mass}}$  can be changed to absorb the changes in density.

3. SHM gives the product  $\alpha G$  where  $G$  is the shear modulus, lbs/inch<sup>2</sup>, and  $\alpha$  is the shape factor for shear (for circular cross-sections:  $\alpha \approx 0.75$ ).

#### Rotor Data (8E9.2)

The rotor is represented by a number of stations connected by shaft sections of uniform diameter. Thus, rotor stations are introduced wherever the shaft diameter changes (or changes significantly). Also, there must be a rotor station at each end of the rotor, at each bearing centerline and at any thrust bearing. Furthermore, a rotor station is introduced wherever the shaft has a concentrated mass which cannot readily be represented in terms of an inner and outer shaft diameter (impellers, turbine wheels, alternator poles, and so on). In this way the rotor is assigned a total of NS stations (card 2, item 1) which are numbered consecutively starting from one end of the rotor. There can be a maximum of 100 stations. Each station can be assigned a concentrated mass  $m$  with a polar mass moment of inertia  $I_p$  and a transverse mass moment of inertia  $I_T$  (any of these quantities may, of course, be zero). Also, each station can be assigned a shaft section with which it is connected to the following station. This shaft section has a length  $l$ , and outer diameter  $(d_o)_{\text{stiff}}$ , an outer diameter

$(d_o)_{\text{mass}}$  and an inner diameter  $d_i$ . The outer diameter  $(d_o)_{\text{stiff}}$  is used to specify the stiffness of the shaft section such that the cross-sectional moment of inertia of the shaft is:  $I = \frac{\pi}{64} \left[ (d_o)^4_{\text{stiff}} - d_i^4 \right]$  and the shear area is:

$\frac{\pi}{4} \left[ (d_o)^2_{\text{stiff}} - d_i^2 \right]$ . The outer diameter  $(d_o)_{\text{mass}}$  is used in calculating the mass of the shaft such that the mass per unit length is:  $\rho \frac{\pi}{4} \left[ (d_o)^2_{\text{mass}} - d_i^2 \right]$  where  $\rho$  is the mass density (see card 3, item 2).

In the computer input there must be a card for each rotor station (NS cards). Each card specifies the 7 values for the station:

1. The concentrated mass:  $m$ , lbs. (may be zero).
2. The polar mass moment of inertia of the station mass;  $I_p$  lbs-inch<sup>2</sup> (may be zero).
3. The transverse mass moment of inertia of the station mass;  $I_T$  lbs-inch<sup>2</sup> (may be zero).
4. The length of the shaft section to the next station:  $l$ , inch (may be zero). For the last station, set  $l = 0$ .
5. The outer diameter,  $(d_o)_{\text{stiff}}$  of the shaft section, inch.  $(d_o)_{\text{stiff}}$  is used in calculating the stiffness of the shaft section,  $(d_o)_{\text{stiff}} \neq 0$ . For the last station, set  $(d_o)_{\text{stiff}} = 1.0$ .
6. The outer diameter,  $(d_o)_{\text{mass}}$  of the shaft section, inch (may be zero).  $(d_o)_{\text{mass}}$  is used in calculating the mass of the shaft section. For the last station, set  $(d_o)_{\text{mass}} = 0$ .
7. The inner diameter,  $d_i$  of the shaft section, inch (may be zero).  $d_i$  is used both in calculating the stiffness and the mass of the shaft section. For the last station, set  $d_i = 0$ .

### Bearing Stations (1415)

The rotor station numbers at which there are bearings, are listed in sequence. This includes both journal bearings and any thrust bearings. There can be up to 10 bearings.

### Pedestal Data (1P6E12.5)

The program provides for the option that the pedestals supporting the bearings may be flexible. In that case, data for the pedestals must be given and NPST must be set equal to 1 (card 2, item 3). If the pedestals are rigid, set NPST = 0 and omit giving any data for the pedestals.

When NPST = 1, each bearing is supported in a "two-dimensional" pedestal. The pedestal is represented as two separate masses, each mass on its own spring and dashpot. The one mass-spring-dashpot system represents the pedestal characteristics in the x-direction, (the vertical direction) and the other system represents the y-direction (the horizontal direction). There is no coupling between the two systems. In the computer input there must be one card for each rotor bearing and each card contains the 6 items necessary to specify the pedestal characteristics:

1. The pedestal mass for the x-direction, lbs.
2. The pedestal stiffness for the x-direction, lbs/inch.
3. The pedestal damping coefficient for the x-direction, lbs-sec/inch.  
(Note: For the bearing films the damping is given in lbs/inch, whereas the damping coefficient in lbs-sec/inch is used for the pedestals).
4. The pedestal mass for the y-direction, lbs.
5. The pedestal stiffness for the y-direction, lbs/inch.

6. The pedestal damping coefficient for the y-direction, lbs-sec/inch.

When the bearings also have angular stiffness (i.e., NANG = 1, item 4, card 2) and the pedestals are flexible (i.e., NPST = 1), the above NB cards must be followed by additional NB cards, one for each bearing, on which are specified the dynamic model of the pedestals for angular motion. Each card contains six values:

1. The pedestal mass moment of inertia in the x-plane (around the y-axis),  
lbs-inch<sup>2</sup>.

2. The pedestal angular stiffness in the x-plane (around the y-axis), lbs.  
inch/radian.

3. The pedestal angular damping coefficient in the x-plane (around the y-axis),  
lbs-inch-sec/radian.

4. The pedestal mass moment of inertia in the y-plane (around the x-axis)  
lbs-inch<sup>2</sup>.

5. The pedestal angular stiffness in the y-plane (around the x-axis), lbs.  
inch/radian.

6. The pedestal angular damping coefficient in the y-plane (around the x-axis),  
lbs-inch-sec/radian.

Whirl Frequency Ratios (1P6E12.5)

When the rotor becomes unstable it whirls in a closed orbit with an angular frequency  $\nu$  which normally is equal to approximately one half the rotational frequency  $\omega$ . However, the exact value depends on the rotor and the supporting bearings, and to determine this the program searches for the zero points of the stability determinant. The present input list gives NFR values (card 2, item 5) in sequence of the whirl frequency ratio  $\nu/\omega$  and these values are used

directly by the program in computing the stability determinant. Thus, the program is unable to detect any possible solution outside the specified range. Furthermore, a zero point of the determinant is only detected when the determinant changes sign from one calculation to the next. Hence, if there are two zero points between two consecutive frequency ratios, the program is unable to find them. It is, therefore, necessary to make the increments sufficiently small (approximately 0.01 or less). This is most readily done by giving, say 5 or 6 frequency ratios in the present input list, and then specify an additional subdivision of the intervals by means of NIT, item 7, card 2. As an example, the present list may give 6 values for the frequency ratio: 0.7, 0.6, 0.51, 0.49, 0.4, 0.3 (NFR = 6). In addition, NIT may be set equal to 5. Thereby, the stability determinant is computed at the following 26 frequency ratios: 0.7, 0.68, 0.66, 0.64, 0.62, 0.6, 0.582, 0.564, 0.546, 0.528, 0.51, 0.506, 0.502, 0.498, 0.494, 0.49, 0.472, 0.454, 0.436, 0.418, 0.40, 0.38, 0.36, 0.34, 0.32 and 0.30. Whenever the determinant changes sign, its value is also computed at the mid-point of the interval and these three values are then used to compute the zero point by quadratic interpolation. A second quadratic interpolation is employed to get a more accurate solution.

#### Speed Data (1P6E12.5)

This data and the following bearing data must be repeated NCAL times (item 9, card 2). The speed data is given on one card with three values:

1. The initial speed of the speed range, rpm
2. The final speed of the speed range, rpm
3. The speed increment, rpm.

Thus, the first calculation is performed at a rotor speed equal to the initial speed. Thereafter, the speed is incremented by the speed increment, and this is repeated until reaching the final speed. The zero points of the instability determinant are found for each speed and by plotting the results as previously

discussed, the rotor speed can be determined at which instability sets in. The selected speed range should, therefore, be sufficiently large that it includes the threshold speed.

#### Bearing Data (8E9.2)

Each bearing is represented by 8 dynamic coefficients for radial motion such that the dynamic bearing reactions can be expressed by means of Eq. (1) (or more correctly, by Eq. (5)). The 8 coefficients are given on one card:

$K_{xx}$   $K_{xy}$   $K_{yx}$   $K_{yy}$   $\omega_B_{xx}$   $\omega_B_{xy}$   $\omega_B_{yx}$   $\omega_B_{yy}$       lbs/inch

where  $\omega$  is the angular speed, radians/sec, and the 8 coefficients are computed from the lubrication equation (Reynolds equation) as described in volumes III and VII. When the lubricant is incompressible ( $INC = 0$ , card 2, item 6) the coefficients are independent of whirl frequency and only one set of values should be given. When the lubricant is compressible ( $INC \neq 0$ ), the coefficients are frequency dependent and one set of coefficients must be given for each of the whirl frequency ratios in the input list, i.e. a total of  $NFR$  cards (card 2, item 5). The cards must be given in the same sequence as the values in the frequency ratio list.

When, in the search for the zero points of the instability determinant, the program performs calculations at frequency ratios different from the specified values, the proper dynamic coefficients are obtained by quadratic interpolation of the input data. Hence, a minimum of 3 sets of coefficients is required when  $INC \neq 0$ , which means  $NFR \geq 3$ . When  $INC = 0$ , interpolation is, of course, not necessary and only one set of coefficients is required.

If  $NANG = 0$  (card 2, item 4) the above data is repeated for the next bearing until the coefficients are specified for all  $NB$  bearings. If  $NANG \neq 0$ , the above data is followed by a similar set of data of dynamic coefficients for angular motion. Let the dynamic moment acting on the rotor have the components  $M_x$  and  $M_y$  where  $M_x$  is in the  $x$ - $z$  plane and  $M_y$  is in the  $y$ - $z$  plane ( $z$  is the

coordinate along the rotor axis). The rotor amplitudes are  $x$  and  $y$  and the corresponding rotor slopes are:  $\theta = dx/dz$  and  $\varphi = dy/dz$ . The equations defining the angular dynamic coefficients are:

$$M_x = -G_{xx}\theta - D_{xx} \frac{d\theta}{dt} - G_{xy}\varphi - D_{xy} \frac{d\varphi}{dt} \quad (34)$$

$$M_y = -G_{yx}\theta - D_{yx} \frac{d\theta}{dt} - G_{yy}\varphi - D_{yy} \frac{d\varphi}{dt}$$

where  $t$  is time. These equations are completely analogous to Eq. (1). The coefficients apply to a given bearing geometry, a known static bearing load and are functions of the rotor speed. For compressible lubricants, the coefficients also depend on the whirl frequency ratio such that Eq. (34) more properly should be written:

$$M_x = -Y_{xx}\theta - Y_{xy}\varphi \quad (35)$$

$$M_y = -Y_{yx}\theta - Y_{yy}\varphi$$

where:

$$Y_{xx} = G_{xx} + i(\frac{v}{\omega}) \omega D_{xx} \quad (36)$$

and similarly for  $Y_{xy}$ ,  $Y_{yx}$  and  $Y_{yy}$ . Eq. (35) is analogous to Eq. (5) and is derived in the same way.

In the computer input, the 8 coefficients are given on one card:

$G_{xx} \ G_{xy} \ G_{yx} \ G_{yy} \ \omega D_{xx} \ \omega D_{xy} \ \omega D_{yx} \ \omega D_{yy}$  lbs.inch/radian

In complete analogy to the input for the radial dynamic coefficients, only one

set of coefficients is required for an incompressible lubricant ( $INC = 0$ ) whereas NFN cards are required for a compressible lubricant ( $INC \neq 0$ ).

When all the required input, both the radial coefficients and the angular coefficients, has been given for one bearing, the input is repeated for the next bearing until all NB bearings are specified.

Whereas a journal bearing usually has both radial and angular coefficients, a thrust bearing has only angular coefficients and its radial coefficients should be set equal to zero. In general, the angular coefficients for a journal bearing are of minor importance and may be set equal to zero except in unusual circumstances.

#### COMPUTER OUTPUT

Referring to the sample calculation given later it is seen that the first couple of pages of computer output lists the input data. Thus, any mistake in the input data is readily found.

The listing in the output of the bearing data gives the 8 dynamic bearing coefficients for radial and angular motion. The angular coefficients are identified as "ANG.KXX", meaning  $G_{xx}$ , "ANG.W.BXX", meaning  $\omega D_{xx}$ , and so on. The first column in the list gives the whirl frequency ratio at which the coefficients apply. For an incompressible lubricant, the coefficients are independent of frequency but to simplify the output routine a value of the frequency ratio is still given although it has no particular meaning.

After the listing of the input, follow the results of the calculations. There is a list of output for each rotor speed. The list is preceded by a title giving the rotor speed in rpm, and then follows a four column list of results. The first column gives the whirl frequency ratio  $v/\omega$ , the second column is the corresponding frequency  $\nu$ , radians/sec, the third column is the real part of the instability determinant, and the fourth column is the imaginary part of the determinant.

The purpose of the calculations is to determine those frequency ratio values at which either the real part or the imaginary part of the instability determinant are zero. The program does this in the following way: to illustrate, assume that the real part is positive at a frequency ratio of 0.51 but becomes negative at the next frequency ratio in the sequence, say 0.50. Then the program calculates the determinant at the midpoint of the interval (i.e. at  $\nu/\omega = 0.505$ ) and through these three values of the determinant (at  $\nu/\omega = 0.51$ , 0.505 and 0.50), it passes a second order polynomial and calculates where it becomes zero. Let this be at  $\nu/\omega = 0.5024230$ . This represents a "first solution". To improve the accuracy, an additional calculation is performed with  $\nu/\omega = 0.5024230$ , and the corresponding determinant value is used together with two neighboring values to compute a "second solution" which, then, is taken as the final solution. Obviously, the corresponding determinant is not exactly zero but it is usually  $10^{-6}$  to  $10^{-8}$  of the neighboring values. To spot the solutions in the list of output, simply go through the column of frequency ratios and each time the results show that an interpolation takes place, the finally obtained frequency ratio is a solution. By checking in the columns for the real part and the imaginary part of the instability determinant, it is readily found which part has a zero point.

INPUT FORM FOR COMPUTER PROGRAM

PN400: THE THRESHOLD OF INSTABILITY FOR A FLEXIBLE ROTOR IN FLUID FILM BEARINGS

Card 1 (72H)      Text

Card 2 (1415)

1. NS = Number of rotor stations ( $1 \leq NS \leq 100$ )
2. NB = Number of bearings ( $1 \leq NB \leq 10$ )
3. NPST =  
= 0: rigid pedestals  
= 1: flexible pedestals
4. NANG =  
= 0: no angular bearing stiffness  
= 1: bearings (and pedestals if NPST ≠ 0) have angular stiffness
5. NFR = Number of input values of frequency ratio ( $3 \leq NFR \leq 50$ )
6. INC =  
= 0: bearing lubricant is incompressible (liquid)  
= 1: bearing lubricant is compressible (gas)
7. NIT = Number of subdivisions of frequency ratio intervals ( $1 \leq NIT$ )
8. METR = 0: no diagnostic METR = 0 1: diagnostic
9. NCAL = Number of speed ranges
10. INP =  
= 0: more input follows, starting with card 1  
= 1: last set of input data

Card 3 (1P6E12.5)

1. YM = Youngs modulus for shaft material,  $\text{lbs/inch}^2$
2. DENST = Weight density of shaft material,  $\text{lbs/inch}^3$
3. SHM =  $\alpha G$ , where  $G$  is shear modulus,  $\text{lbs/inch}^2$ , and  $\alpha$  is shape factor for shear

Rotor Data (8E9.2)

Give NS cards with 7 values on each card:

1. Weight at rotor station, lbs.
2. Polar mass moment of inertia at rotor station, lbs.inch<sup>2</sup>
3. Transverse mass moment of inertia at rotor station, lbs.inch<sup>2</sup>
4. Length of shaft section to next station, inch
5. Outer shaft diameter for cross-sectional moment of inertia, inch
6. Outer shaft diameter for shaft mass, inch
7. Inner shaft diameter, inch

Bearing Stations (14I5)

List the NB rotor stations at which there are bearings

Pedestal Data (1P6E12.5)

This data only applies when NPST ≠ 0 (card 2, item 3). Give NB cards with 6 values per card, one card per bearing:

1. Pedestal vibratory mass, x-direction, lbs.
2. Pedestal stiffness, x-direction, lbs/inch
3. Pedestal damping coefficient, x-direction, lbs.sec/inch
4. Pedestal vibratory mass, y-direction, lbs.
5. Pedestal stiffness, y-direction, lbs/inch
6. Pedestal damping coefficient, y-direction, lbs.sec/inch

If also NANG ≠ 0 (card 2, item 4), give additional NB cards, 6 values per card

1. Pedestal vibratory mass moment of inertia, x-plane, lbs.inch<sup>2</sup>
2. Pedestal angular stiffness, x-plane, lbs.inch/radian
3. Pedestal angular damping coefficient, x-plane, lbs.inch.sec/radian
4. Pedestal vibratory mass moment of inertia, y-plane, lbs.inch<sup>2</sup>
5. Pedestal angular stiffness, y-plane, lbs.inch/radian
6. Pedestal angular damping coefficient, y-plane, lbs.inch.sec/radian

Whirl Frequency Ratios (1P6E12.5)

List NFR values of the whirl frequency ratio in sequence, 6 values per card

Note: The remaining data must be repeated NCAL times

Speed Data (1P6E12.5)

1. Initial speed, rpm
2. Final speed, rpm
3. Speed increment, rpm

Bearing Data (8E9.2)

Give NFR cards if INC  $\neq$  0, or 1 card only if INC = 0, with 8 dynamic translatory coefficients per card:

$K_{xx}$   $K_{xy}$   $K_{yx}$   $K_{yy}$   $\omega_B_{xx}$   $\omega_B_{xy}$   $\omega_B_{yx}$   $\omega_B_{yy}$  lbs/inch

If also NANG  $\neq$  0, this data is followed by NFR or 1 card with 8 dynamic angular coefficients per card:

$G_{xx}$   $G_{xy}$   $G_{yx}$   $G_{yy}$   $\omega_D_{xx}$   $\omega_D_{xy}$   $\omega_D_{yx}$   $\omega_D_{yy}$  lbs.inch/radian

There is one set of coefficients per bearing, i.e. the above bearing data is repeated NB times.

```

C      DIMENSION RM( 80),RIP( 80),RIT( 80),RL( 80),RS( 80),RW( 80) *
C      PN400=STABILITY THRESHOLD OF FLEXIBLE ROTOR
1RD( 80),RJ( 80),DV( 80),DM( 80),DMH( 80),AI( 80),A2( 80),
2A3( 80),A4( 80),A5( 80),A6( 80),A7( 80),AN( 80),BN( 80),DN( 80),
3FHQ1(40),XL(4),SL(4),ML(4),JL(4),XR(4),SR(4),BR(4),VR(4),LB(10)
DIMENSION PMX(2+10),PKA(2+10),PDX(2+10),PMY(2+10),PKY(2+10),          6
1PDY(2+10),SB(2+8)                                                 7
DIMENSION DC(4+40+10),DA(4+40+10),DV(2+8+10)                         1
COMMON AC(4+4),AS(4+4),UTC,DTS
200 READ(5+100)
READ(5+101) NS,NF,NPS1,NANG,NFR,INC,NIT,METR,NCAL,INP           10
READ(5+102) YF,DENST,SHM
WRITE(6+100)
WRITE(6+103)
WRITE(6+104) NS,NF,NPS1,NANG,NFR,INC,NIT,METR,NCAL,INP           14
WRITE(6+105)
WRITE(6+106) YF,DENST,SHM
WRITE(6+107)
WRITE(6+108)
DO 201 J=1+NS
READ(5+109) RM(J),RIP(J),RIT(J),RL(J),RS(J),RW(J),RD(J)          19
201 WRITE(6+110) J,RIP(J),RIT(J),RL(J),RS(J),RW(J),RD(J)           20
READ(5+101) (I+(J)+J=1+NH)
WRITE(6+111)
WRITE(6+101)(LR(J),J=1+NH)                                         21
202 AMS=386.064
AMSL=0.000001
204 RS(NS)=1.0
DENST=DENS1/AMS
DO 210 J=1+NS
RM(J)=RM(J)/AMS
RIP(J)=RIP(J)/AMS
RIT(J)=RIT(J)/AMS
C2=RD(J)
C3=RS(J)
RS(J)=0.0490H/245*YF*( (C3**4)-(C2**4))                      25
C4=RW(J)
RW(J)=0.78534*16*(C4**4-C2**4)*DENST                         36
IF(C4) 205,205,205
205 RJ(J)=0.0
GO TO 207
206 RJ(J)=(C4*C4+C2*(C2))/42.0                                 41
207 C2=1.5707463*SHM*(C3+C3-C2*C2)                            42
IF(C2) 208,209,204
208 RD(J)=RS(J)/C2
GO TO 210
209 RD(J)=0.0
210 CONTINUE
IF(NPS1) 211,215,c11
211 WRITE(6+112)
WRITE(6+113)
DO 212 J=1+NH
READ(5+102) PMA(1,J),PKA(1,J),PDX(1,J),PMY(1,J),PKY(1,J),    51
1PDY(1,J)                                                       52
WRITE(6+110) LR(J),PMA(1,J),PKA(1,J),PDX(1,J),PMY(1,J),PKY(1,J), 53
1PDY(1,J)                                                       54
PMX(1,J)=PMX(1,J)/AMS                                         55
212 PMY(1,J)=PMY(1,J)/AMS                                         56
IF(NANG) 213,215,213                                         57
213 WRITE(6+114)
DO 214 J=1+NH
READ(5+102) PMX(2,J),PKA(2,J),PDX(2,J),PMY(2,J),PKY(2,J),    60
1PDY(2,J)                                                       61
WHITE(6+110) LR(J),PMX(2,J),PKA(2,J),PDX(2,J),PMY(2,J),PKY(2,J), 62
1PDY(2,J)                                                       63
PMX(2,J)=PMX(2,J)/AMS                                         64
214 PMY(2,J)=PMY(2,J)/AMS                                         65

```

```

215 READ(5,102) (FR01(J):J=1,NFR)
  WRITE(6,115)
  WRITE(6,106) (FR01(J)+J=1,NFR)
  IC=1
  301 READ(5,102) SPST,SPFN,SPNC
    K1=NFR
    IF(INC) 303+302+303
  302 K1=1
  303 WRITE(6,116)
    WRITE(6,106) SPST,SPFN,SPNC
    WRITE(6,117)
    DO 310 K=1,NH
      WRITE(6,118)LH(K)
      WRITE(6,119)
      DO 306 J=1,K1
        READ(5,109)(DC(I,J,K)+I=1,8)
  306 WRITE(6,121)FR01(J)+(DC(1,J,K)+I=1,8)
    IF(NANG) 307+310+307
  307 WRITE(6,120)
    DO 308 J=1,K1
      HFAU(5,109)(DA(I,J,K)+I=1,8)
  308 WRITE(6,121)FR01(J)+(DA(1,J,K)+I=1,8)
  310 CONTINUE
    SP0=SPST
  320 ANSP=0.1047147E+SP0
    WRITE(6,122)SP0
    WRITE(6,123)
    I0=1
    FRw=FR01(1)
    KR=0
    KE=0
    K1=1
    K2=0
    K3=0
    DF=NIT
    DFK=(FR01(2)-FRw)/I0,E*
  325 FRQ=ANSP*FRw
    FRQ2=FRw*FRq
    DO 326 J=1,NS
      DVA(J)=FRQ2*PK(J)
      DMA(J)=-FRQ2*NIT(J)
  326 DMR(J)=FRQ*ANSP*HIR(J)
  330 DO 375 J=1,NH
    IF(INC) 332+331+332
  331 I1=1
    GO TO 334
  332 IF(K2) 335+333+334
  333 I1=I0
  334 DO 336 I=1,M
    SH(1,I)=DC(I,I1,J)
    IF(NANG) 337+335+335
  335 Sh(2,I)=DA(I,I1,J)
  336 CONTINUE
    GO TO 359
  338 I1=I0
    I2=2
    I3=0
    IF(K3) 340+340+337
  339 I1=I0+1
  340 IF(NFP-I1) 356+356+341
  341 C4=FR01(I1)
    C1=FR01(I1+1)-C4
    C2=C4-FR01(I1-1)
    C3=C1+C2
    C4=FRw-C4
    DO 355 I=1,8
      CS=DC(I,I1,J)
      C6=(DC(I,I1+1,J)-CS)/(C1*C3)
      CR=(DC(I,I1-1,J)-CS)/(C2*C3)

```

C7=C6+C8	136
C6=C2*C6-C1*C8	137
C8=C5+C9*(C6+C9*C7)	138
IF(I1-I2) 343,342,343	139
342 SB(1,I)=C8	140
IF(NANG) 347,355,347	141
343 IF(I3) 344,344,345	142
344 SB(1,I)=C8/C2*(FR#-FH#(I1-1))	143
IF(NANG) 347,355,347	144
345 SB(1,I)=SH(1,I)+C8/C1*(FR#(I1+1)-FR#)	145
IF(NANG) 347,355,347	146
347 C5=DA(I,I1,J)	147
C6=(DA(I,I1+1,J)-C5)/(C1*C3)	148
C8=(DA(I,I1-1,J)-C5)/(C2*C3)	149
C7=C6+C8	150
C6=C2*C6-C1*C8	151
C8=C5+C9*(C6+C9*C7)	152
IF(I1-I2) 349,344,349	153
348 SH(2,I)=C8	154
GO TO 355	155
349 IF(I3) 350,350,352	156
350 SH(2,I)=CH/C2*(FR#-FH#(I1-1))	157
GO TO 355	158
352 SH(2,I)=SH(2,I)+C8/C1*(FR#(I1+1)-FR#)	159
355 CONTINUE	160
356 IF(I3) 359,357,354	161
357 IF(I1-I2) 359,359,358	162
358 I1=I1-1	163
I2=NFR-1	164
I3=1	165
GO TO 341	166
359 DO 360 I=1..4	167
DV(1,I,J)=0.0	168
360 DV(2,I,J)=0.0	169
I1=1	170
361 DO 362 I=5..8	171
362 SH(I1,I)=FR#*SH(I1,I)	172
IF(NPST) 365,363,365	173
363 DO 364 I=1..8	174
DV(I1,I,J)=SH(I1,I)	175
GO TO 370	176
365 C1=PKX(I1,J)-FR#*PMX(I1,J)	177
C2=FR#*PLX(I1,J)	178
C3=PKY(I1,J)-FR#*PMY(I1,J)	179
C4=FR#*PY(I1,J)	180
C5=SH(I1,I)+C1	181
C6=SH(I1,5)+C2	182
C7=SH(I1,4)+C3	183
C8=SH(I1,4)+C4	184
D1=C5*C7-C6*C4-SH(I1,2)*SB(I1,3)+SB(I1,6)*SH(I1,7)	185
D2=C5*C4+C6*C7-SH(I1,2)*SH(I1,7)-SH(I1,3)*SH(I1,6)	186
IF(ABS(D1)-ABS(D2)) 367,366,366	187
366 D3=D2/D1	188
D4=D1+D3*D2	189
D1=1.0/U4	190
D2=-D3*D1	191
GO TO 368	192
367 D3=D1/U2	193
D4=D2*D3*D1	194
D2=-1.0/U4	195
D1=-D3*D2	196
368 D3=C1*D1-C2*D2	197
D4=C1*D2+C2*D1	198
D5=1.0-D3*C7+D4*C8	199
D6=-D3*C8-D4*C7	200
DV(I1,I,J)=C1*D5-C2*D6	201
DV(I1,5,J)=C1*D6+C2*D5	202
D5=C3*SH(I1,2)-C4*SH(I1,6)	203
D6=C4*SH(I1,2)+C3*SH(I1,6)	204

DV(II+2,J)=D3*D5-D4*D6	205
DV(II+6,J)=D3*D6+D4*D5	206
D5=C3*S4(II+3)-C4*S4(II+7)	207
D6=C4*S4(II+3)+C3*S4(II+7)	208
DV(II+3,J)=D3*D5-D4*D6	209
DV(II+7,J)=D3*D6+D4*D5	210
D3=C3*D1-C4*D2	211
D4=C3*D2+C4*D1	212
D5=1.0-D3*C5+D4*C6	213
D6=-D3*C6-D4*C5	214
DV(II+4,J)=C3*D5-C4*D6	215
DV(II+8,J)=C3*D6+C4*D5	216
370 IF(NANG) 371,375,371	217
371 IF(II-1) 372,372,375	218
372 II=2	219
GO TO 361	220
375 CONTINUE	221
IF(METH) 381,382,382	222
381 I1=IAHS(METH)	223
WRITE(6,1c1) FHW*(DV(II+1,J)+I1+3)	
GO TO 400	225
382 CONTINUE	226
I1=NS-1	227
DO 420 J=1,I1	228
C1=PS(J)	229
C2=FR02*M4(J)	230
C3=R0(J)	231
C10=RJ(J)	232
C4=C2/C1	233
C5=SQRT(C4)	234
C6=SQRT(C5)	235
C7=RL(J)	236
IF(C6*C7=0.03) 411,411,412	237
411 C4=C2*C7	238
D1=C7*C7*C4	239
D2=C7*D1	240
D3=C7*D2	241
D4=D1*(C3-C10)	242
D5=C7/C1	243
D6=C7*D5/2.0	244
D7=C7*D6/3.0	245
DA=C3-C10	246
DF=UM*D8*C3*C10	247
A1(J)=1.0+D3/24.0	248
A2(J)=R1(J)-D4	249
A3(J)=(1.0-D4/3.0+D3/120.0)*C7	250
A4(J)=D2/6.0	251
A5(J)=C1*A4(J)	252
A6(J)=C2*A3(J)	253
AN(J)=(1.0+D1*D4*C4+C3*(1.0+D3/120.0)*D5	254
M(J)=1.0-D4/6.0+D3/360.0	255
A7(J)=C5*MN(J)/C1*D7	256
BN(J)=UM*D8*(J)	257
DM(J)=(1.0+D1*(C4*D8)*D7-(C3-C10)*2.0*D5	258
GO TO 400	259
412 C4=(4*((C3+C1)*2))	260
C4=C5*(C3-C1)	261
IF((M=0.002)->13+13+14	262
413 C11=1.0+0.27*CH	263
CA=1.0+0.5*CH	264
GO TO 415	265
414 CM=SQRT(1.0+CH)	266
C11=SQRT(CH)	267
415 DS=CS*(CH-C4)	268
DA=CS*(CH+C4)	269
DD=DS*DH	270
IF(4HS(C4/CH)=0.0002) 416,416,417	271

416	DR=0.5*C8+C9	272
	D3=C6+C11*(1.0-DR)	273
	D4=C6+C11*(1.0+DR)	274
	GO TO 41c	275
417	D3=SQRT(D5)	276
	D4=SQRT(D6)	277
418	D7=D3*D5	278
	DR=D4*D6	279
	D1=P3*C7	280
	D2=D4*C7	281
	VC=COS(D2)/D4	282
	VS=SIN(D2)/D4	283
	BMC=EXP(C1)	284
	BMS=1.0/EXP	285
	D1=0.5*(BMC+BMS)/D4	286
	D2=0.5*(BMC-BMS)/D4	287
	A1(J)=D4*D1+D5*VC	288
	A2(J)=D5*D1+D4*VS	289
	A3(J)=D3*D2+D4*VS	290
	A6(J)=C2*A3(J)	291
	RN(J)=(D1-VC)/C1	292
	A7(J)=C2*(D1-VC)	293
	A4(J)=C5*(D4*D2-D3*VS)	294
	A5(J)=C1*A4(J)	295
	CA=C1*C5	296
	AN(J)=(D6*D2+D7*VS)/C6	297
	DN(J)=(D7*D2-D6*VS)/C6	298
420	CONTINUE	299
	DO 470 I=1,4	300
	DO 452 J=1,4	301
	XL(J)=0.0	302
	SL(J)=0.0	303
	BL(J)=0.0	304
452	VL(J)=0.0	305
	I1=I+I-1	306
	IF(I>2) 453+453+454	307
453	XL(I1)=AMSL	308
	GO TO 455	309
454	I1=I1-4	310
	SL(I1)=AMSL	311
455	I1=1	312
	I2=LH(I)	313
	DO 465 J=1,NS	314
	DO 456 L=1,4	315
	PR(L)=HL(L)+DMA(J)*SL(L)	316
	VR(L)=VL(L)+DVA(J)*XL(L)	317
	XR(L)=XL(L)	318
456	SR(L)=SL(L)	319
	BR(1)=BR(1)-DMH(J)*SL(4)	320
	BR(2)=BR(2)+DMH(J)*SL(3)	321
	BR(3)=BR(3)+DMH(J)*SL(2)	322
	BR(4)=BR(4)-DMH(J)*SL(1)	323
	IF(I2>J) 460+457+460	324
457	BR(1)=BR(1)+SL(1)*DV(z+1,I1)-SL(2)*DV(2,5,I1)+SL(3)*DV(2,2,I1)-	325
	1SL(4)*DV(2,6,I1)	326
	BR(2)=BR(2)+SL(1)*DV(2,5,I1)+SL(2)*DV(2,1,I1)+SL(3)*DV(2,6,I1)+	327
	1SL(4)*DV(2,2,I1)	328
	BR(3)=BR(3)+SL(1)*DV(2,3,I1)-SL(2)*DV(2,7,I1)+SL(3)*DV(2,4,I1)-	329
	1SL(4)*DV(2,8,I1)	330
	BR(4)=BR(4)+SL(1)*DV(2,7,I1)+SL(2)*DV(2,3,I1)+SL(3)*DV(2,8,I1)+	331
	1SL(4)*DV(2,4,I1)	332
	VR(1)=VR(1)-XL(1)*DV(1,1,I1)+XL(2)*DV(1,5,I1)-XL(3)*DV(1,2,I1)+	333
	1XL(4)*DV(1,6,I1)	334
	VR(2)=VR(2)-XL(1)*DV(1,5,I1)-XL(2)*DV(1,1,I1)-XL(3)*DV(1,6,I1)-	335
	1XL(4)*DV(1,2,I1)	336
	VR(3)=VR(3)-XL(1)*DV(1,3,I1)+XL(2)*DV(1,7,I1)-XL(3)*DV(1,4,I1)+	337
	1XL(4)*DV(1,8,I1)	338
	VR(4)=VR(4)-XL(1)*DV(1,7,I1)-XL(2)*DV(1,3,I1)-XL(3)*DV(1,8,I1)-	339
	1XL(4)*DV(1,4,I1)	340

11=11+1	341
IF(NH=11) 458+459+459	342
458 I2=NS+2	343
GO TO 460	344
459 I2=LH(11)	345
460 IF(NS=J) 465+466+467	346
461 DO 462 L=1+0	347
XL(L)=A2(J)*X-(L)+A3(J)*SH(L)+BN(J)*BR(L)+DN(J)*VR(L)	348
SL(L)=A4(J)*X-(L)+A1(J)*SH(L)+AN(J)*BR(L)+BN(J)*VR(L)	349
BL(L)=A7(J)*X-(L)+A5(J)*SH(L)+A1(J)*BN(L)+A3(J)*VR(L)	350
VL(L)=AH(J)*X-(L)+A7(J)*SH(L)+A4(J)*BR(L)+A2(J)*VR(L)	351
465 CONTINUE	352
AC(1,I)=VR(1)	353
AC(2,I)=VR(3)	354
AC(3,I)=BR(1)	355
AC(4,I)=BR(3)	356
AS(1,I)=VR(2)	357
AS(2,I)=VR(4)	358
AS(3,I)=BR(2)	359
AS(4,I)=BR(4)	360
470 CONTINUE	361
CALL CUE1K	
NH TH (6+105) FHN+FHW+0 L+0 TS	
IF(KH) 476+477+478	364
480 IF(KF) 478+479+480	365
481 IF(KI) 479+480+482	366
482 K1=0	367
DC1=UTC	368
TC1=FHW	369
GO TO 483	370
483 IF(UTC>DC1) 478+479+484	371
484 DC1=UTC	372
TC1=FHW	373
485 IF(DTS>0 S1) 505+456+456	374
486 DS1=0 S	375
TS1=FHW	376
IF(NFH=16) 550+551+487	377
487 IF(NIT=1-K3) 489+489+489	378
488 K3=K3+1	379
K2=1	380
FHW=FHW+FHW	381
GO TO 489	382
489 K3=0	383
K2=0	384
I0=10+1	385
FHW=FHW(I0)	386
IF(NFH=16) 440+440+441	387
440 DFw=0.1	388
GO TO 490	389
491 DFw=0 1	390
DFw=(FHW*(I0+1)-FHW)/DFw	391
GO TO 492	392
492 Kw=1	393
DC3=UTC	394
TC4=FHW	395
DS3=0 S	396
TS4=FHW	397
FHW=(FHW+TC1)/2.0	398
K2=1	399
GO TO 495	400
495 Kp=-1	401
X1=TC1	402
X2=FHW	403
X3=TC3	404
Y1=DC1	405
Y2=UTC	406
Y3=DC3	407
GO TO 520	408
496 IF(KH+1) 501+497 497	409

497	KR=-2	410
	IF(FRW-X2) 499,498,49d	411
498	X1=X2	412
	Y1=Y2	413
	GO TO 500	414
499	X3=X2	415
	Y3=Y2	416
500	X2=FRW	417
	Y2=DTC	418
	GO TO 520	419
501	KR=0	420
	DTS=DS3	421
	FRW=TS3	422
	DC1=DC3	423
	TC1=TC3	424
	GO TO 485	425
505	KE=1	426
	DS3=DTS	427
	TS3=FRW	428
	FRW=(FRW+TS1)/2.0	429
	K2=1	430
	GO TO 325	431
506	KE=-1	432
	X1=TS1	433
	X2=FRW	434
	X3=TS3	435
	Y1=DS1	436
	Y2=DTS	437
	Y3=DS3	438
	GO TO 520	439
507	IF(KE+1) 512,508,508	440
508	KF=-2	441
	IF(FRW-X2) 510,504,504	442
509	X1=X2	443
	Y1=Y2	444
	GO TO 511	445
510	X3=X2	446
	Y3=Y2	447
511	X2=FRW	448
	Y2=DTS	449
	GO TO 520	450
512	KF=0	451
	DTS=DS3	452
	FRW=TS3	453
	GO TO 484	454
520	C1=X3-X2	455
	C2=X2-X1	456
	C3=X3-X1	457
	C4=(Y3-Y2)/(C1*C3)	458
	C5=(Y1-Y2)/(C2*C3)	459
	C6=C2*C4-C1*C5	460
	C4=C4+C6	461
	IF(C4) 522,521,522	462
521	C6=-Y2/C5	463
	GO TO 525	464
522	C5=0.5/C4*C5	465
	C4=AH5(C5*C5-Y2/C4)	466
	C4=SQR(T(C4))	467
	IF(C5) 523,524,524	468
523	C4=-C4	469
524	C6=C4-C5	470
525	FR'v=XP+C6	471
	GO TO 325	472
550	SPD=SPD+SP1IC	473
	IF(SPFN+0.00001-SPD) 552,552,320	474
552	IF(NCAL-1C) 554,554,553	475
553	IC=IC+1	476
	GO TO 301	477
554	IF(INP) 555,200,555	478

```

555 CALL EXIT          480
100 FORMAT(1ZH        481
      1)              482
101 FORMAT(14I5)       483
102 FORMAT(6E12.5)     484
103 FORMAT(1H0,1STATIONS NO.BRGS RAD.FLEX ANG.FLEX NO.FREQ INCUMPR
      1SUHDIVS MTHIC SPEEDS INPUT) 485
104 FORMAT(16.9I9)     486
105 FORMAT(1SH0 YOUNGS MOD.SAxDENSITY (SHEAR FACT)*6) 487
106 FORMAT(HE14.5)     488
107 FORMAT(1IH0,ROTOR DATA) 489
108 FORMAT(104H0,STATION MASS POLAR MOM.IN. TRANSV.MOM.IN L
      LENGTH OUT.DIA(STIFF) UNIT.DIA(MASS) INNER DIA.) 490
109 FORMAT(3E9.2)       491
110 FORMAT(15.8E16.5,7E14.5) 492
111 FORMAT(17H0,REARING STATIONS) 493
112 FORMAT(14H0,TESTAL DATA) 494
113 FORMAT(10H0,STATION MASS-X STIFFNESS-X DAMPING-X MA
      ISS-Y STIFFNESS-Y DAMPING-Y) 495
114 FORMAT(10H0,STATION MM4.INSERT-X ANG-STIFFN-X ANG.DAMP-X MOM.
      1INPHT-Y ANG-STIFFN-Y ANG.DAMP-Y) 496
115 FORMAT(23H0,INITIAL FREQUENCY RATIOS) 497
116 FORMAT(42H0,INITIAL SPEED FINAL SPEED SPEED INCH.) 498
117 FORMAT(12H0,DYNAMIC READING COEFFICIENTS) 499
118 FORMAT(12H0,READING AT ROTOR STATION) 500
119 FORMAT(13H0, FREQUENCIES XMASRAX10X3HKYX10X3HKYY9X5HW*8XX8X5
      1HRYAYXASRAX, YAHAYHAYKYY) 501
120 FORMAT(13H0, FREQ.RATIOS X/HANG,X/XA/X7HANG,X/X6X7HANG,KY
      1Y5XHAN,X/X4X4X4HANG,X/X4Y4A/XHANG,W/X4X4YHANG,W/BYY) 502
121 FORMAT(2E14.5,7E12.5) 503
122 FORMAT(11H0,ROTOR SPEED=13.6+4H RPM) 504
123 FORMAT(5DH0, FREQUENCIES FREQUENCY RE(DETERM) IM(DETERM)) 505
      END          506
      SUBROUTINE COEFH 507
C      SUBROUTINE FOR PN400          508
      DIMENSION INDX(4,5)          509
      COMMON AC(4,4),AS(4,4),DTC,DT5          510
C      INITIALIZATION          511
      N=4
      DTC=1.0
      DT5=0.0
      DO 10 J=1,N          6
      10 INDX(J,J)=0          7
C      CHECK FOR ZERO MATRIX          8
      DO 15 I=1,N          9
      IRW=1
      ICL=1
      DO 14 J=1,N          10
      IF(ABS(AC(I,J))+ABS(AS(I,J))) .LT. 1E-11          11
      11 IRW=0
      12 IF(ABS(AC(J,I))+ABS(AS(J,I))) .LT. 1E-11          12
      13 ICL=0
      14 CONTINUE
      IF(IRW+ICL) 15,15,46          13
      15 CONTINUE
C      SEARCH FOR PIVOT ELEMENT          14
      DO 41 I=1,N          15
      TST=0.0
      DO 24 J=1,N          16
      IF(INDX(J,J)-1) 17,24,17          17
      17 DO 23 K=1,N          18
      IF(INDX(K,J)-1) 18,23,46          19
      18 C1=SQRT(AC(J,K)*AC(J,K)+AS(J,K)*AS(J,K))
      IF(TST-C1) 22,23,23          20
      22 IRW=J
      ICL=K
      TST=C1
      23 CONTINUE          21

```

```

24 CONTINUE 33
INDEX(ICL+3)=INUX(ICL+3)+1 34
INDEX(I,1)=IRW 35
INDEX(I,2)=ICL 36
C INTERCHANGE ROWS TO PUT PIVOT ELEMENT ON DIAGONAL 37
IF(IRW-ICL) 25,29,25
25 DTC=-DTC
DTS=-DTS
DO 26 L=1,N
C1=AC(IRW,L)
C2=AS(IRW,L)
AC(IRW,L)=AC(ICL,L)
AS(IRW,L)=AS(ICL,L)
AC(ICL,L)=C1
26 AS(ICL,L)=C2 45
C DIVIDE PIVOT ROW BY PIVOT ELEMENT 46
29 C1=AC(ICL,ICL) 47
C2=AS(ICL,ICL) 48
TST=DTC
DTC=C1*TST-C2*DTS
DTS=C2*TST+C1*DTS
AC(ICL,ICL)=1.0 49
AS(ICL,ICL)=0.0 50
IF(ABS(C1)-ABS(C2)) 31,30,30 51
30 TST=C2/C1 52
C1=1.0/(C1+TST*C2) 53
C2=TST*C1 54
GO TO 32 55
31 TST=C1/C2 56
C2=1.0/(C2+TST*C1) 57
C1=TST*C2 58
32 DO 33 L=1,N 59
TST=AC(ICL,L) 60
AC(ICL,L)=C1*TST+C2*AS(ICL,L) 61
AS(ICL,L)=C1*AS(ICL,L)-C2*TST 62
C REDUCE NON-PIVOT ROWS 63
33 DO 41 L1=1,N 64
IF(L1-ICL) 37,41,37 65
37 C1=AC(L1,ICL) 66
C2=AS(L1,ICL) 67
AC(L1,ICL)=0.0 68
AS(L1,ICL)=0.0 69
DO 38 L=1,N 70
AC(L1,L)=AC(L1,L)-C1*AC(ICL,L)+C2*AS(ICL,L) 71
38 AS(L1,L)=AS(L1,L)-C2*AC(ICL,L)-C1*AS(ICL,L) 72
41 CONTINUE 73
C INTERCHANGE COLUMNS 74
DO 44 I=1,N 75
L=N+1-I 76
IF(INDX(L+1)-INDEX(L+2)) 42,44,42 77
42 IRW=INDEX(L+1) 78
ICL=INDEX(L+2) 79
DO 43 K=1,N 80
C1=AC(K,IRW) 81
C2=AS(K,IRW) 82
AC(K,IRW)=AC(K,ICL) 83
AS(K,IRW)=AS(K,ICL) 84
AC(K,ICL)=C1 85
AS(K,ICL)=C2 86
43 CONTINUE 87
44 CONTINUE 88
DO 45 K=1,N 89
IF(INDX(K+3)-1) 46,45,46 90
45 CONTINUE 91
ID=1 92
GO TO 47 93
46 ID=2 94
DTC=0.0
DTS=0.0
47 RETURN
END

```

#### REFERENCES

1. Rotor-Bearing Dynamics Design Technology, Part V: "Computer Program Manual for Rotor Response and Stability," Technical Report AFAPL-TR-65-45, Part V, J. W. Lund, May 1965.
2. Rotor-Bearing Dynamics Design Technology, Part VII: "The Three Lobe Bearing and Floating Ring Bearing," Technical Report AFAPL-TR-65-45, Part VII, J. W. Lund, February 1968.
3. Rotor-Bearing Dynamics Design Technology, Part VI: "The Influence of Electromagnetic Forces on the Stability and Response of an Alternator Rotor," Technical Report AFAPL-TR-64-45, Part VI, J. W. Lund and T. Chiang, September 1967.
4. Lund, J. W., "The Stability of an Elastic Rotor in Journal Bearings with Flexible, Damped Supports", Trans. ASME, Journal of Applied Mechanics, Series E Volume 87, pp. 911-920.
5. Lund, J. W., Wernick, R. J. and Malanoski, S. B., "Analysis of the Hydrostatic Journal and Thrust Bearing for the NASA AB-5 Gyro Gimbal Bearing", Mechanical Technology Inc., Report No. MTI-62TR26, 1962.
6. Hildebrand, F.B., "Introduction to Numerical Analysis", McGraw-Hill Book Co., 1956, pp. 41-43.
7. Tang, I.C. and W.A. Gross, "Analysis and Design of Externally Pressurized Gas Bearings", ASLE Paper No. 61LC-20, 1961.
8. Design of Gas Bearings, Vol. I, Mechanical Technology Inc., 1969, Section 5.6.

Unclassified

Security Classification

**DOCUMENT CONTROL DATA - R & D**

(Security classification of title, body of abstract and indexing annotation must be entered when the overall report is classified)

1. ORIGINATING ACTIVITY (Corporate author)		2a. REPORT SECURITY CLASSIFICATION <b>Unclassified</b>
Mechanical Technology Incorporated 968 Albany-Shaker Road Latham, New York 12110		2b. GROUP <b>N/A</b>
3. REPORT TITLE  Rotor-Bearing Dynamics Design Technology Part IX: Thrust Bearing Effects on Rotor-Bearing Stability		
4. DESCRIPTIVE NOTES (Type of report and inclusive dates) Final Report for Period October 1968 to January 1969		
5. AUTHOR(S) (First name, middle initial, last name)  R.A. Cundiff and J. Vohr		
6. REPORT DATE August 10, 1970		7a. TOTAL NO. OF PAGES <b>97</b>
8a. CONTRACT OR GRANT NO. AF33(615)-3238		9a. ORIGINATOR'S REPORT NUMBER(S)  MTI 70TR40
b. PROJECT NO. 3048		9b. OTHER REPORT NO(S) (Any other numbers that may be assigned this report)  AFAPL-TR-65-45, Part IX
c. Task Nr: 304806		
d. Task Nr: 304806		
10. DISTRIBUTION STATEMENT  This document is subject to special export controls and each transmittal to foreign governments or foreign nationals may be made only with prior approval of the Air Force Aero Propulsion Laboratory (APFL), Wright-Patterson Air Force Base, Ohio 45433.		
11. SUPPLEMENTARY NOTES  None		12. SPONSORING MILITARY ACTIVITY  Air Force Aero Propulsion Laboratory Wright-Patterson AFB, Ohio 45433
13. ABSTRACT  This volume presents a study conducted to determine the effects thrust bearings on rotor-bearing stability. A computer program, written in order to study these effects, permits the inclusion of the thrust bearing characteristics into the rotor system. A program manual is provided, containing a listing of the program and detailed instructions for preparation of input data. A technique is also presented which provides for the user a convenient method of evaluating the stability of a rotor system with and without the thrust bearing data. Extensive design data are presented for gas-lubricated, externally pressurized thrust bearings.		

DD FORM 1 NOV 68 1473 (PAGE 1)

S/N 0101-807-6801

Unclassified

Security Classification

Unclassified  
Security Classification

14 KEY WORDS	LINK A		LINK B		LINK C	
	ROLE	WT	ROLE	WT	ROLE	WT
Bearings Critical Speed Lubrication Fluid Film Hybrid Hydrodynamic Hydrostatic Rotor-Bearing Dynamics Stability Stiffness and Damping Gas Lubrication Gas Bearings						